



**UNIVERSITY of the
WESTERN CAPE**

**AN ASSESSMENT OF THE RIVER FLOW CONTRIBUTIONS OF TRIBUTARIES
AND THE EFFECTS OF FLOODPLAIN WETLANDS ON SPATIO-TEMPORAL
VARIATIONS OF RIVER FLOWS IN THE NUWEJAARS RIVER CATCHMENT,
CAPE AGULHAS**

Daniel James Gustav Mehl

*A thesis submitted in fulfilment of the requirements for the degree of Magister Scientiae in the
Department of Earth Sciences*

Supervisor: Professor D. Mazvimavi

KEY WORDS

Heuningnes Catchment; flood prediction; ungauged catchments; wetland classification



UNIVERSITY *of the*
WESTERN CAPE

ABSTRACT

Improved knowledge is required on the quantity and source of water resources, particularly evident during periods of drought currently being faced in South Africa. There is inadequate knowledge with regards to the flood attenuating properties of wetlands, particularly evident in the ungauged catchments of Southern Africa. This study aims to improve the knowledge on the contribution of flow from tributaries with headwaters in mountainous regions to low lying areas and the effects of wetlands on river flow patterns. Several river flow monitoring sites were established along the major upper tributaries of the Nuwejaars River at which daily water levels were recorded and bi-weekly discharge measurements were conducted. Weather data was collected using four automatic weather stations and three automatic rain gauges' setup throughout the catchment. Rainfall data coupled with rating curves and daily discharges were used to assess the flow responses of these tributaries to rainfall events. Additionally, stable isotope analysis and basic water quality analysis was used to determine the major sources of flow within the major tributaries. The rainfall and river flow data collected, coupled with the characterization of the wetland was used to determine the flood attenuation capabilities of the wetland. Lastly, a conceptual model based on a basic water balance was developed to further explain the role of the wetland and its effects on river flows. The results showed a 27-hour lag time in peak flows from the upper tributaries at the inflows of the wetland to the outflow. Two of the upper tributaries had flow throughout the year and were fed by springs in the upper mountainous regions of the catchment and all tributaries were largely reliant on rainfall for peak flows. The temporary storage of flows within the wetland occurred as a result of the Nuwejaars River bursting its banks, filling of pools, or ponds and the Voëlvlei Lake. It was concluded that the wetland increased the travel time and decreased the magnitude of flows of the Nuwejaars River. However, due to the fact that wetlands are interlinked on a catchment scale and have a collective effect on flood attenuation this study may be improved by looking at the wetlands within the catchment holistically.

PLAGARISM DECLARATION

I Daniel Mehl declare that Assessing the Influence of floodplain wetlands on wet and dry season river flows along the Nuwejaars River, Western Cape, South Africa.is my own work, that it has not been submitted for any other degree or examination in any other university and that all the sources I have used or quoted have been indicated and acknowledged by complete references.

Full Name: Daniel James Gustav Mehl

Date: ...16/01/2019.....

Signature:|.....



UNIVERSITY *of the*
WESTERN CAPE

ACKNOWLEDGEMENTS

After many consultations, weekends of reviewing my thesis and fording me the opportunity to receive funding from Applied Centre for Climate and Earth Systems Science (ACCESS), I would like to express my gratitude to my supervisor Prof. D. Mazvimavi. He always went the extra mile, as far as correcting poor grammar and spelling “mistakes”. I am truly grateful to have had such an amazing supervisor.

To my colleagues and team mates, Damian Hans and Yonela Mkunyana a big thank you for hanging upside down, dealing with mood swings, terrible weather, break-downs and accidents. All in all, a pretty epic experience and memories I will always cherish. **THANK YOU**

From dodging of tortoises to near death encounters with snakes these few years were truly amazing and memories I will look upon fondly in many years to come.

To my family and friends who put up with all the stress alongside me, shoulders to cry on and the oh so necessary drink every now and then to keep the sanity up, I am extremely grateful.

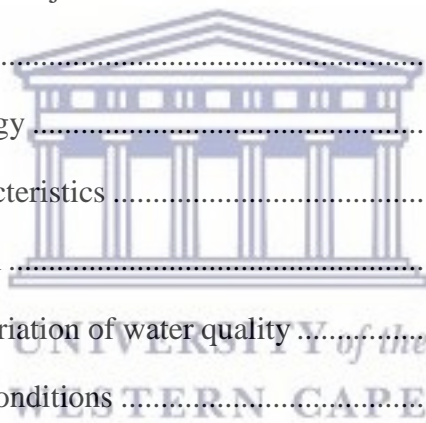
Last but definitely not least a huge thank you to my small big sister for putting up with me for a month, without which I doubt I would ever have completed this journey!

TABLE OF CONTENTS

Key Words.....	i
Abstract.....	ii
Plagiarism declaration.....	iii
Acknowledgements.....	iv
List of figures.....	viii
List of tables.....	xi
List of Symbols.....	xvii
List of Acronyms.....	xix
1. INTRODUCTION	20
1.1 Background.....	20
1.2 Problem Statement.....	24
1.3 Research Question and Hypothesis.....	24
1.4 Aim and Objectives.....	25
1.5 Thesis outline.....	25
2. LITERATURE REVIEW	26
2.1. Introduction.....	26
2.2. Assessing the flood attenuating capabilities of wetlands.....	26
2.2.1 Wetland Topography	26
2.2.2. Wetland Shape, Size and Location	27
2.2.3. Vegetation.....	28
2.2.4. Soil Properties.....	30
2.2.5. Flow regime	30
2.2.6. Wetland classification.....	31
2.3. Use of models to predict the influence of wetlands on flow.....	32

2.3.1. Lumped models.....	33
2.3.2. Physically distributed models	34
2.4. Summary	35
3. STUDY AREA	36
3.1. Introduction.....	36
3.2. Geology.....	38
3.3. Vegetation	39
3.4. Land uses	40
4. HYDROLOGICAL RESPONSES TO RAINFALL EVENTS	42
4.1 Introduction.....	42
4.2. Methods.....	42
4.2.1. Weather data collection.....	42
4.2.2. Selection of river flow monitoring sites.....	46
4.2.3. Topography of tributaries and channel cross-sections.....	47
4.2.4. Stage-discharge measurements	47
4.2.5. Derivation of rating curves	49
4.2.6. Analysis of hydrologic responses	49
4.3. Results.....	50
4.3.1. Seasonal variation of rainy days	50
4.3.2. Rainfall intensity	54
4.3.3. Estimation of catchment rainfall	57
4.3.4. River flow monitoring sites	61
4.3.5. Rating curves	75
4.3.6. Daily variations of river water levels.....	81
4.3.7. Discharge estimates of sub-catchments	84
4.3.8. Sub-catchment responses to rainfall events	88
4.3.9. Rainfall requirements for flows to occur	91

4.4. Discussion	93
5. INFLUENCE OF THE NUWEJAARS WETLAND ON RIVER FLOWS	97
5.1 Introduction	97
5.2 Methods.....	97
5.2.1. Wetland morphology	97
5.2.2. Determination of soil texture and infiltration rates.....	98
5.2.3. Spatial distribution of wetland vegetation	99
5.2.4. Wetland flow regimes and water sources	99
5.2.5. Wetland climatic conditions	100
5.2.6. Conceptual model of the floodplain wetland.....	101
5.2.7. Modelling of the Nuwejaars Wetland	102
5.3 Results	106
5.3.1. Wetland morphology	106
5.3.2. Wetland soil characteristics	111
5.3.3. Wetland vegetation	112
5.3.4. Spatio-temporal variation of water quality	113
5.3.5. Wetland climatic conditions	117
5.3.6. Spatio-temporal variations of flows through the wetland.....	119
5.3.7. Predicting the wetland response to inflows	126
5.4 Discussion	128
6. CONCLUSION AND RECOMMENDATIONS	131
7. REFERENCES	134
8. ANNEXURES	144



LIST OF FIGURES

Figure 3.1: Location of the Nuwejaars River and its tributaries.	36
Figure 3.2: Geology and spatial distribution of wetlands of the Nuwejaars Catchment area within the Heuningnes Catchment.	39
Figure 3.3: Land cover and land uses of the Nuwejaars Catchment.	40
Figure 4.1: Locations of the rain gauges and weather stations.	43
Figure 4.2: Thiessen polygons used to estimate the weights of each rainfall station for estimating daily rainfall.	46
Figure 4.3: Record lengths for the Weather Stations and Rain Gauges in the Nuwejaars Catchment.	50
Figure 4.4: Number of rainy days per month at each of the rainfall stations for 2015.	52
Figure 4.5: Number of rainy days per month at each of the rainfall stations for 2016.	53
Figure 4.6: Number of rainy days per month for each of the rainfall stations from January 2017 to July 2017.	54
Figure 4.7: Average daily rainfall intensity for the Tiersfontein, Spanjaardskloof and Vissersdrift rainfall stations, from 27 th January to 31 st December 2015.	55
Figure 4.8: Average daily rainfall intensity for the Moddervlei, Tiersfontein, Spanjaardskloof and Vissersdrift rainfall stations for 2016.	56
Figure 4.9: Average daily rainfall intensity for the Moddervlei, Tiersfontein, Spanjaardskloof and Vissersdrift rainfall stations, from 1 st January to 30 th June 2017.	57
Figure 4.10: Daily rainfall of all the rainfall stations for 2015 and 2016.	58
Figure 4.11: Daily rainfall of all the rainfall stations from January to 31 st July 2017.	69
Figure 4.12: Estimated rainfall received for each of the sub-catchments for 2015, 2016 and January to 31 st July 2017.	60

Figure 4.13: Flow monitoring sites established from 2014 to 2016 in the Nuwejaars Catchment.	61
Figure 4.14: Flow monitoring site on the Jan Swartskraal River and the channel bed and bank coverage downstream of the flow monitoring site (A), bridge and stilling well installed (B), cross-section selected for flow measurements (C) and invaded channel and banks upstream of the bridge (D).	63
Figure 4.15: Shaded active channel of the cross-section of the Jan Swartskraal flow monitoring site.	64
Figure 4.16: Confluence of the Jan Swartskraal and Koue Rivers with the upper tributaries of the Nuwejaars River.	65
Figure 4.17: Downstream of the Elim Waste Water Treatment Plant flow monitoring site before and after clearing (A, B) and upstream of the site before and after clearing (C, D).	66
Figure 4.18: Installation of the stilling well and a flow measurement being done during one of the peak flows at Elim Water Treatment Plant.	67
Figure 4.19: Shaded active channel of the cross-section on the upper Nuwejaars River at the Water Treatment Plant flow monitoring site used to estimate Q using Manning's Equation.	67
Figure 4.20: The cross-section where flow measurements were conducted on the Nuwejaars River at the Elim-Boskloof Road Bridge (A), Meander and vegetation on banks downstream of the selected cross-section (B), dense vegetation in and around the channel upstream of the bridge (C) and hidden PVC pipe with the logger installed (D).	68
Figure 4.21: Shaded active channel of the cross-section of the Nuwejaars River at the Melkery Bridge flow monitoring station.	69

Figure 4.22: Flow measuring site along the Upper Nuwejaars River at the Elim Flow Diversion.	70
Figure 4.23: Cross-section where flow measurements were conducted and the stilling well installed (A) and cross-section along the straight channel with sandy bed and banks invaded by alien <i>Acacia</i> species at the Pietersielieskloof flow monitoring site (B). Erosion of Palmiet wetlands along the Pietersielieskloof River upstream of the flow monitoring site located on Farm 299 (C).	71
Figure 4.24: Shaded active channel of the cross-section of the Pietersielieskloof River.	72
Figure 4.25: Stilling well installed at Elandsdrift (A) and the Elandsdrift bridge during the selection of the flow monitoring site in 2014 (B).	72
Figure 4.26: Completed setup of the Voëlvlei site with stilling well fixed to the Elim-Struisbaai Road Bridge alongside the gauge plate (A) and installation of the stilling well (B).	73
Figure 4.27: Stilling well installed at the Blomkraals site and the culverts used for the initial flow measurements (A), pond upstream of the Blomkraals flow monitoring station which requires flooding before flow occurs through the bridge (B), cross-section of the area where flow measurements were done for the remainder of the study (C).	74
Figure 4.28: Shaded active channel of the cross-section of the Blomkraals River.	74
Figure 4.29: Rating curve derived for the Nuwejaars River at Elandsdrift using discharge measurements from 2015 – 2016.	76
Figure 4.30: Rating curve derived for the Voëlvlei tributary using the discharge measurements from 2015 to 2016.	77
Figure 4.31: The rating curve derived for the Blomkraals River.	78

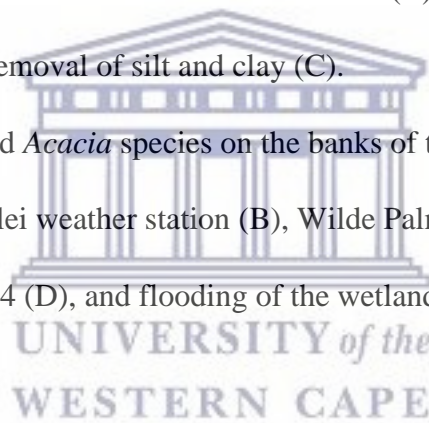
Figure 4.32: Rating curve produced for the Melkery Bridge tributary from 0 m to 1m (A), 1 m to 2m (B) and the combined rating curves with measured discharges (C).	79
Figure 4.33: Rating curves produced using Manning's equation and the measured Q values for Pietersielieskloof tributary.	80
Figure 4.34: Rating curves produced using Manning's equation and the measured Q values for the Jan Swartskraal tributary.	81
Figure 4.35: The record lengths of collected water level data for all the sites until the 5th September 2017.	82
Figure 4.36: Daily variation of water levels for 2016.	83
Figure 4.37: Daily variations of water levels from January 2017 to 5th September 2017.	84
Figure 4.38: Monthly discharge (Mm^3/month) of 7 of the flow monitoring sites for 2016.	85
Figure 4.39: Annual contribution to flows from the each of the sub-catchments of the Nuwejaars Catchment for 2016.	86
Figure 4.40: Monthly discharge (Mm^3/month) of 6 of the flow monitoring sites from January 2017 to the 4th of September 2017.	87
Figure 4.41: Annual contribution to flows from each of the sub-catchments of the Nuwejaars Catchment from January 2017 to the 4th of September 2017.	88
Figure 4.42: Hourly responses of the monitored tributaries to selected rainfall events during the wet season, from the 28 th April to 30 th April 2016 (A) and from the 9 th June to 13 th June 2016 (B) prior to the major event which occurred between the 25 th and 26 th July 2016 (C).	89

Figure 4.43: Hourly responses of the monitored tributaries to selected rainfall events from mid to the end of the wet season. (A) 18 th August to 27 th August 2016, (B) from the 1 st September to the 4 th September 2016 and (C) from the 16 th September to the 18 th September.	90
Figure 4.44: Daily discharge of the Janswarskraal and the combined Janswarskraal and Koue sub-catchments (measured at the Melkery Bridge) to the cumulative rainfall received in 2016.	91
Figure 4.45: Daily discharge of the Pietersielieskloof tributary and the cumulative rainfall received by the sub-catchment in 2016.	92
Figure 4.46: Daily discharge of the Voëlvelei and Blomkraals tributaries to the cumulative rainfall received by the sub-catchment in 2016.	93
Figure 5.1: Diagrammatic representation of the conceptual model adapted from Schulze and Pike, (2004).	101
Figure 5.2: Diagrammatic representation of the conceptual model adapted from Savenije (2010).	103
Figure 5.3: Drainage network of the Nuwejaars Wetland and the locations at which transects were conducted.	106
Figure 5.4: Transects 1 to 3 of the upper section of the Nuwejaars Wetland.	107
Figure 5.5: Meandering of the Nuwejaars River at the Zoetendal Vineyard. (Source: Google Earth Pro – 05/18/2017).	107
Figure 5.6: Transects 4 to 6 of the middle section of the Nuwejaars Wetland.	108
Figure 5.7: Meandering and oxbow lakes in the middle section of the Nuwejaars Wetland. (Source: Google Earth Pro – 05/18/2017).	108

Figure 5.8: Transects 9 and 10 of the lower section of the Nuwejaars Wetland and transect 11 along the Pietersielieskloof's convergence with the wetland.	109
Figure 5.9: Spatial distribution of pools before (A) and after (B) the major rainfall event that occurred on the 25 th July 2016. Derived using NDWI.	110
Figure 5.10: The spatial distribution of surface soil types across the Nuwejaars Wetland and infiltration rate estimates in mm/day.	111
Figure 5.11: The spatial distribution of sub-surface soil types across the Nuwejaars Wetland and infiltration rate estimates in mm/day.	112
Figure 5.12: Spatial distribution of vegetation in the Nuwejaars Wetland and the locations at which cross-sections and soil samples were collected.	113
Figure 5.13: Variation of electrical conductivity (EC) and pH of river water along the Nuwejaars River and tributaries in June 2016 (A) and July 2016 (B). At each location EC value is separated from pH by “- “.	114
Figure 5.14: Variation of electrical conductivity (EC) and pH of river water along the Nuwejaars River and tributaries in August 2016 (A) and September 2016 (B). At each location EC value is separated from pH by “- “.	116
Figure 5.15: Variation of electrical conductivity (EC) and pH of river water along the Nuwejaars River and tributaries in October 2016 (A) and November 2016 (B). At each location EC value is separated from pH by “- “.	117
Figure 5.16: Average monthly maximum and minimum air temperatures, maximum and minimum relative humidity, wind speed, solar radiation and air pressure measured at the Moddervlei weather station from the 16 th June 2016 to 16 th June 2017.	118
Figure 5.17: Daily rainfall recorded at the Moddervlei station and the daily ET estimated using the Penman-Monteith method from the 16 th June 2016 to the 16 th June 2017.	119

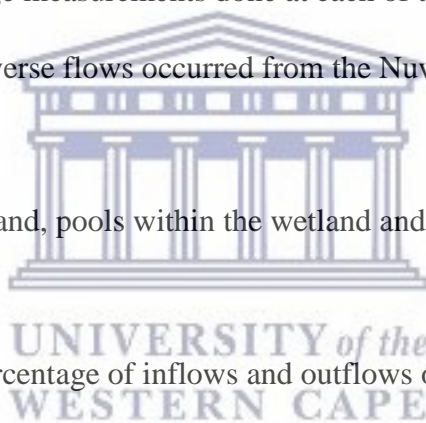
Figure 5.18: Daily water level responses of the Nuwejaars River at the Elim Melkery Bridge (inflow to the wetland) and Elandsdrift (wetland outflow) to rainfall recorded at the Spanjaardskloof station, from the 13 th May 2016 to 2 nd December 2016.	120
Figure 5.19: Average hourly discharge of the Nuwejaars River at the Melkery Bridge (upstream of the wetland) vs the outflow of the wetland at Elandsdrift in response to a selected rainfall event during the early stages of the wet season.	121
Figure 5.20: Average hourly discharge of the Nuwejaars River at the Melkery Bridge (upstream of the wetland) vs the outflow of the wetland at Elandsdrift in response to the major rainfall event on the 25 th July 2016 mid-wet season.	122
Figure 5.21: Average hourly discharge of the Nuwejaars River at the Melkery Bridge (upstream of the wetland) vs the outflow of the wetland at Elandsdrift in response to a selected rainfall event during the end of the wet season.	123
Figure 5.22: Isotopic results of the rainfall water samples (triangles) and river water samples (circles) collected in June 2016.	124
Figure 5.23: Isotopic results of the rainfall water samples (triangles) and river water samples (circles) collected in July 2016.	125
Figure 5.24: Isotopic results of the rainfall water samples (triangles) and river water samples (circles) collected in August 2016.	125
Figure 5.25: Isotopic results of the rainfall water samples (triangles) and river water samples (circles) collected in September 2016.	126
Figure 5.26: The predicted daily discharge at Elandsdrift estimated using the water balance vs the measured daily discharge at Elandsdrift from 17 th June 2016 to the 17 th June 2017.	127
Annexure 1: Rainfall data of each of the sites used for infilling of the rainfall data.	144

Annexure 2: Fabric mesh (A), PVC cap and 14 mm bolt with lock-nut (B), and slits being cut into the 75 mm PVC pipes used as stilling wells (C).	145
Annexure 3: High flows experienced on the 26 th July 2016 during the peak flows at Pietersielieskloof (A), the Melkery Bridge (B) and Jan Swartskraal flow monitoring site (C) which limited the ability of conducting flow measurements.	146
Annexure 4: Internal structure (A), cone and rubber seal (B), table tennis ball inside the cone (C), anti-bird and insect net (D), and the Isotope sampler installed alongside the Tiersfontein weather station (E).	147
Annexure 5: Soil samples being filtered after the organic matter was removed (A), soil samples placed in settling tubes before the 8-hour extraction (B) and the sand portion of the analysis following the removal of silt and clay (C).	148
Annexure 6: Grasses, reeds and <i>Acacia</i> species on the banks of the Nuwejaars River (A), upstream of the Moddervlei weather station (B), Wilde Palmiet upstream of transect 5 (C), downstream of transect 4 (D), and flooding of the wetland on 25 th July 2016 (E).	149



LIST OF TABLES

Table 4.1: Locations of the automatic weathers stations and rain gauges in the Nuwejaars Catchment established by the University of the Western Cape.	43
Table 4.2: Equations used to infill missing rainfall data.	44
Table 4.3: Number of dry and wet days for each of the rainfall stations of Nuwejaars catchment for 2015, 2016 and 2017.	51
Table 4.4: Locations, altitude, logger types, presence of gauge plates and the starting date of the flow monitoring sites.	62
Table 4.5: Number of discharge measurements done at each of the flow monitoring sites.	75
Table 4.6: Occasions when reverse flows occurred from the Nuwejaars River into Voëlvlei.	77
Table 5.1: Volume of the wetland, pools within the wetland and the amount of water required to fill the pools.	110
Table 5.2: The volume and percentage of inflows and outflows of the Nuwejaars Wetland and the measured vs predicted outflow from the 17 th June 2016 to 17 th June 2017.	127



LIST OF SYMBOLS

Symbol	Parameter Description	Unit
q_n	Discharge of the segment	m^3s^{-1}
v_1	Mean velocity at the first vertical	m/s
v_2	Mean velocity at the second vertical	m/s
d_1 and d_2	Total depths at verticals 1 and 2	m
b	Horizontal distance between the verticals	m
Q	Total discharge of the stream or cross-section	m^3/s
V	Cross-sectional velocity	m/s
A	Area	m^2
n	Manning's roughness coefficient	
R	Hydraulic radius	m
S	Channel slope	$^\circ$
Et_0	Reference ET rate	$mm.d^{-1}$
R_n	Net radiation	$MJ.m^{-2}.d^{-1}$
G	Soil heat flux density	$MJ.m^{-2}.d^{-1}$
T	Mean daily air temperature	$^\circ C$
u_2	Wind speed at 2m	$m.s^{-1}$
e_s	Saturation vapour pressure	kPa
e_a	Actual vapour pressure	kPa
$e_s - e_a$	Saturation vapour pressure deficit	kPa
Δ	Slope of saturation vapour curve	$kPa\ ^\circ C^{-1}$
γ	Psychometric constant	$kPa\ ^\circ C^{-1}$
ΔS	Change in wetland storage	m^3/day
$I(t)$	Inflows	m^3/s
$O(t)$	Outflows	m^3/s
t	Time	s
P	Precipitation	mm
GW_D	Groundwater discharge	m^3/s
GW_R	Groundwater recharge	m^3/s
Q_{in}	Surface water inflow	m^3/s

Q_{out}	Wetland outflows	m^3/s
S_{max}	Max storage of wetland before overland flow	m^3 .
S_{min}	Min storage required in wetland for discharge to occur downstream of the wetland	m^3 .
D_w	Interception threshold for P	m^3
Symbol	Parameter Description	Unit
WP	standard subsurface storage always present in the wetland	m^3/day
$Q_{sim}(t)$	Predicted outflow or simulated discharge	m^3/day
$Q_{sof}(t)$	Saturation excess overland flows	m^3/day
$(Q_{sub}(t))$	Subsurface flow	m^3/day
C_w	Runoff coefficient	
$P_e(t)$	Effective rainfall	m^3/day
$P(t)$	Rainfall	m^3/day
$S(t)$	Storage of the subsurface reservoir	m^3
$Q_{obs}(t)$	Observed discharge	m^3/day
$Q_{sim}(t)$	Simulated flow	m^3/day



LIST OF ACRONYMS

RMSE	Root Mean Square Error
IAHS	International Association of Hydrological Sciences
PUB	Prediction in Ungauged Basins
IWRM	Integrated Water Resource Management
ET	Evapotranspiration
NDWI	Normalized Difference Water Index
SANBI	South African National Biodiversity Institute
DWA	Department of Water Affairs
NFEPA	National Freshwater Ecosystems Priority Areas
NGI	Chief Directorate of National Geo-Spatial Information, South Africa
DGPS	Differential Global Positioning System
EWWTTP	Elim Waste Water Treatment Plant



1. INTRODUCTION

1.1 Background

Water resources planning and management are an integral part of mankind's survival. It is therefore imperative that the physical processes governing water resources are well understood. Understanding river flows or runoff may be the most important process thereof, as it is one of the key sources of water for domestic and commercial uses. River flow data provide the foundation for water resources management as they provide information on the quantity and spatial and temporal variability of water resources. The collection and analysis of river flow data are therefore critical aspects of water resources management.

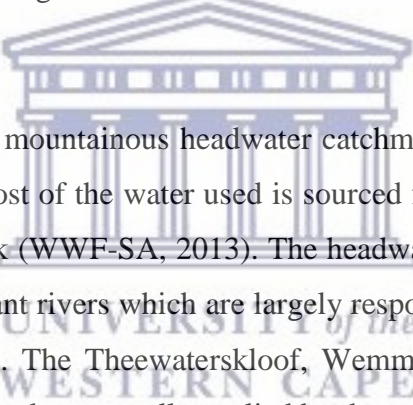
About a decade ago, the International Association of Hydrological Sciences (IAHS) launched a global scientific initiative known as Prediction in Ungauged Basins (PUB) (Blöschl *et al.*, 2013). Blöschl *et al.* (2013) noted that PUB was a global issue as most catchments around the world are ungauged, meaning that they have inadequate or no hydrological data. As PUB is directly linked to flood predictions it is a great asset to disaster risk management and may aid in preventing the adverse effects of large floods such as the major flood which struck Mozambique, leaving 50 000 people removed from their homes in 2007 (Blöschl *et al.*, 2013).

Flood predictions do not only aid in disaster risk management but also for reservoir management, flow routing and river restoration amongst others (Blöschl *et al.*, 2013). On the other hand, low flow predictions are essential for determining the ecological flow requirements, drought preparedness, river restoration, and Integrated Water Resource Management (IWRM) (Blöschl *et al.*, 2013). Additionally, runoff prediction as part of the IWRM and risk management approach aids in determining how much water is available, when the water will be available, for how long the water will be available and the magnitude and duration of a flood.

Blöschl *et al.* (2013), and Tanner & Hughes (2015) reported that there were no universally accepted methods for runoff prediction at a catchment scale. This was attributed to the fact that

catchments are for the most part heterogeneous and it is therefore easy to study them in isolation rather than holistically. Therein lies the problem, as studies are isolated to individual catchments, models are developed and analysed based on the parameters being studied and the inputs being used. Furthermore, Blöschl *et al.* (2013), and McCartney, *et al.* (2013) noted that each catchment acts as an organism susceptible to and shaped by its environment (climate) and the processes which form it. These include runoff generation, evapotranspiration (ET), climatic factors, and the factors which control these processes.

Improved knowledge is required about the quantity and source of water resources available in South Africa. This is particularly evident during periods of drought, which result in water use restrictions. It is therefore imperative that ungauged catchments such as the Heuningnes Catchment in the Cape Agulhas have well established flow monitoring programmes as part of water resource planning and management activities.



South Africa is home to many mountainous headwater catchments. These are evident in the Western Cape region where most of the water used is sourced from the mountainous regions of Boland and Grootwinterhoek (WWF-SA, 2013). The headwaters of these areas supply the Breede, Berg, Doring and Olifant rivers which are largely responsible for the supply of water in the Western Cape Province. The Theewaterskloof, Wemmershoek, Voëlvlei, upper and lower Steenbras, and Berg River dams are all supplied by these mountainous regions.

These mountainous regions are protected as priority areas for water supply and no development of any kind is allowed in these areas. River flows in mountainous areas have high water quality due to a lack of contamination from urban and farming areas. However, urbanization, farming and industrial developments which occur along these rivers, further downstream may be a particular concern for water quality.

The hydrology of mountainous regions is susceptible to highly variable precipitation and water movement through and over steep landscapes. Weathered or fractured rock types underlying soil and macropores resulting from decaying roots and burrowing animals have the ability to

transmit subsurface flow downslope rapidly. In certain cases, this may result in the formation of hillside springs (Schulze, 2011; Blöschl *et al.*, 2013). During dry seasons or periods, flows may be sustained by discharge from groundwater systems. In some cases, during the wet season or periods, soils on the hillslope are saturated quickly and water reaches streams rapidly by means of overland flow. At the foot of hillslopes, the water table may rise to the surface resulting in overland flow. If precipitation continues over the saturated area this may lead to continued overland flow further down the catchment (flooding). This phenomenon is particularly noticeable in arid and semi-arid regions where overland flow is generated when the infiltration capacity of the soil is exceeded by the rate of rainfall (Schulze, 2011; Blöschl *et al.*, 2013).

In some cases, at or near foothills, the water table is intersected by a steep valley wall, which may result in an almost constant discharge of groundwater and in some cases the formation of wetlands. A more common process resulting in wetland formation at the base of foothills results from the discharge of groundwater or high water table in the flatter areas which saturates the soil. This discharge is the result of the change in slope or head from the steep mountainside to the flatter floodplain area. Additionally, ponding and flooding in floodplains with thick clayey soils with low infiltration rates may hold moisture and therefore result in the formation of wetlands.



Wetlands affect runoff generation, ET, habitats and contaminant control. The effects of wetlands on river flows are not well understood. Many studies have shown that wetlands may contribute to flood attenuation, while others have shown that wetlands may increase river flows (McCartney, *et al.*, 2013). Kotzé (2000), and Cleaver and Brown (2005) noted that wetlands are usually gently sloping and river flows spread through the wetland by means of diffuse flow, lowering the velocity of the flow and therefore the discharge of the river. Additionally, wetlands are in most cases highly vegetated and therefore increase flood attenuation by decreasing flow velocities. McCartney, *et al.* (2013) found through a review of literature that in 30 out of 66 studies wetlands located in headwaters drastically reduced flood peaks. However, 27 out of 66 studies showed that flood peaks were increased. Additionally, McCartney, *et al.* (2013) reported that most studies (65%) showed that wetlands increased average ET, thus reducing annual river flows. On the other hand, 10% of studies showed the

opposite, while 25% of the studies showed no significant results (McCartney, *et al.*, 2013). Kotzé (2000) and McCartney, *et al.* (2013), noted that biophysical factors such as flow regime; wetland shape, size and location within the catchment, topography, geology, climate, soil properties and vegetation all need to be considered when assessing the effects of wetlands on flow.

Bullock and McCartney (1996) examined the river flow maintenance by wetlands in Zimbabwe. Prior to this period, it was believed that wetlands aided in the maintenance of dry season flows. The perceived idea of wetlands sustaining dry season flows resulted in legislation in Zimbabwe such as the Water Resources Act of 1927 and the Natural Resources Act of 1952 protecting wetlands from being used for agricultural purposes. Bullock and McCartney (1996) by means of a conceptual water balance analysis and flow measurements found that wetlands did not maintain dry season flows, however it was noted that this was highly dependent on the presence of vegetation. These results were further substantiated by McCartney, *et al.* (2013). Bullock and McCartney (1996) concluded that the water retention characteristics of wetlands depended on soil texture and any impermeable underlying rock or clay layer. Bullock and McCartney (1996) noted that there was a lack of detailed water balance investigations of small catchments and that these studies may improve the understanding of these processes and the contributions of wetlands to downstream flows.

Cleaver and Brown (2005) noted that the low gradients of the Agulhas Plain resulted in the formation of several wetlands. Kraaij *et al.* (2009) reported that freshwater supplies in the Agulhas Region were available to meet human demands in 2009. However, the demand for freshwater exceeded the supply during the drier summer season. Intensive cultivation of grapes and deciduous fruits, water abstraction, alterations of drainage patterns (i.e. roads, canalization, ploughing), and the spread of woody alien vegetation posed a particular threat to the ecological integrity and water resources of the Heuningnes Catchment (Rowntree, 1991; King *et al.*, 2003; Kraaij *et al.*, 2009; Kotzé *et al.*, 2010). Cleaver & Brown (2005) noted that the draining of wetlands for various land uses, channelization of tributaries, damming of water and over-abstraction of water pose potential threats to the water supply within the Heuningnes Catchment.

Improved knowledge is required on the effects of wetlands in regulating high flows and sustaining dry season flows for management and planning purposes in the Agulhas region. Furthermore, improved knowledge is required on the importance of the contribution of mountainous catchments to dry and wet season flows.

1.2 Problem Statement

There inadequate knowledge with regards to the flood attenuation properties of wetlands, particularly in the ungauged catchments of Southern Africa. Kraaij *et al.* (2009) noted that the tributaries and wetlands along the Nuwejaars River are important in controlling the volume and quality of water which flows through the Nuwejaars River. The main tributaries of the Nuwejaars River include Pietersielieskloof River, Koue River and Jan Swartskraal River. However, the contribution of flow from each of these tributaries is not well understood. Bickerton (1984) reported that many developments occur within the 1 in 50-year flood range in the Agulhas Plain and therefore are in danger if such a flood were to occur. These dangers include loss of cattle, crops and impact adversely on livelihoods. It is therefore imperative to understand the contributions of flow from each of these tributaries for planning and management of water resources. Furthermore, improved knowledge is required about the effects of the wetlands on the flows of the Nuwejaars River.



1.3 Research Question and Hypothesis

Does the presence of a flood-plain wetland reduce the magnitude of river flows and increase the travel times of flows from the hillslopes to lower-lying areas?

It was hypothesized that the presence of a flood-plain wetland would decrease the magnitude of river flows (Q) and increase the travel time of floods from the hillslopes to the lower-lying areas.

1.4 Aim and Objectives

This study aims to improve the knowledge on the contribution of flow from tributaries with headwaters in mountainous regions to low lying areas and the effects of wetlands on river flow patterns. The objectives thereof are:

- 1- To determine the nature of the hydrological responses of catchments with headwaters in mountainous regions.

- 2- To assess the influence of flood-plain wetlands on river flows.

1.5 Thesis outline

The thesis is structured as follows, Chapter 2 provides a review of the relevant literature about the flood attenuation of wetlands and how it is assessed and modelled. Chapter 3 provides a brief look at the study area, including climate, geology, vegetation and land uses. Chapter 4 is focused on the hydrological responses of the Nuwejaars Catchment to rainfall events and further discusses the hydrological functions of the catchment. Chapter 5 is solely focused on the observed influences of the Nuwejaars wetland on the flows of the Nuwejaars River and attempts to predict the effects of the wetland on the Nuwejaars River flows using the Flex-topo model. Chapter 6 is the concluding chapter, including the limitations and recommendations for further studies.

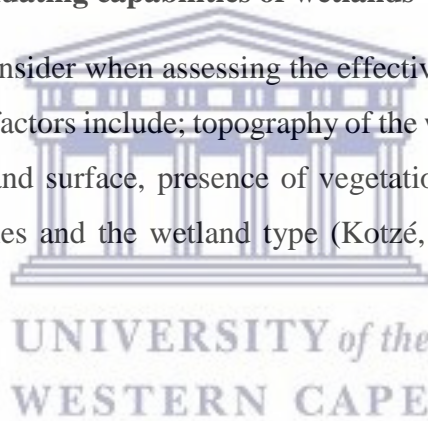
2. LITERATURE REVIEW

2.1. Introduction

Knighton (1984), Morisawa (1985) and Stroosnijder (1992) stated that runoff is related to the discharge, velocity and transport capacity of the river flow. The stream velocity and transport capacity are determined by relief, soil properties and the source of water. The presence of wetlands is dependent on these factors and therefore influences the flow regime of streams. This section reviews the literature on the flood attenuating capabilities of wetlands. Additionally, it summarises the factors to be consider when analysing the flood attenuating capabilities of wetlands and reviews literature on the methods used to assess the flood attenuating capabilities of wetlands.

2.2. Assessing the flood attenuating capabilities of wetlands

There are several factors to consider when assessing the effectiveness of the flood attenuating properties of wetlands. These factors include; topography of the wetland, wetland size, wetland shape, roughness of the wetland surface, presence of vegetation, location in the catchment, flow regime, the soil properties and the wetland type (Kotzé, 2000 and McCartney, *et al.*, 2013).



2.2.1 Wetland Topography

The topography of the wetland includes the slope, landform features (channels or depressions) and the nature of the wetland outlet. Kotzé (2000) reported that wetlands with constricted outlets have a higher flood attenuation potential than that of unconstructed outlets. Additionally, Kotzé (2000) and McCartney, *et al.*, (2013) noted that the gentler the slope of the wetland the greater its flood attenuating abilities will be. This includes the slope of the floodplain and the channels present within the wetland. Additionally, depressions or landform features such as oxbow lakes and pools may add to the flood storage capacity of wetlands and therefore increase flood attenuation potential.

There are two methods used to determine the topography of a wetland or area. The Normalized Difference Water Index (NDWI) is a method which uses remotely sensed data to detect surface

waters in wetland environments and to determine the spatial extent of areas with water. It was first proposed by McFeeters (1996). The index was initially created for use with Landsat Multispectral Scanner (MSS) image data. However, it has been successfully used with other sensor systems (McFeeters, 2013; Doña, *et. al.*, 2016). The recently launched Sentinel-2 satellite provides fine spatial resolution multispectral images with a spectral resolution of 10 m. This new dataset is free and has a frequent revisit time. The Normalized Difference Water Index (NDWI) is calculated from the green (band 3) and band 8 which is the Near-Infrared (NIR) band (Equation 2.1) and is one of the most popular methods used to identify water bodies today (Du, *et. al.*, 2016).

$$NDWI = \frac{\rho_{Green} - \rho_{NIR}}{\rho_{Green} + \rho_{NIR}} \quad (2.1)$$

where: ρ_{Green} = reflectance value of the green band

ρ_{NIR} = reflectance value of the NIR band

The main limitation of the NDWI is that it does not suppress the signal of land cover features in built up areas (Du, *et. al.*, 2016). However, in an area such as the Nuwejaars Catchment where there is very little to no built up areas this effect is limited and the NDWI can therefore be used at a 10 m resolution at a sub-catchment scale (Doña, *et. al.*, 2016; Du, *et. al.*, 2016). In addition, the use of satellite imagery is subject to errors resulting from climatic conditions, human error or technical failure. Huang *et al.* (2001), Cleaver & Brown (2005), Azizi, *et al.* (2008), Wu (2002) and Kotzé *et al.* (2010) emphasize the importance of ground truthing when using satellite derived data. It is imperative that the results obtained are validated by field verification.

2.2.2. Wetland Shape, Size and Location

Kotzé (2000), noted that a large wetland area provides a great area for flood storage and reduction in velocity and therefore increasing the flood attenuation potential of the wetland. However, this is provided that other factors such as the flow regime and slope of the wetland

remain constant. Kotzé (2000) noted that the wetland shape, specifically length parallel to flow is more effective than width in increasing the flood attenuation potential of a wetland. Additionally, Bullock and McCartney (1996), Kotzé (2000) and McCartney *et al.* (2013) noted the importance of the wetlands location within the catchment and its effect on flood attenuation capabilities, as wetlands located in the upper parts of the catchment were less effective in flood attenuation than those in the lower parts.

Kotzé (2000) noted that headwater wetlands when compared to downstream wetlands tend to be more susceptible to degradation due to steep slopes. However, it is important to analyse wetlands at a catchment scale. This is due to the fact that wetlands are interlinked on a catchment scale and therefore have a collective effect on flood attenuation. This being said, headwater wetlands when studied in isolation may produce inaccurate conclusions and it is imperative that these wetlands are studied collectively (Kotzé, 2000 and Blöschl *et al.*, 2013). Additionally, Kotzé (2000) noted that headwater wetlands by reducing storm flows reduce the potential erosion of downstream wetlands and therefore improve the possibility of the establishment of vegetation in downstream wetlands.

2.2.3. Vegetation

Vegetation is one of the key factors affecting soil erosion. It has the ability to slow overland flow, increase the critical shear stress of the soil by binding soil particles, stabilize banks and reduce surface scour (Rowntree, 1991; Wynn & Mostaghimi, 2006 and Gholami & Khaleghi, 2013). McCartney *et al.* (2013) noted that the presence of vegetation within the wetlands increased the ET. However, this depends on the type of vegetation present within the wetland.

The roughness of the wetland surface is determined largely by the nature of the vegetation present within the wetland (Kotzé 2000). The effect of vegetation on surface roughness relies mainly on the nature of vegetation. This differs in floating aquatics, rooted aquatics, herbaceous vegetation and woody vegetation. Research by Rowntree (1991), Wynn & Mostaghimi (2006), Holmes *et al.* (2008) and Gholami & Khaleghi (2013) showed that herbaceous vegetation and grasses have shallow but denser rooting systems which provide a good surface cover and therefore was most effective at protecting against surface scour. On the other hand, woody trees

were associated with a lower surface cover but deeper rooting systems which allowed for a more efficient stabilization and cohesion of bank material. Kotzé (2000) noted that tall robust or woody vegetation (characteristic of many wetlands) offers more frictional resistance than that of softer vegetation, therefore contributing to the hydraulic resistance of wetlands. Furthermore, Kotzé (2000) stated that the effectiveness of the flood attenuating capabilities of vegetation is closely related to its effectiveness in sediment trapping as both have the ability to reduce flow velocities.

There are two commonly used methods to map the distribution of vegetation in an area. The first being remotely sensed methods and field based surveys. Azizi *et al.* (2008) reported that remote sensing has proven to be the most cost effective method of mapping and monitoring environmental changes, specifically in terms of vegetation. Particularly in the 21st Century, technological improvements have motivated the use of digitally based methods such as the use of remote sensing. LANDSAT 7 ETM+ and Lidar imagery are commonly used satellite imagery in mapping the distribution of vegetation over large areas.

Huang *et al.* (2001), Wu (2002), Azizi *et al.* (2008) and Dilts *et al.* (2010) made use of high resolution satellite imagery to map the distribution of vegetation over large areas. Using vegetation indices such as the Normalized Differential Vegetation Index (NDVI) in conjunction with a Bare Soil Index and Shadow Index, Azizi *et al.* (2008) were able to evaluate the effectiveness of remote sensing imagery to predict forest canopy cover. Huang *et al.* (2001) and Wu (2002) reported that although these methods proved effective, images are highly dependent on climatic conditions. Images may be affected by cloud cover, deciduous trees being incorrectly classified as they shed their leaves in autumn or a lower elevation angle of the sun could affect results during seasonal changes. However, Huang *et al.* (2001) and Dilts *et al.* (2010) recommended that high resolution images provide an accurate representation of the real world.

Huang *et al.* (2001) and Dilts *et al.* (2010) reported that although remote sensing methods are effective, vegetation mapping mainly rely on field based surveys which estimate the distribution of plant communities along transects perpendicular to the river. However, this

method is not cost effective and highly time consuming over large areas. Cleaver (2005) and Kotzé *et al.* (2010) used similar methods in which a helicopter was used to map the distribution of woody alien vegetation. The latter study however mapped the distributions of South Africa, Swaziland and Lesotho, while the study by Cleaver & Brown (2005) was conducted within the Heuningnes Catchment.

2.2.4. Soil Properties

Soil erodibility refers to the degree to which soil material can be detached and transported by the influence of a force. Soil erodibility is controlled by particle size, aggregate stability, critical shear stress, soil moisture and soil fertility (Knighton, 1984; Morisawa, 1985; Piegay *et al.*, 1997; Bartley *et al.*, 2006; Zaines *et al.*, 2006; Tal & Paola, 2010; Sang *et al.*, 2015). For example, a fine sandy soil with a particle size of 0.064 mm would be more vulnerable to erosion than a coarser sand of 2 mm. Additionally, the particle size is related to the stability of the soil; the more stable the soil the less vulnerable it is to erosion. Furthermore, the higher the critical shear stress of the soil the less vulnerable it is to erosion.

Although there are several methods used to determine soil types, one of the most common methods used to date is the settling tube method (Tennessee Valley Authority, *et al.*, 1941). The settling tube method relies on Stokes Law of falling particle velocities in liquid, in order to separate the fine sediments of sand, silt and clay. The foundation of Stokes Law is built on the falling of sediments in a liquid medium and allows the sediment to remain in a near natural state (Tennessee Valley Authority, *et al.*, 1941). This method has been around for decades and is still one of the most commonly used methods as it is cost effective and time efficient.

2.2.5. Flow regime

Kotzé (2000) noted that the potential for a wetland to attenuate floods relies on the flow regime. For example, provided that other factors are constant, a seasonally or temporarily flooded wetland would have a greater flood attenuating capability than that of a permanently wetted wetland. Wetlands fed by groundwater sources tend to be perennial and therefore have lower flood attenuating capabilities. On the other hand, seasonally or temporarily wetted wetlands

are fed by surface water flows from non-perennial streams or direct precipitation and ponding and therefore may have higher flood attenuating capabilities.

2.2.6. Wetland classification

The wetland classification system developed for SANBI (South African National Biodiversity Institute) was formally known as the National Wetland Classification. That name has now changed to a Classification System for Wetlands and other Aquatic Ecosystems in South Africa (Ollis *et al.*, 2013). Ollis *et al.*, (2013) noted that a wetland is defined as “an ecosystem that is permanently or periodically inundated by flowing or standing water, or which has soils that are permanently or periodically saturated within 0.5 m of the soil surface”. The classification system has six levels used to classify wetlands.

At level 1, wetlands are classified into three broad groups, inland systems, estuarine systems and marine systems. Firstly, inland systems are defined as aquatic ecosystems with no existing connection to the ocean. They are characterized by the lack of tidal influence and or absence of marine exchange. Secondly, an estuarine system is defined as body of surface water that is part of a water course, that is permanently or periodically open to the sea; in which a rise and fall of the water level as a result of the tides is measurable at spring tides when the water course is open to the sea; or in respect of which the salinity is measurably higher as a result of the influence of the sea. Lastly, marine systems are defined as that part of the open ocean overlying the continental shelf and/ or its associated coastline, up to a depth of ten metres at low tide (Ollis *et al.*, 2013).

Level 2 inland systems are classified based on their regional setting. Here the regional setting is either based on the spatial framework of the Department of Water Affairs (DWA) Ecoregions, National Freshwater Ecosystems Priority Areas (NFEPA) (Ollis *et al.*, 2013) or another spatial framework reference. These spatial frameworks use regional characteristics such as vegetation types or biomes to classify areas. Ollis *et al.*, (2013) noted that for the classification of aquatic ecosystems in the context of water resource management, the DWA Ecoregions is more effective while the NFEPA is more appropriate for fine-scale wetland conservation planning.

Level 3, classifies the inland system based on its landscape setting or units. Within this level the four categories are valley floor, slope, plain and bench. The Agulhas Plain is an example of an inland system located on a plain. At level 4, the hydrogeomorphic (HGM) units are identified. These are based on the landform, which defines the shape and localized setting of the wetland, the hydrological characteristics which describe the nature of water movement through the system and the hydrodynamics which describe the direction and strength of flow through the aquatic ecosystem (Ollis *et al.*, 2013). At this level inland systems are further classified into rivers, floodplain wetlands, valley-bottom wetlands, depressions, seeps and wetland flats.

Although the HGM unit is influenced by the source water, the hydrological regime at level 5 of the classification system describes the behaviour of water within the system as well as the soils. Here the river flow types, hydroperiod and depth of inundation are considered.

Finally, at level 6 descriptors are used to further classify inland systems or wetlands. The descriptors rely on the structural, chemical and biological characterization of inland systems. The descriptors have no hierarchy but can be applied in order based on the purpose and availability of information. The factors in broad terms that are considered are whether the inland system is natural or artificial, salinity and pH of the water, the substratum type, vegetation cover and the geology or lithology of the system.

2.3. Use of models to predict the influence of wetlands on flow

Williams, *et al.* (2012) noted that flood attenuation estimates should be conducted by means of continuous hydrological modelling which considers local factors. The spatial and temporal variations of soil moisture and precipitation, storage capacity, outflow rate, flood route and past and present disturbances need to be considered as they influence the hydrological processes of individual wetlands (Williams, *et al.*, 2012). Where there is high quality hydrologic data covering long periods these flow estimations are easy to model. However, in reality most catchments are ungauged and have limited or no hydrological data (Vaze *et al.*, 2012 and Blöschl *et al.*, 2013).

Rainfall-runoff models can be used to estimate flows for ungauged periods. These models are also used for forecasting and assessing the impacts of human influence and climate variability on flows. The two types of approaches used to predict the influence of wetlands on flow are lumped/black-box type models and physically distributed models.

2.3.1. Lumped models

The foundation of every hydrological model is based on a simple water balance (Williams, *et al.*, 2012). Lumped models simply consider the change in storage associated with inflows and outflows and do not have a spatial representation of the processes involved. Lumped models can also be considered “semi-distributed” as they can be divided into a number of sub-basins in which hydrological parameters may differ. However, they are not considered physically based because the physical processes are not explicitly represented (Williams, *et al.*, 2012; Asadi, 2013; Brirhet & Benaabidate, 2016).

Williams, *et al.*, (2012) noted that flood attenuation is achieved when there is a notable change in flood peak and or a delay in flood peaks between inflow and outflow. The water balance of a wetland allows one to estimate the storage capacity of the wetland based on the inputs to and outputs of a wetland. By comparing hydrographs at the inflow and outflow of the wetland the lag time between peak flows can be determined (Bullock and McCartney, 1996; Williams, *et al.*, 2012 and McCartney *et al.*, 2013). Therefore, a delay in flood peaks between the inflow and outflow of the wetland provides insight into the flood attenuating capabilities of the wetland. This is a simple and cost effective method, however the delay in flood peaks cannot only be attributed to the wetland itself but other factors such as evapotranspiration, drainage, groundwater recharge and overland flow need to be considered (Bullock and McCartney, 1996; Williams, *et al.*, 2012 and McCartney *et al.*, 2013). In addition, this method is only applicable if the floodplain is small compared to the gauged catchment (McCartney, *et al.*, 2013).

An example of a lumped or conceptual model is the FLEX-topo model proposed by Savenije, *et al.* (2010). The FLEX-topo model divides the catchment into three different parts based on topography and each part has its own conceptual model and parameters that are considered. The topographic parts are the plateau, hillslope and wetland (Savenije, *et al.*, 2010). The FLEX-topo model is adaptable and can be calibrated and altered to represent various catchments. Due

to its adaptability and short data requirements a conceptual model such as the FLEX-topo model is ideal for modelling a wetland such as the Nuwejaars Wetland where there is very little to no hydrological data as it can perform effectively and adequately with limited data over a short period of time.

McCartney, *et al.*, (2013) recommended an alternate method for assessing the flood attenuating capabilities of wetlands. This approach simulates the time series of flow that may have occurred in the absence of an upstream wetland and is dependent on the analysis of flow within various locations of the catchment. The method is based on an analysis of flow duration curves (FDC's) which represents the relationship between any given discharge and the percentage of time that flow is equalled or exceeded (McCartney, *et al.*, 2013). FDC's are developed by dividing all daily flows by the long term mean annual discharge and all the flows are then represented as a ratio of the long term mean. These discharges are then compared in the absence and presence of the wetland. The study by McCartney, *et al.*, (2013) proved this method to be effective, and it was found that different wetlands affect flow regimes in different ways.

2.3.2. Physically distributed models

Physically based hydrological models are based on the hydrological processes which control catchment responses and use physically based equations to describe these processes. These models allow for quantification of individual catchment processes within discrete grids for the entire catchment and can be highly accurate. An example would be the SWAT model, which is a continuous event based hydrological model that is used in GIS. This model predicts stream flow in watersheds with wetlands by means of 9 parameters and requires extensive long term hydrological data. The SWAT model performs well for long term predictions and is commonly used in the agricultural sector (Brauer *et al.*, 2014; Ameli & Creed, 2017). However, it is prone to errors, data hungry and requires large sets of spatial and temporal data. It is very time consuming to calibrate and not ideal for a catchment with little to no hydrological data.

2.4. Summary

There are 5 key factors that need to be considered when analysing the effect of wetlands on river flows. These factors are the topography, shape, size and location, vegetation, soil properties and flow regime of the wetland. These factors all play an integral role in the flood attenuating capabilities of the wetland.

There have been several studies conducted assessing the flood attenuating capabilities of wetlands. However, the results of these studies vary. Many studies support the notion that wetlands contribute to flood attenuation, while others show the opposite. The major issue in Southern Africa is that most catchments are ungauged and therefore have very poor or inadequate hydrological data.

The lack of hydrological data is a driving force behind hydrological modelling. In order to predict or estimate hydrological responses of catchments for planning and management of water resources. As most of these catchments are ungauged one cannot rely on complex physically distributed models such as SWAT. Although these models are capable of quantifying individual catchment processes they are data hungry, complex and time consuming and are therefore not ideal for an ungauged catchment.

For this study a simpler, lumped or conceptual model is ideal as it requires much less hydrological data and is based on simple water balance equations. In addition, these models are easier to calibrate and therefore make them more suited to modelling ungauged catchments, with very little to no hydrological data. The FLEX-topo model proposed by Savenije, *et al.* (2010) is adaptable and can be altered to suite various catchments and was therefore ideal for this study.

3. STUDY AREA

3.1. Introduction

The Nuwejaars River is located in the Agulhas Plain which is approximately 150 km east of Cape Town (Figure 3.1). This river originates north east of Elim and flows down to Soetendalsvlei east of the Agulhas National Park. The main upper tributaries of the Nuwejaars River include the Pietersielieskloof River, Koue River and Jan Swartskraal River (Figure 3.1). The rivers in the northern parts of the catchment have headwaters in mountainous regions. These are followed by wetlands which occur throughout the lowlands of the catchment (Figures 3.1). The Nuwejaars Wetland is formed at the convergence of these tributaries and is the focus of this study (Figure 3.1).

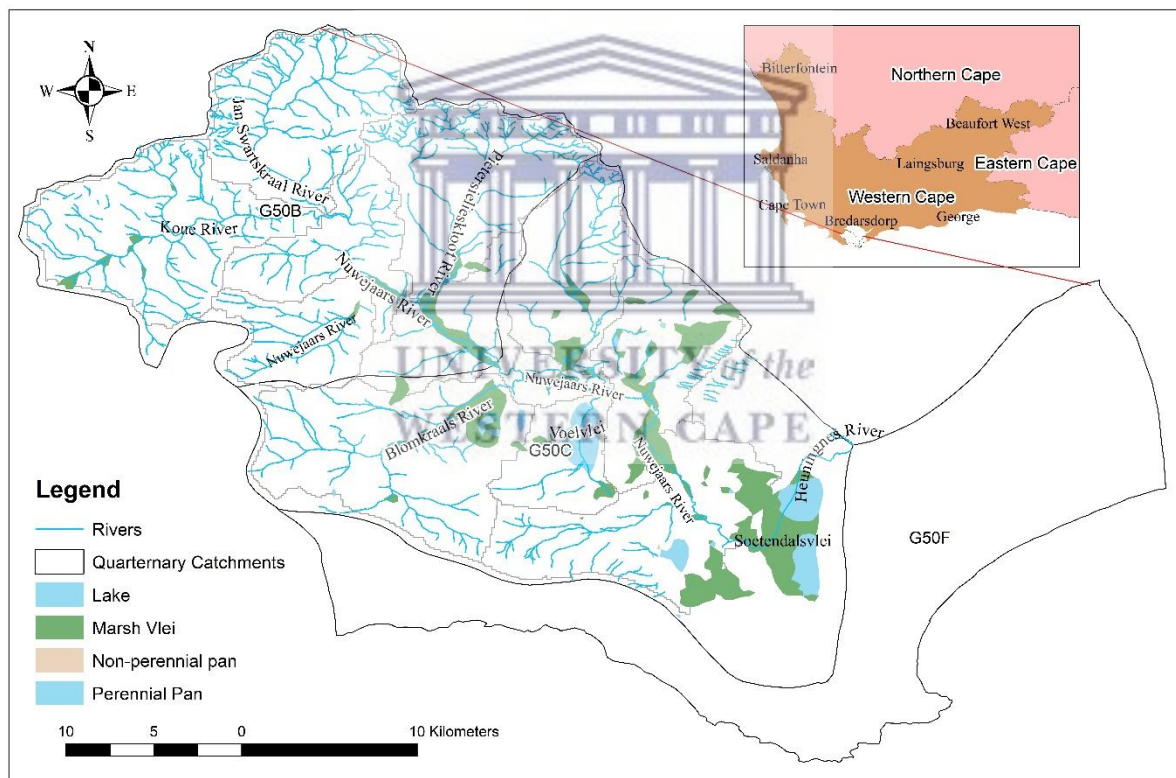
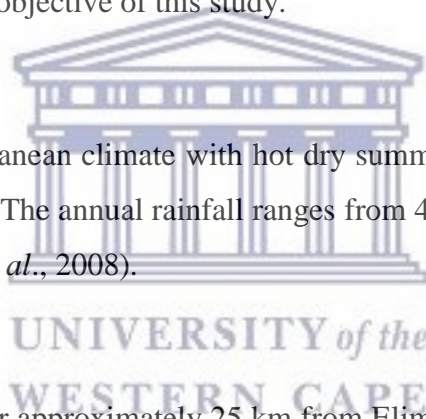


Figure 3.1: Location of the Nuwejaars River and its tributaries (Source: Chief Directorate of National Geographic Information Surveys and Mapping, Private Bag X10, Mowbray).

The transition from the mountainous headwater regions to the lowlands in the Nuwejaars Catchment makes it an ideal case study to address the first objective of the study. In addition, river flow monitoring sites and weather stations were established prior to this study. The maintaining and improvement of the already established monitoring system would help improve knowledge on the ungauged catchment.

Previous studies showed that the longitudinal length of a wetland was more important in flood attenuation than the width of the wetland (Kotzé, 2000). The Nuwejaars Wetland is 8.5 km in length and 0.9 km in width at its widest point. In addition, the wetland is formed at the confluence of most of the tributaries of the Nuwejaars Catchment and therefore provides a better understanding of the flows contributed by each of the tributaries. Furthermore, the Nuwejaars Wetland was previously classified as a floodplain wetland and therefore is an ideal case study to meet the second objective of this study.

The study area has a Mediterranean climate with hot dry summers and with 60 % – 75 % of precipitation falling in winter. The annual rainfall ranges from 445 mm/year in the east to 540 mm/year in the west (Kraaij *et al.*, 2008).



The Nuwejaars River flows for approximately 25 km from Elim into Soetendalsvlei, which is the second largest lacustrine wetland in South Africa (Figure 3.1). The flows exit Soetendalsvlei via the Heuningnes River to Die Mond estuary. The Voëlvlei and Waskraals wetlands are linked to the Nuwejaars River (Figure 3.1).

The Jan Swartskraal River is 18.3 km in length from its source at an elevation of 534 m to the confluence with the Koue River at 50 m. The average slope of the river is 3.9° with a maximum of 30.8° in the mountainous region (Figure 3.1). The Koue River is 18.9 km in length from its source at an elevation of 327 m to 50 m at the confluence with the Jan Swartskraal River. The average slope is 2.4°, with a maximum of 20.7° in the mountainous region (Figure 3.1). The Pietersielieskloof River is 14.7 km long and has an elevation of 365 m at its source and 27 m at its confluence with the Nuwejaars River. The average slope along this river is 2.9° with a

maximum of 27.5° in the mountainous region (Figure 3.1). The Nuwejaars Wetland is formed at the confluence of the Jan Swartskraal, Koue and Pietersielieskloof Rivers.

The Voëlvlei tributary is 9.7 km long from its source at an elevation at 124 m to its lowest point of 12 m. The maximum slope is 5.6° in the undulating plains, while the average slope of the stream is 1.9° (Figure 3.1). The Blomkraals River is 17.3 km from its source at an elevation of 104 m to the lowest elevation at 15 m at the flow measuring site. The average slope of the river is 5.1° and the maximum slope was 8.2° (Figure 3.1).

3.2. Geology

The coastal mountains of the Nuwejaars Catchment are Cape Fold Belt sandstone, capped in sections by limestone (Figure 3.2). The foothills of these mountains are followed by undulating plains, largely comprising Bokkeveld shale, which together with Cape Fold Belt sandstone form part of the Cape Supergroup (Bickerton, 1984; Kraaij *et al.*, 2009). The area is largely underlain by Palaeozoic sediments of the Cape Supergroup and Sandstones, and the low mountains and coastal ridges comprise quartzite of the Table Mountain Group (Figure 3.2). Soils derived from these rocks are highly acidic and therefore tend to be infertile in most cases.



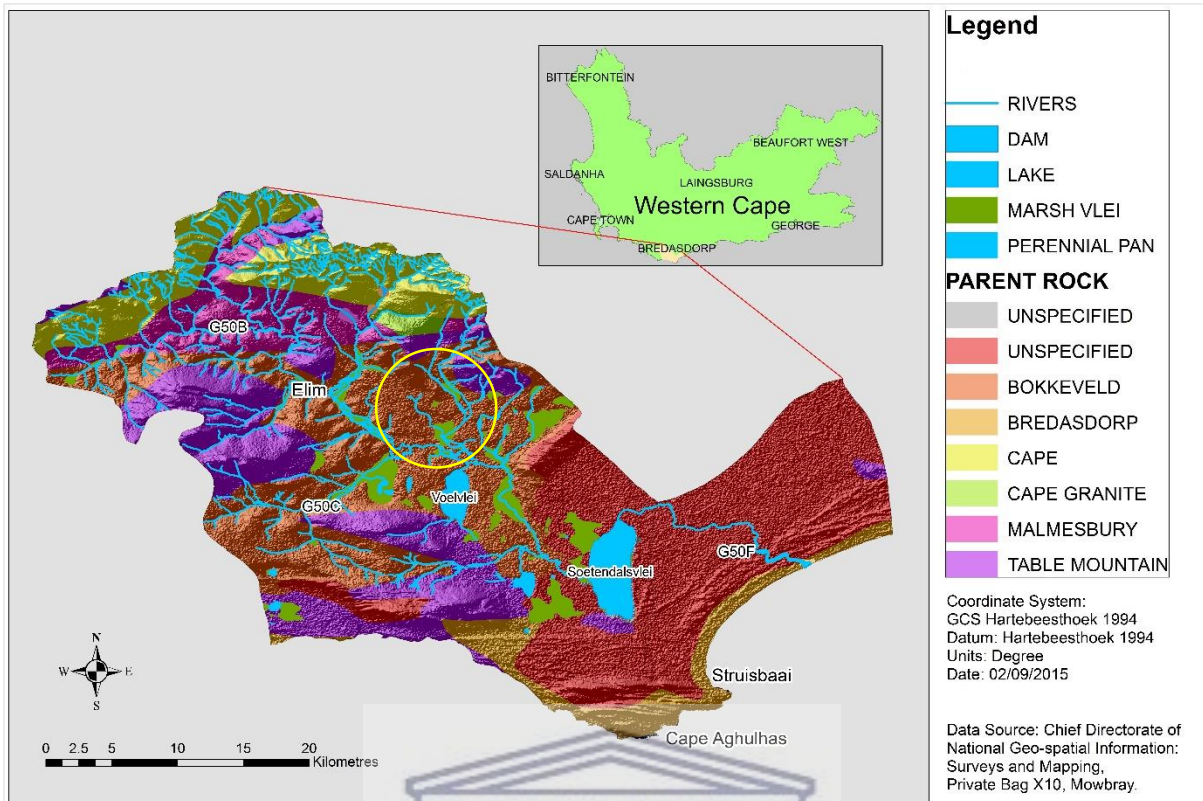
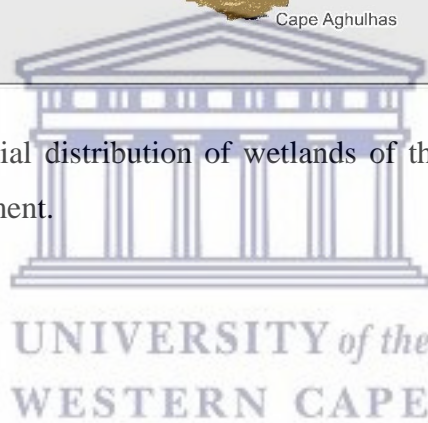


Figure 3.2: Geology and spatial distribution of wetlands of the Nuwejaars Catchment area within the Heuningnes Catchment.



3.3. Vegetation

The Jan Swartskraal sub-catchment has been extensively invaded by various alien *Acacia* species. However, in the northern parts of Jan Swartskraal farmers are rehabilitating lands and replanting natural fynbos (Figure 3.3). Likewise, the Koue sub-catchment is invaded by various alien *Acacia* species.

The northern parts of the Pietersielieskloof sub-catchment is partially invaded by various alien *Acacia* species and Black Wattle. However, the mountainous regions is covered largely in natural fynbos and invasions of woody alien vegetation increases downstream towards the Nuwejaars Wetland (Figure 3.3). The Elim, Blomkraals and Voëlvlei sub-catchments are largely covered in natural fynbos (Figure 3.3).

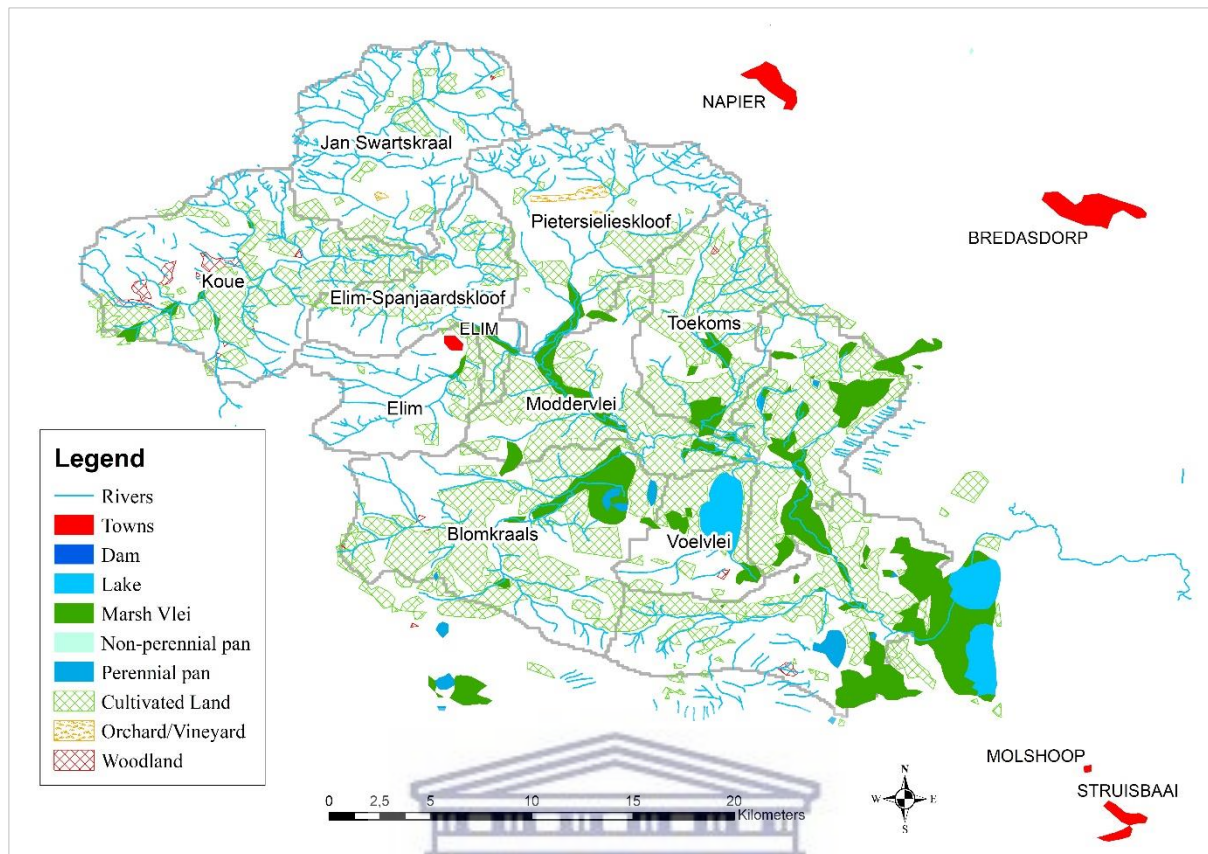


Figure 3.3: Land cover and land uses of the Nuwejaars Catchment. (Source: Chief Directorate of National Geographic Information Surveys and Mapping, Private Bag X10, Mowbray).

3.4. Land uses

Most of the Nuwejaars catchment is cultivated land with woodlands present mostly in the mountainous regions. There are pine plantations in the mountainous regions of the Pietersielieskloof, Koue and Jan Swartskraal. Fynbos and Protea flower farms are found in the Jan Swartskraal, Koue, Pietersielieskloof and Elim sub-catchments (Figure 3.3).

Most of the area is used for pastures, cattle farming, raising of livestock, livestock grazing, crops (wheat and canola). The Elim-Spanjaardskloof sub-catchment has dairy production and owned by the Elim community (Figure 3.3). In addition, vineyards are present in the Moddervlei and upper Pietersielieskloof sub-catchments.

The Voëlvlei sub-catchment has the smallest area of 27.6 km². On the other hand, the Blomkraals sub-catchment is the largest with an area of 90.3 km². The Voëlvlei sub-catchment is largely under a natural state (Figure 3.3). The Blomkraals sub-catchment has a variety of wildlife and was protected by the Nature Reserve, while other parts are used for cultivation and raising of livestock (Figure 3.3).



4. HYDROLOGICAL RESPONSES TO RAINFALL EVENTS

4.1 Introduction

In order to determine the hydrological responses of a catchment, there are several factors that need to be examined. These include climatic conditions, topography, geology, soil characteristics, surface and groundwater flow patterns, spatial distribution of vegetation, and land uses (Blöschl et al., 2013; McCartney, et al., 2013). This chapter addresses the first objective of the study and will therefore examine the hydrologic responses of the sub-catchments to rainfall events.

4.2. Methods

4.2.1. Weather data collection

For the purpose of this study, rainfall data for the Nuwejaars catchment were collected at 4 automatic weather stations at Tierfontein, Spanjaardskloof, Moddervlei and Vissersdrift farms, and two automatic rain gauges at the Toekoms and Tussenberge farms. The density of the rainfall stations is 1 rainfall station per 127 km² which meets the minimum density of 250 km² – 575 km² (WMO, 2008) (Figure 4.1).

Rainfall data were recorded at 15 minute intervals by the automatic weather stations and rain gauges. Data records ranged from 584 days to 960 days (Figure 4.2) as the weather stations were not established at the same time (Table 4.1). The periods of missing data were the result of equipment malfunction and periods of servicing the equipment. The first record for Moddervlei from 15th August 2014 to 16th November 2015 was recorded using a rain gauge, while the latter was recorded by the weather station installed on the 17th June 2016.

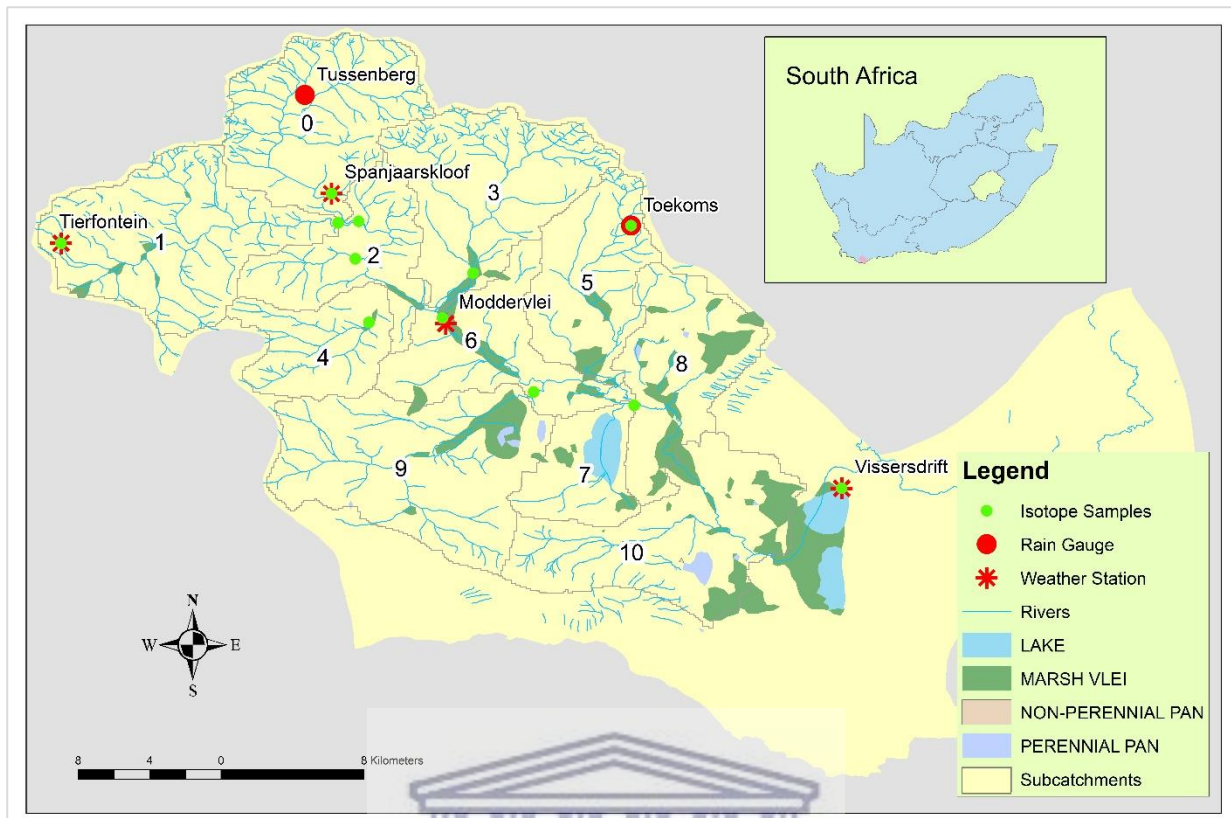


Figure 4.1: Locations of the rain gauges and weather stations

Table 4.1: Locations of the automatic weathers stations and rain gauges in the Nuwejaars Catchment established by the University of the Western Cape.

Location	Coordinates	Altitude (m)	Equipment Type	Date Started
Weather Stations				
Tierfontein	34.5650° S, 19.6033° E	197	HOBO US30	15 Aug 2014
Spanjaardskloof	34.5400° S, 19.7396° E	159	HOBO USO30	15 Aug 2014
Moddervlei	34.6051° S, 19.7963° E	25	Campbell Scientific with CR1000 data logger	17 June 2016
Vissersdrift	34.6880° S, 19.9955° E	7	HOBO US30	21 Dec 2014

Rain Gauging Stations				
Tussenberg	34.474363° S, 19.743775° E	231	HOBO 0.2 mm with Event data logger	4 June 2015
Toekomst	34.556116° S, 19.890188° E	162	HOBO 0.2 mm with Event data logger	4 June 2015

Based on the recommendations by Penna *et al.*, (2010), missing rainfall data were infilled using the linear regression method (Annexure 1). The station with the highest correlation was used to infill the missing data for each station (Table 4.2).

Table 4.2: Equations used to infill missing rainfall data.

Station with missing data	Station used to infill	Equation used to infill	R ² Value
Tiersfontein (2015)	Spanjaardskloof	$y = 1.0792x + 0.1432$	0.78
Tiersfontein (2016)	Vissersdrift	$y = 0.616x + 0.4716$	0.62
Moddervlei	Vissersdrift	$y = 1.0904x - 0.1213$	0.79
Toekoms	Spanjaardskloof	$y = 0.6912x + 0.642$	0.44
Tussenberg	Spanjaardskloof	$y = 0.8059x + 0.2648$	0.8
Spanjaardskloof	Tierfontein	$y = 0.7234x + 0.1865$	0.78
Vissersdrift	Spanjaardskloof	$y = 0.7143x + 0.0948$	0.53

Where: y = "daily rainfall at station with missing data" and x = "daily rainfall at station used to fill gaps"

i) Analysis of wet and dry spells

The analysis of wet and dry spells was done for all of the stations for 2015, 2016 and January 2017 to July 2017. Wet spells were determined by adding the number of days during which rain occurred irrespective of the intensity or duration. Rainfall intensity was estimated using hourly rainfall data. Thiessen polygons were produced and used to estimate the rainfall for of each of the sub-catchments.

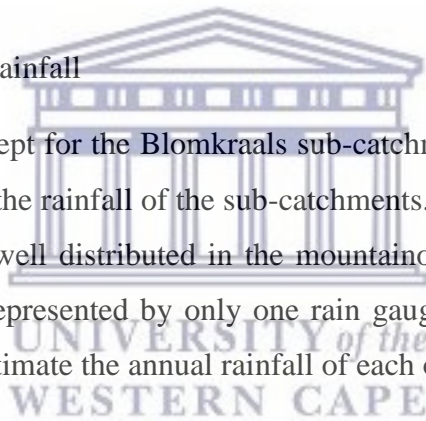
ii) Determining rainfall intensity

The rainfall intensity was analysed for each event, where an event was classified as a period during which rainfall was recorded consecutively for an hour or more. The rainfall intensity was estimated using only the hours during which rainfall occurred. The hours during which rainfall did not occur were not included.

The rainfall intensity was analysed for each event at the Tiersfontein, Spanjaardskloof and Vissersdrift rainfall stations for 2015, 2016 and until 30th June 2017. The data for the Moddervlei station was only included for the period of 2016 to 30th June 2017. The average daily rainfall intensity was then estimated for each of the abovementioned sites as the average of rainfall intensity of the events which occur on a particular day.

iii) Estimating catchment rainfall

In all the sub-catchments, except for the Blomkraals sub-catchment, more than one Thiessen polygon was used to estimate the rainfall of the sub-catchments. The Thiessen polygons show that the weather stations are well distributed in the mountainous regions. However, for the lower lands a larger area is represented by only one rain gauge (Figure 4.2). The Thiessen polygons were then used to estimate the annual rainfall of each of the sub-catchments.



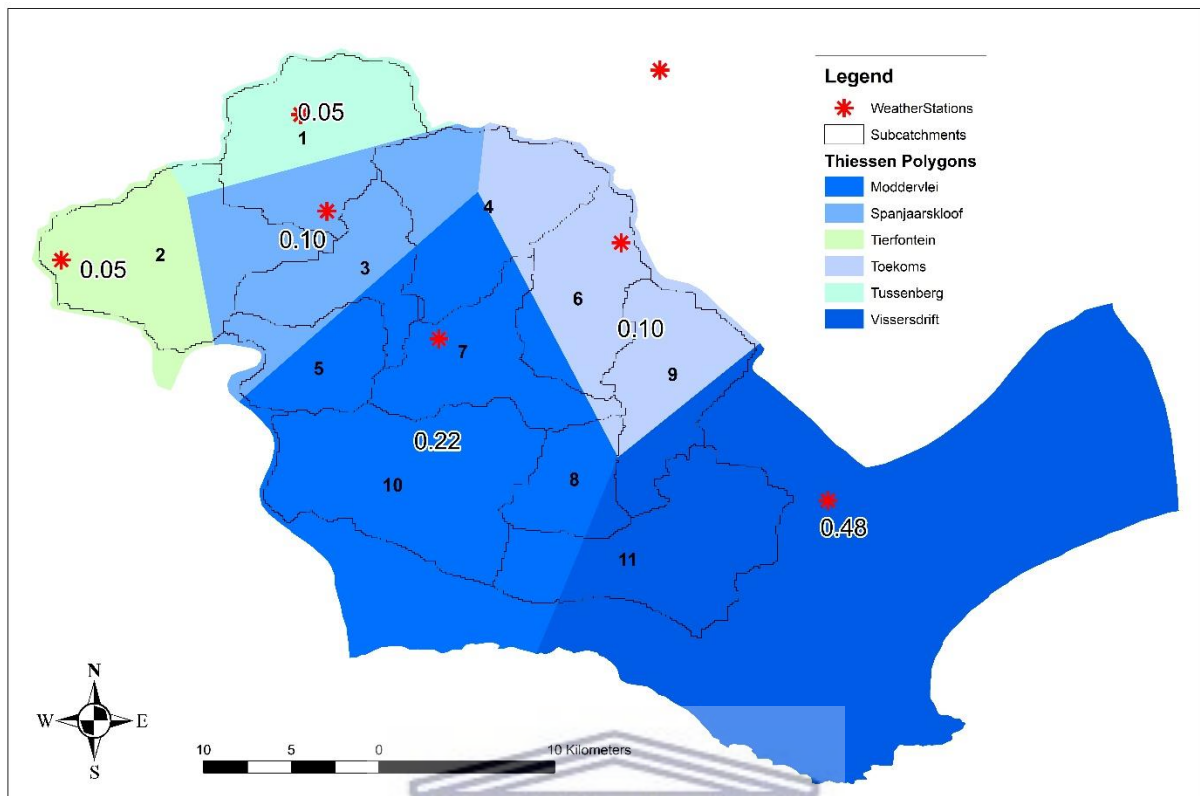


Figure 4.2: Thiessen polygons used to estimate the weights of each rainfall station for estimating daily rainfall.

4.2.2. Selection of river flow monitoring sites

It was imperative that flow monitoring sites be selected to accurately represent the contributions of flows of each of the selected sub-catchments in Chapter 3. Sites were selected based on the following recommendations by WMO, (2008) and WMO, (2010):

- The general course of the stream should be straight for approximately 100 m upstream and downstream of the gauging site;
- The total flow should be confined to one channel at all stages and no flow should bypass the gauging site as subsurface flow
- The stream bed is not subject to scour and fill and should be free of weeds;
- Banks should be stable, high enough to contain floods, and free of brush;
- An adequate reach for measuring discharge at all stages is available as close to the gauge site as possible.
- The site is readily accessible to ensure ease in the installation and operation of the gauging site

4.2.3. Topography of tributaries and channel cross-sections

Based on the recommendations by Blöschl, *et al.* (2013) and McCartney, *et al.* (2013), the main properties considered for this project were the topography and geology of the sub-catchments. One of the key aspects of this study was to determine the response times of each of the tributaries as well as the contributions they have to the Nuwejaars River. The most important characteristics were therefore slope, channel length and width, the area of the sub-catchment and the amount of rainfall it received. The characterization of the sub-catchments was done using remotely sensed data to determine the geology, slope and length of tributaries of each sub-catchment.

The geology, slope, length of the river and area of the sub-catchments were determined using 1:50 000 maps provided by the NGI (Chief Directorate of National Geo-Spatial Information South Africa). River lengths and slopes were measured using satellite imagery on Google Earth Pro on 18 May 2017.

Elevation data for describing the longitudinal profiles and cross-sections at the flow monitoring sites were collected using a Leica Zeno 15 DGPS (Differential Global Positioning System) with an accuracy of 10 cm to 50 cm. These profiles were used to estimate channel slope. Photographs and notes were taken during these visits in order to identify the type of vegetation present in and around the selected sites and notes were made on the bed material present in each of the channels during and after installation of the stilling wells and water level loggers.

4.2.4. Stage-discharge measurements

A pressure transducer with automatic water-level logger inside a stilling well was installed at each site to continuously measure water levels. The OTT Orpheus Mini water level logger with a depth range of 50 m and accuracy of 0.05 % (OTT Hydromet, 2011) or Hobo water level U20L-02 logger with a depth range of 30 m and accuracy of 3 cm – 6 cm (Onset C. C., 2010) were used (Table 4.4). For Elandsdrift, Voëlvlei, Blomkraals, and Jan-Swarskraal sites, stilling wells made of a 75 mm diameter PVC pipe were fixed to bridge piers (Figure 4.25 A). At the Elim Flow Diversion flow monitoring site, the stilling well was mounted inside a weir (Figure

4.22). On the Nuwejaars River at the Elim Waste Water Treatment Plant flow monitoring site, and at the Pietersielieskloof flow monitoring site stilling wells were installed by sinking a pipe into the bed of the river (Figure 4.18).

Stilling wells consisted of a blue 75 mm PVC pipe with thin slits of 5 mm cut into them to allow for water flow and covered with a fabric mesh to limit the amount of sediment which entered the stilling well (Annexure 2 A & C). The stilling wells were then capped with a PVC cap and a 14 mm bolt with a lock-nut were used to secure the logger within the well (Annexure 2 B).

For the Elandsdrift, Voëlvlei, Elim Flow Diversion and Elim-Boskloof Road Bridge (herein further referred to as the Melkery Bridge site) flow monitoring sites where gauge plates had previously been installed, water level readings were noted during every visit to the field (Table 4.4). For those sites that did not have a gauge plate, a measurement was taken using a handheld measuring staff at a fixed location.

Discharge measurements were done using the OTT MF Pro electromagnetic current meter and the One-point, Two-point or Three-point methods recommended by WMO, (2008) were used depending on the stage of flow at the time of measurement. If flows were less than 0.75 m the one-point method was used, for flows between 0.75 m and 1.2 m the two-point method was used, and the three-point method was used when flows exceeded 1.2 m. The cross-section was divided into segments. The mean-section method was used to calculate discharge (q) as follows:

$$q = \left(\frac{v_1 + v_2}{2} \right) \left(\frac{d_1 + d_2}{2} \right) b \quad (4.1)$$

where q is the discharge of the segment, v_1 is the mean velocity at the first vertical, v_2 is the mean velocity at the second vertical, d_1 and d_2 are the total depths at verticals 1 and 2, b is the horizontal distance between the verticals and q is the discharge of the segment.

$$Q = \sum_{i=1}^n q_n \quad (4.2)$$

where Q is the total discharge of the stream or cross-section, q_n is the discharge of each segment and n is the total number of segments. This is then repeated at each of the selected sites. Measurements were done on a bi-weekly basis and during high episodes of rainfall in order to provide an adequate number of measurements for deriving rating curves.

4.2.5. Derivation of rating curves

The discharge measurements were used to derive rating curves. Manning's equation was used to improve rating curves when a site did not have adequate measurements to cover the range of flows. Rating curves were derived using the Manning's equation (Arcement & Schneider, 1984). The measured stage-discharge values were then used to adjust the n values for each equation accordingly. The cross-sectional profiles at each site were used to estimate flows using Manning's Equation (Equation 4.3).

$$Q = VA = \left(\frac{100}{n}\right) AR^{\frac{2}{3}} \sqrt{S} \quad (4.3)$$

where: Q = Discharge, (m³/s)

V = Cross-sectional Velocity, (m/s)

A = Area, (m²)

n = Manning's Roughness Coefficient

R = Hydraulic Radius, (m)

S = Channel Slope

4.2.6. Analysis of hydrologic responses

In order to determine the hydrologic responses of the rivers to rainfall events, it was imperative to understand the minimum cumulative rainfall required for flows to occur, response times or

time to peak and the recession characteristics of each of the tributaries. The tributaries in most of the cases were dry or not flowing during the time of installation of flow measuring equipment and the initial flows of the tributaries were therefore easily identifiable.

By comparing the hourly rainfall data and hourly water level data one was able to determine the response time of each of the tributaries using the time to peak analysis. To determine the cumulative rainfall required for flow to occur and the initial abstraction of the tributaries it was vital to note the initial or first flow recorded in each of the tributaries. The minimum cumulative rainfall required before flows occur in each tributary can then be estimated by summing all the rainfall received prior to the peak in water level. The derived rating curves are then used to estimate the fluxes in daily discharges for each of the tributaries

4.3. Results

4.3.1. Seasonal variation of rainy days

The rainfall station with the longest record of data is the Spanjaardskloof station which had 960 days of data from 2014 when it was installed (Figure 4.3). The Tussenberg rainfall station had the least amount of rainfall data with only 584 days of data. The periods of missing data were due to servicing of the weather stations or periods where the weather stations were offline (Figure 4.3).

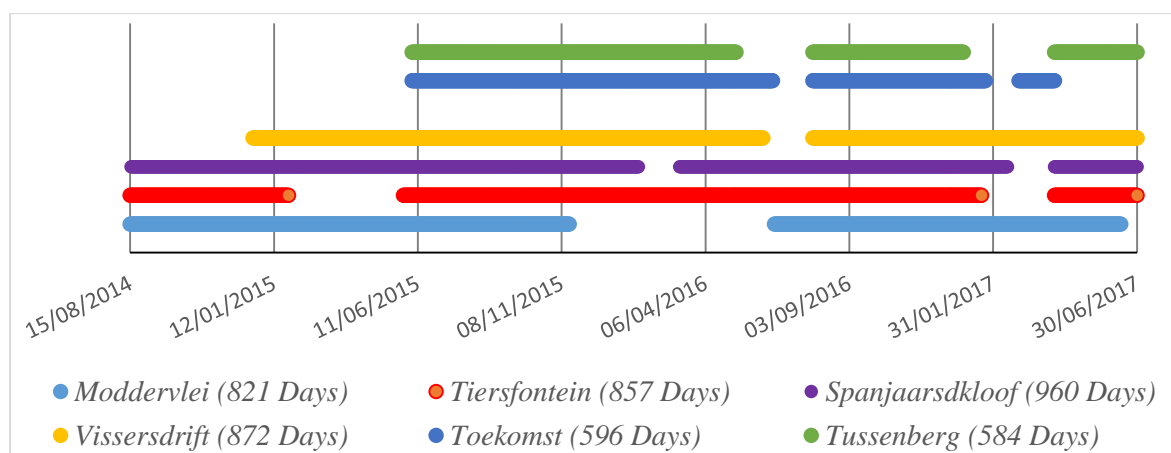


Figure 4.3: Record lengths for the Weather Stations and Rain Gauges in the Nuwejaars Catchment.

In 2015, the longest recorded wet spell was 9 days, measured at the Moddervlei station and occurred from the 22nd June to the 30th June 2015. During this time rain was recorded for 3 days at the Tiersfontein and Vissersdrift stations, 4 days at the Spanjaardskloof and Tussenberg stations and for 5 days at the Toekomst station. The average number of wet days for 2015 was 136 days. The highest number of wet days for 2015 was recorded at the Toekoms station having 151 wet days, while Vissersdrift had the lowest of 103 days (Table 4.3).

Table 4.3: Number of dry and wet days for each of the rainfall stations of Nuwejaars catchment for 2015, 2016 and 2017.

Rainfall Station	2015		2016		Jan-Jul 2017	
	Dry Days	Wet Days	Dry Days	Wet Days	Dry Days	Wet Days
Moddervlei	190	175	239	127	157	55
Tierfontein	245	120	235	131	157	55
Spanjaardskloof	246	119	233	133	157	55
Vissersdrift	262	103	236	130	158	54
Toekoms	214	151	189	177	148	64
Tussenberg	216	149	197	169	125	87

In 2015, the highest number of rainy days were recorded in winter between June and September (Figure 4.4). During winter, the highest number of rainy days are recorded at the Moddervlei station. On the other hand, during the summer months' rainfall is higher in the mountainous areas of Tiersfontein, Toekoms and Tussenberg than elsewhere (Figure 4.4)

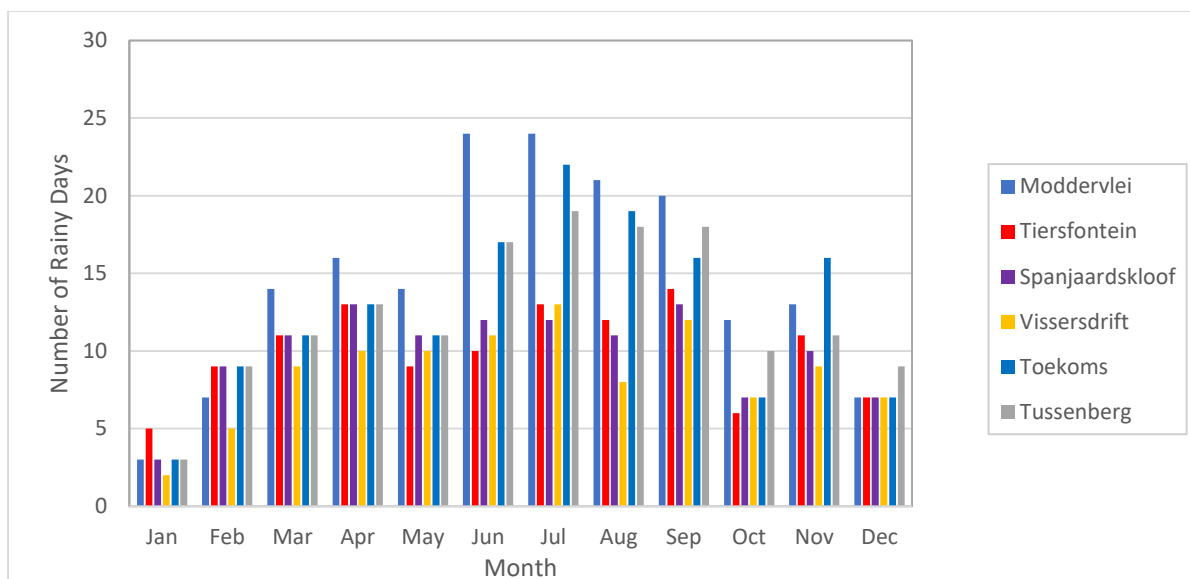
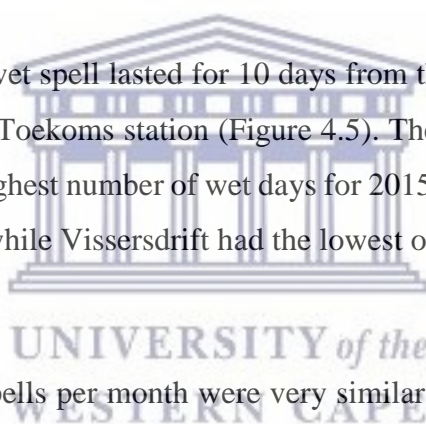


Figure 4.4: Number of rainy days per month at each of the rainfall stations for 2015.

In 2016 the longest recorded wet spell lasted for 10 days from the 27th May 2016 to 5th June 2016 and was recorded at the Toekoms station (Figure 4.5). The average number of wet days for 2016 was 145 days. The highest number of wet days for 2015 was recorded at the Toekoms station having 177 wet days, while Vissersdrift had the lowest of 130 days (Table 4.3).



In 2016, the number of wet spells per month were very similar from February to September, averaging between 10 and 15 wet days per month (Figure 4.5). In 2016, the period from May to July had significantly less rainy days than compared to 2015. In 2016, significantly more wet days were recorded throughout the year except for the Moddervlei station (Table 4.3). However, as will be discussed later, the annual rainfall in 2015 was more than that of 2016.

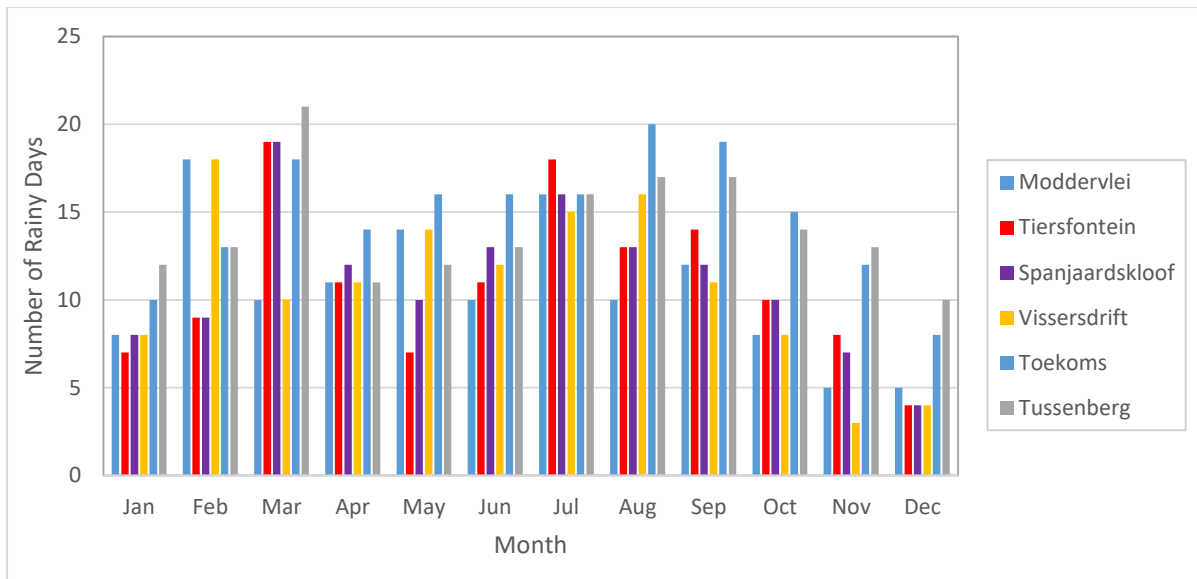


Figure 4.5: Number of rainy days per month at each of the rainfall stations for 2016.

From January to July 2017, the highest recorded average duration of wet spells was 3.1 days and was recorded at the Tussenberg station. The lowest recorded average duration of wet spells was recorded at the Moddervlei station, with an average duration of 1.4 days. The longest recorded wet spell in 2017 lasted for 9 days, from the 17th June to 25th June and this was followed by the second longest spell which lasted 8 days, from the 28th June to 5th July (Figure 4.6). Both these wet spells were recorded at the Tussenberg station and interestingly throughout this period the other stations recorded more sporadic rainfall lasting for three consecutive days at most. The trend of rainy days to dry days is very similar to what was recorded in 2015 and 2016 (Table 4.3).

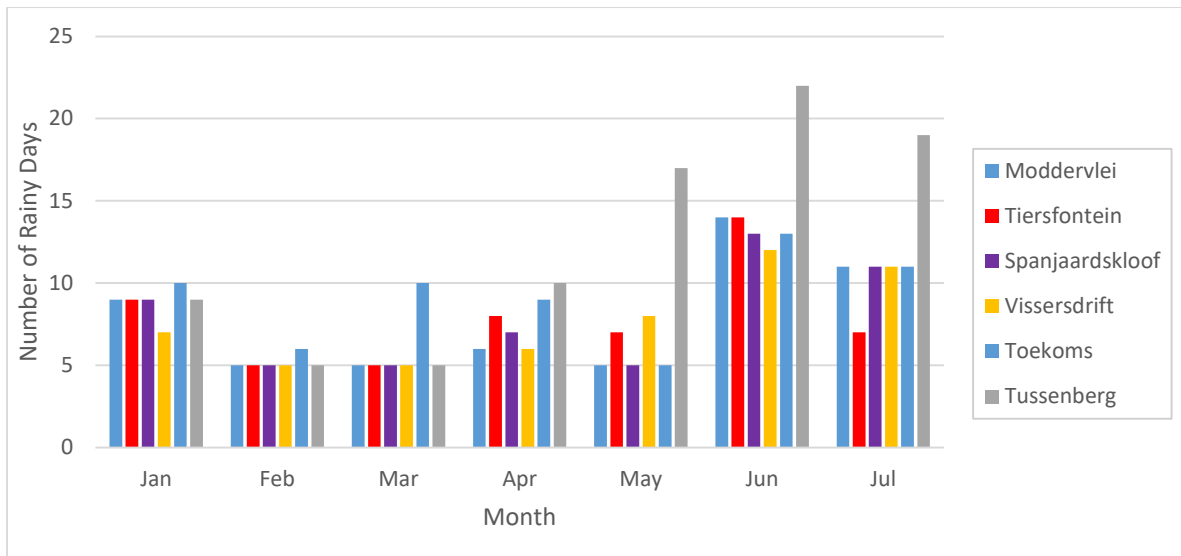


Figure 4.6: Number of rainy days per month for each of the rainfall stations from January 2017 to July 2017.

4.3.2. Rainfall intensity

In 2015, the average daily rainfall intensity was 0.24 mm/hr at Tiersfontein, 0.27 mm/hr at Spanjaardskloof and 0.21 mm/hr at Vissersdrift. The highest average daily rainfall intensities were recorded during July for all three sites, with an average of 0.39 mm/hr recorded at Tiersfontein and a maximum of 2.56 mm/hr (Figure 4.7). The highest average daily rainfall intensity was 0.54 mm/hr at Spanjaardskloof with a maximum rainfall intensity of 4.6 mm/hr. However, the maximum rainfall intensity at Spanjaardskloof was 2.94 mm/hr and was recorded in June 2015. On the other hand, the highest average daily rainfall intensity at Vissersdrift was recorded in June 2015 at 0.39 mm/hr with a maximum of 3.48 mm/hr (Figure 4.7).

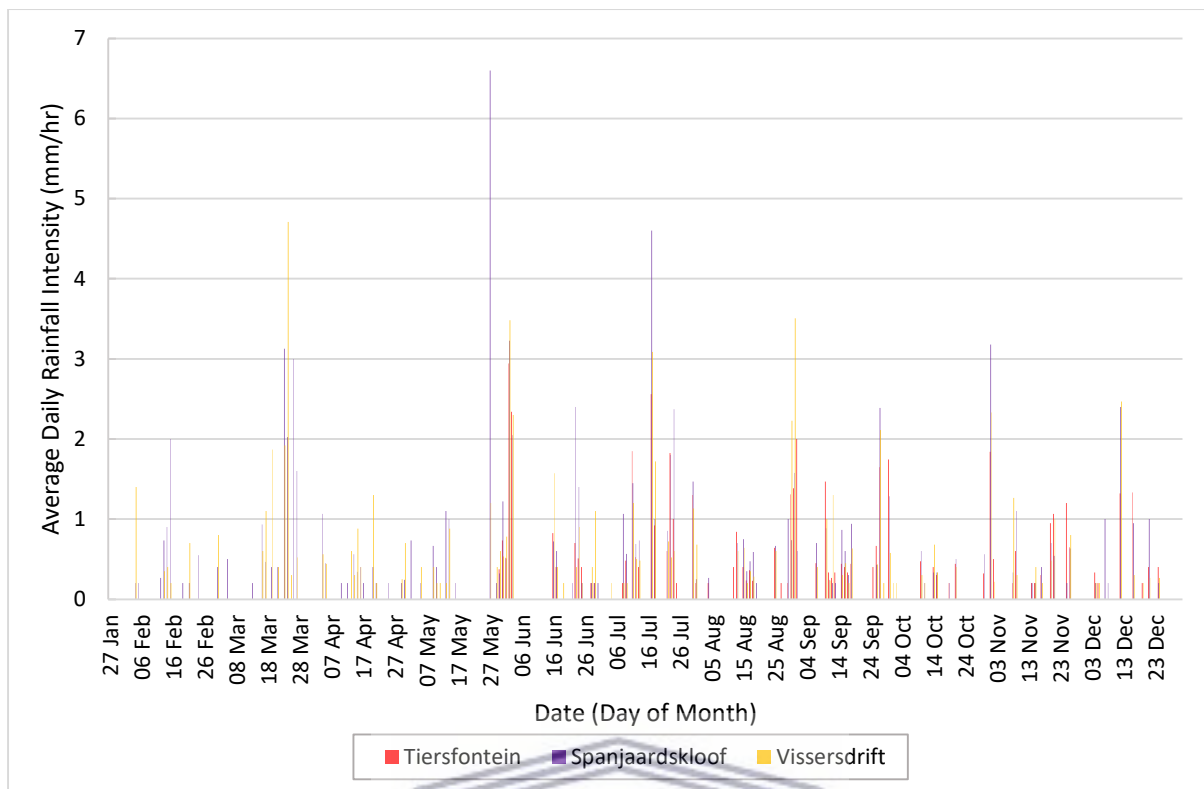


Figure 4.7: Average daily rainfall intensity for the Tiersfontein, Spanjaardskloof and Vissersdrift rainfall stations, from 27th January to 31st December 2015.

In 2016, the average daily rainfall intensity was 0.29 mm/hr at Moddervlei, 0.27 mm/hr at Tiersfontein, 0.25 mm/hr at Spanjaardskloof and 0.18 mm/hr at Vissersdrift. Like in 2015, the highest average rainfall intensities were recorded in July (Figure 4.8). The average daily rainfall intensities in July were 0.66 mm/hr at Moddervlei with a maximum of 4.97 mm/hr, 0.55 mm/hr at Tiersfontein with a maximum of 3.57 mm/hr and 0.5 mm/hr at Spanjaardskloof with a maximum of 3.31 mm/hr (Figure 4.8). The missing data at the Vissersdrift station made it difficult to accurately determine the averages during the wet months of June, July and August. However, it can clearly be seen from the other stations that rainfall intensities were highest during June, July and August.

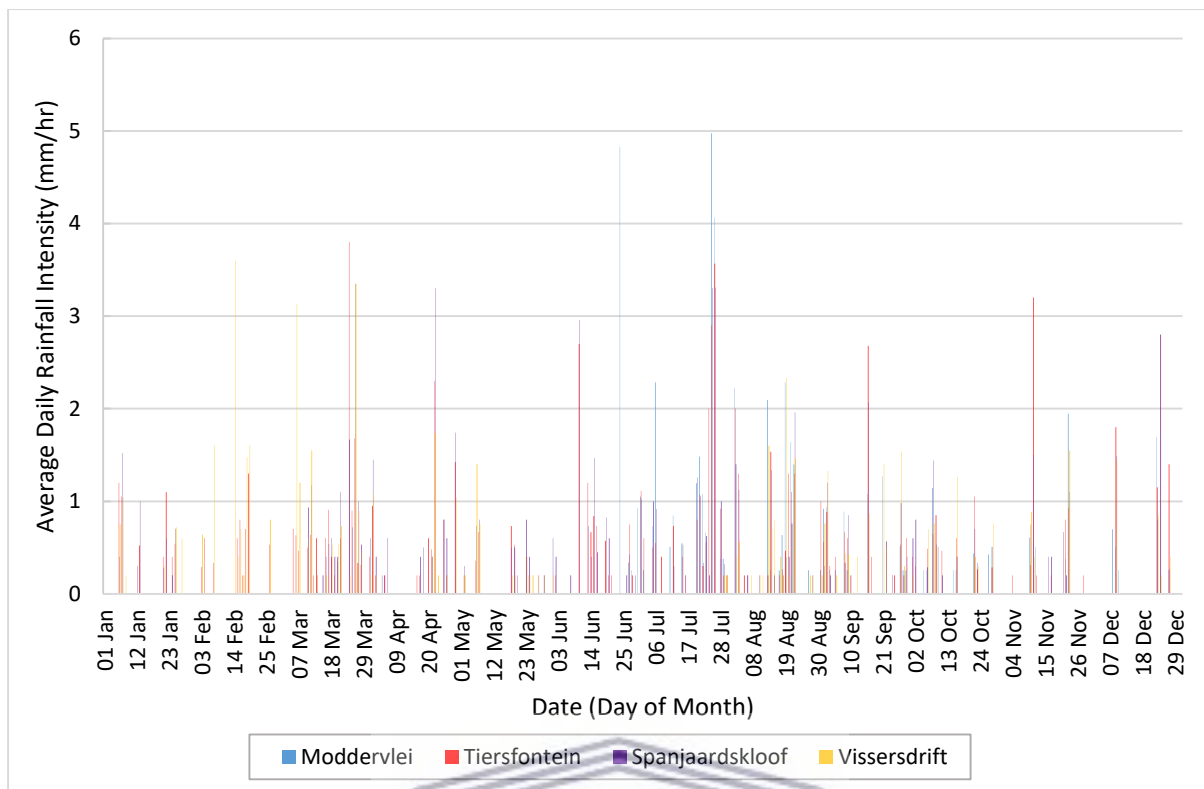


Figure 4.8: Average daily rainfall intensity for the Moddervlei, Tiersfontein, Spanjaardskloof and Vissersdrift rainfall stations for 2016.

The average rainfall intensity was 0.21 mm/hr at Moddervlei, 0.12 mm/hr at Tiersfontein, 0.18 mm/hr at Spanjaardskloof and 0.13 mm/hr at Vissersdrift (Figure 4.9). This was significantly less than the average rainfall intensities of 2015 and 2016. The highest average daily rainfall intensities were recorded in June. Moddervlei had an average daily rainfall intensity of 0.46 mm/hr with a maximum of 1.78 mm/hr in June. However, the maximum rainfall intensity in May was significantly higher at 3.56 mm/hr at the Moddervlei site. The average daily rainfall intensity was 0.39 mm/hr at the Tiersfontein site with a maximum of 1.67 mm/hr, 0.53 mm/hr at Spanjaardskloof with a maximum of 1.92 mm/hr and 0.27 mm/hr at Vissersdrift with a maximum of 1.8 mm/hr (Figure 4.9).

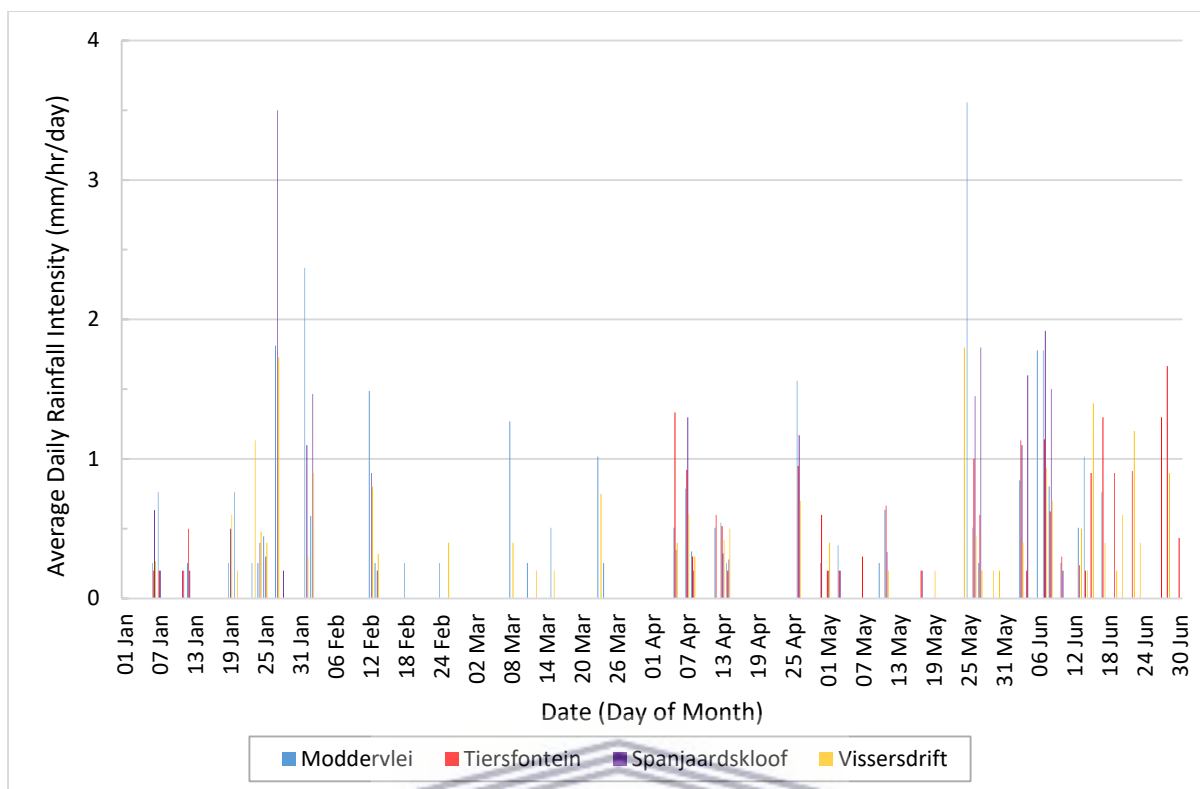


Figure 4.9: Average daily rainfall intensity for the Moddervlei, Tiersfontein, Spanjaardskloof and Vissersdrift rainfall stations, from 1st January to 30th June 2017.

4.3.3. Estimation of catchment rainfall

In 2015, the average rainfall for the catchment was 552 mm/yr. The highest annual rainfall was recorded at the Spanjaardskloof station with 629 mm/yr. The lowest annual rainfall was recorded at the Tiersfontein station of 493 mm/yr (Figure 4.10). In 2016, the average rainfall for the catchment was 516 mm/yr. The highest annual rainfall of 609 mm/yr was recorded at the Toekoms station (Figure 4.10).

There were 8 large rainfall events that occurred during 2015. The first major event occurred between the 23rd and 24th of March 2015. The highest rainfall of 61.4 mm/day was recorded at the Vissersdrift rain gauge while only 26 mm/day was recorded at the Moddervlei station during the first event between the 23rd and 24th March 2015. The largest event in 2015 occurred between the 1st and 3rd of June 2015. The highest rainfall of 99.2 mm/day was recorded for this

period at the Vissersdrift station and the lowest in the Toekoms and Tussenberg mountainous region (Figure 4.10).

For 2016, the Vissersdrift station recorded significantly less rainfall than compared to 2015. In 2016, the Tiersfontein and Tussenberg rain gauges in the Mountainous regions recorded less rainfall than that of the Moddervlei station. In 2016 only two days exceeded rainfall of 30 mm/day. On the other hand, a total of 6 days exceeded 30 mm/day of rainfall in 2015 (Figures 4.10).

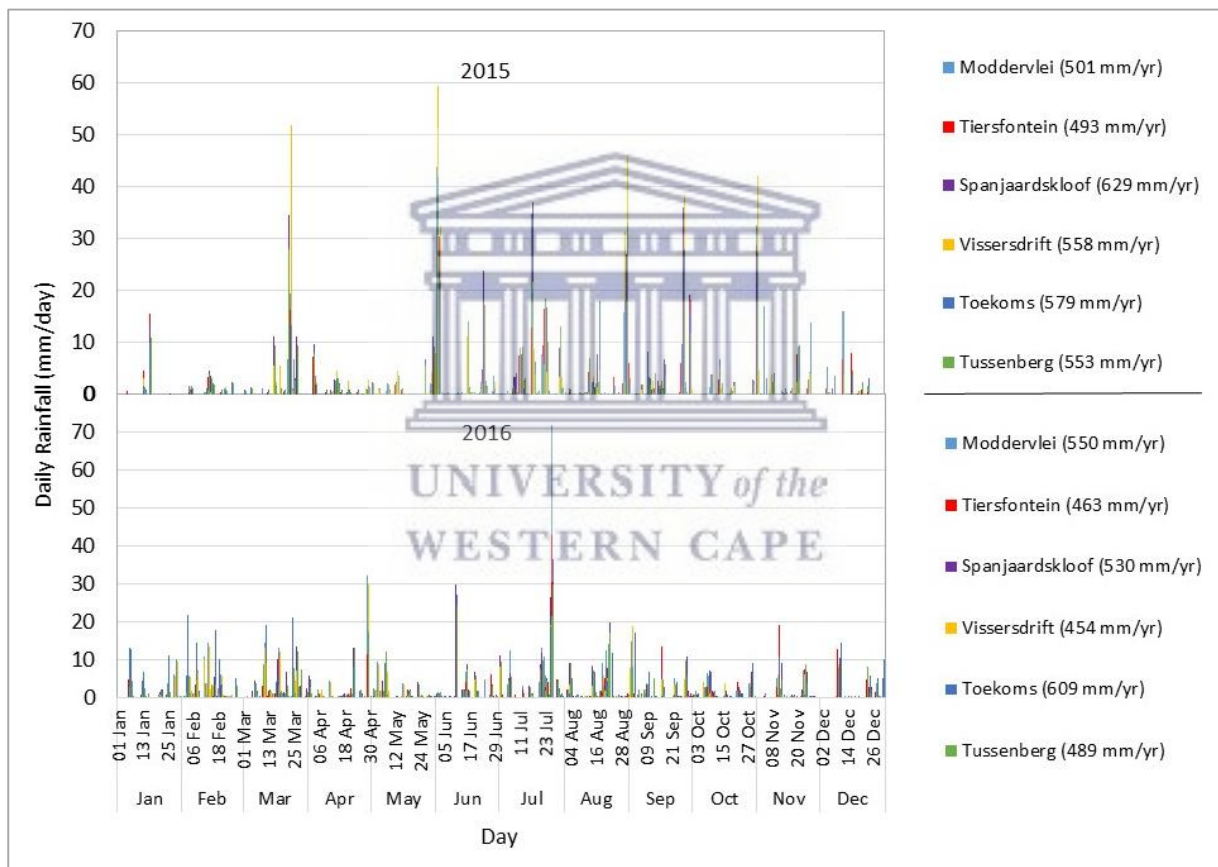


Figure 4.10: Daily rainfall of all the rainfall stations for 2015 and 2016.

The largest rainfall event in 2016 occurred between the 25th and 26th July 2016. A maximum rainfall of 92.2 mm/day was recorded at the Moddervlei station within a 24 hr period at an intensity of 4.51 mm/hr. 60.2 mm/day was recorded at the Tiersfontein station and 62.8 mm/day at the Spanjaardskloof station, with an average intensity of 3.27 mm/hr recorded at

these stations (Figures and 4.7 and 4.10). The number of rainy days in 2016 exceeded that of 2015. However, the intensity of these rainfall events was much less in 2016 than compared to 2015.

In 2017, data was collected up to 31st July 2017. Three major events occurred during this period. The largest event of 2017 occurred between the 7th and 8th June, 49.3 mm/day at Moddervlei station, 23.3 mm/day at Tiersfontein, 62.3 mm/day at Spanjaardskloof, 26.2 mm/day at Vissersdrift, 44.8 mm/day at Toekoms and 65.2 mm/day at Tussenberg (Figure 4.11). The average intensity for this event was 1.24 mm/hr which is significantly less than the rainfall intensities recorded in 2015 and 2016 (Figure 4.8).

The years 2015, 2016 and 2017 had a similar number of rainy days. However, in 2017 these events did not last as long and had significantly lower rainfall intensities than compared to 2015 and 2016. In 2017 most of the daily rainfall did not exceed 5 mm/day and compared to 2015 and 2016.

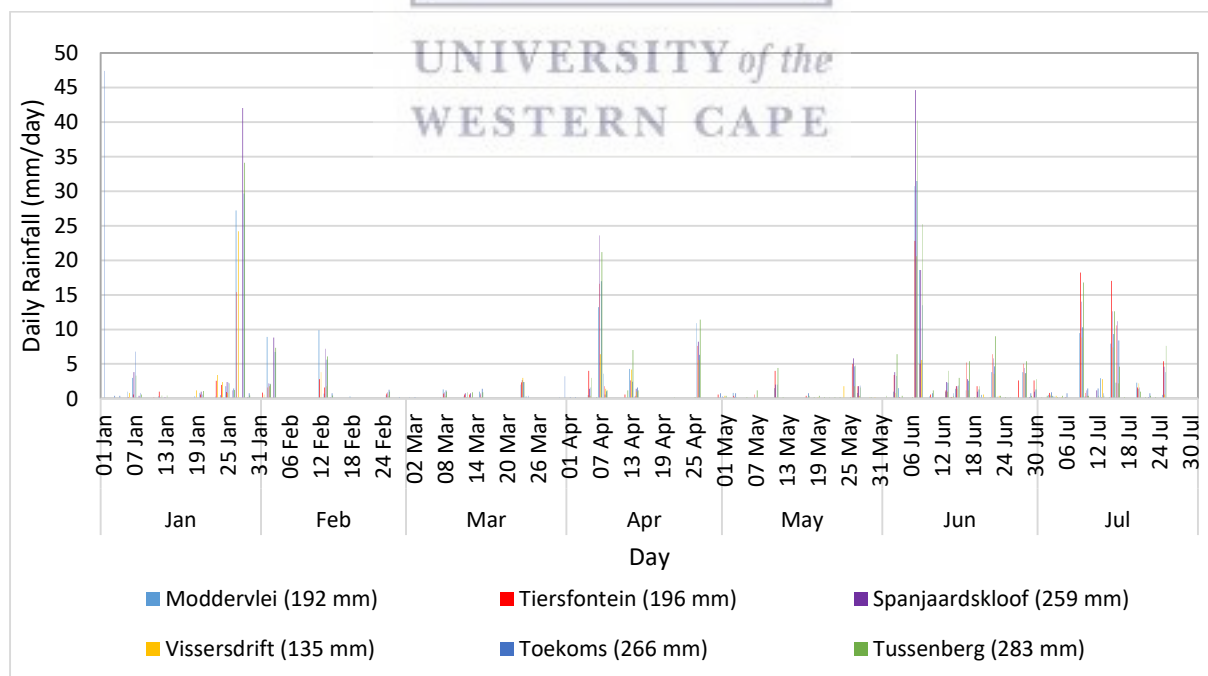


Figure 4.11: Daily rainfall of all the rainfall stations from January to 31st July 2017.

The total annual rainfall received over the catchment in 2015 and 2016 were very similar at 552 mm/yr in 2015 and 516 mm/yr in 2016 (Figure 4.12). In 2015 most of the rainfall fell over the south west of the catchment, with the highest rainfall falling over the Voëlvelei sub-catchment. In 2016, less rainfall was recorded in the south west of the catchment, however the highest rainfall was recorded in the Voëlvelei sub-catchment (Figure 4.12). In 2017, similarly to 2015 and 2016 most of the rainfall occurred in the south west, followed by the Pietersielieskloof sub-catchment in the north east (Figure 4.12).

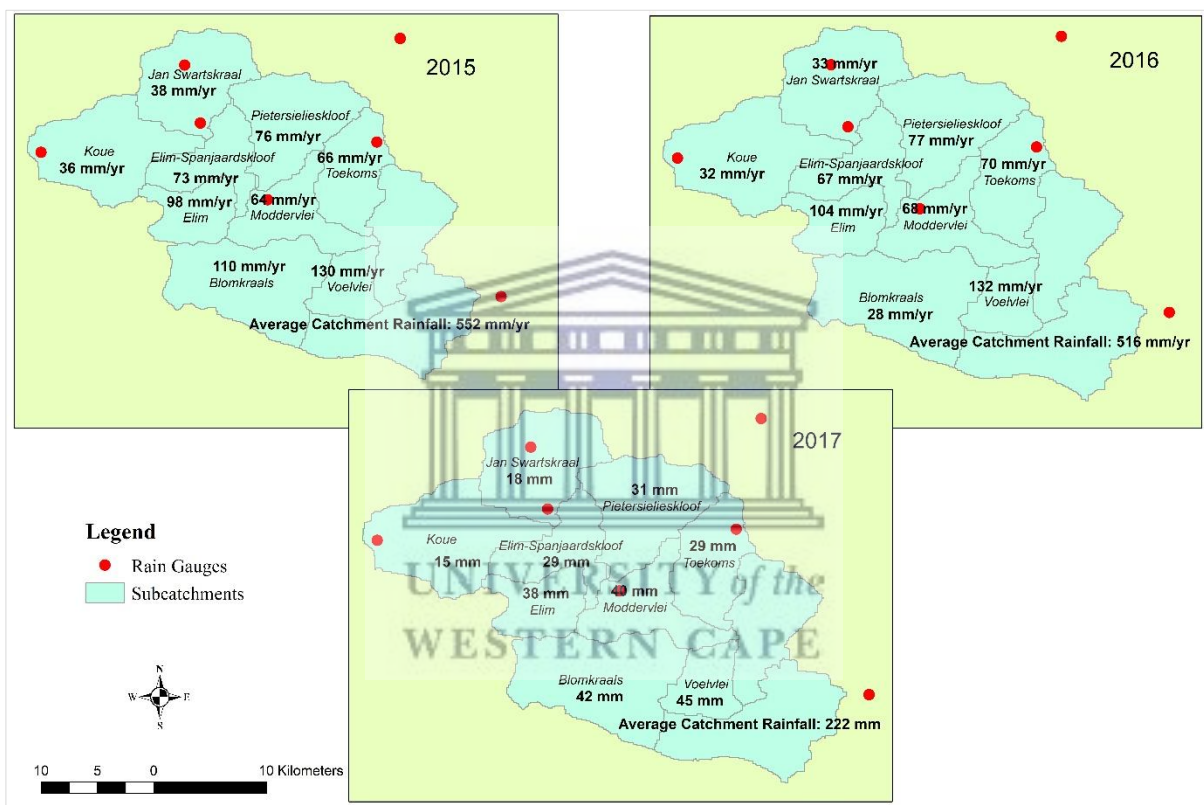


Figure 4.12: Estimated rainfall received for each of the sub-catchments for 2015, 2016 and January to 31st July 2017.

4.3.4. River flow monitoring sites

The main objective of this section was determine the contribution each sub-catchment to the flows of the Nuwejaars River. To meet this objective, 8 river flow monitoring sites were established in the Nuwejaars Catchment (Figure 4.13). However, it was not possible to establish a flow monitoring site on the Koue River as most stretches were densely invaded by alien *Acacia* species. Seven of the flow monitoring sites were established in 2016, while the Elandsdrift, Wiesdrif and Vissersdrift sites were established in 2014 (Table 4.4).

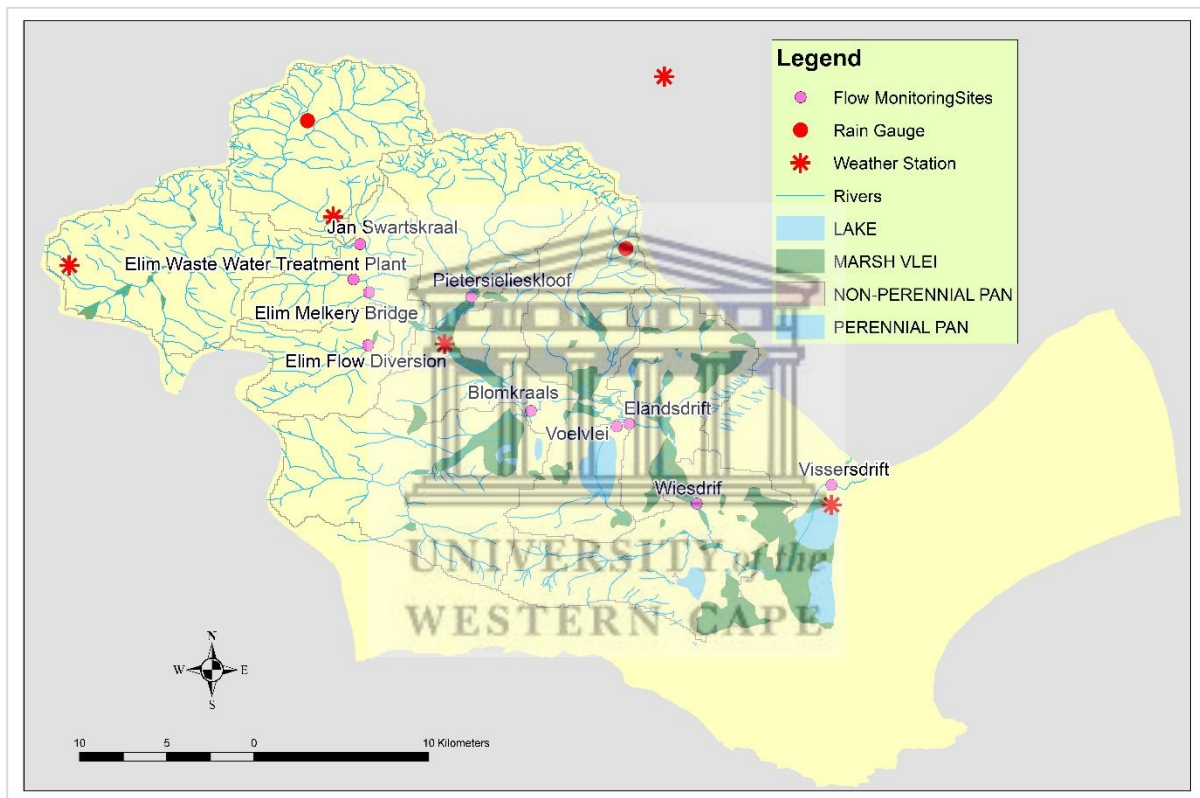


Figure 4.13: Flow monitoring sites established from 2014 to 2016 in the Nuwejaars Catchment.

Table 4.4: Locations, altitude, logger types, presence of gauge plates and the starting date of the flow monitoring sites.

River Name	Location	Coordinates	Altitude (m)	Data Logger Type	Gauge Plate	Starting Date
Jan-Swartzkraal	Elim-Spanjaardskloof Road Bridge	34.554017° S, 19.753187° E	48	Hobo Water Level Data Logger	No	5/5/2016
Upper Nuwejaars River	Elim Waste Water Treatment Plant	34.572228° S, 19.749723° E	41	OTT Orpheus Mini water level logger	No	27/4/2016
Nuwejaars River	Elim-Boskloof Road Bridge	34.578672° S, 19.757813° E	34	Hobo Water Level Data Logger	Yes	13/5/2016
Upper Nuwejaars River	Elim Flow Diversion	34.605981° S, 19.757341° E	49	Hobo Water Level Data Logger	Yes	27/4/2016
Pietersielieskloof	Farm 299	34.581193° S, 19.810442° E	43	OTT Orpheus Mini water level logger	No	27/4/2016
Blomkraals	Elim-Bredarsdorp R43 Road Bridge	34.639819° S, 19.841316° E	15	Hobo Water Level Data Logger	No	27/4/2016
Voëlvlei	Elim-Struisbaai Road Bridge	34.647549° S, 19.885179° E	10	Hobo Water Level Data Logger	Yes	27/4/2016
Nuwejaars River	Elandsdrift Bridge	34.646425° S, 19.891785° E	10	Hobo Water Level Data Logger	Yes	17/10/2014
Nuwejaars River	Wiesdrif Bridge	34.687441° S, 19.926537° E	9	Hobo Water Level Data Logger	Yes	24/10/2014
Heuningnes River	Vissersdrift	34.677811° S, 19.995915° E	7	Solinist water level data logger	Yes	17/10/2014

I) Jan Swartskraal River at Elim-Spanjaardskloof Road

The Jan Swartskraal flow monitoring site was established at the Elim-Spanjaardskloof road bridge (Table 4.4). This site presented a great challenge due to dense invasions of alien species such as; *Acacia longifolia*, *Acacia mearnsi* and further from the channels *Acacia cyclops* (Figure 4.14 A, B, C). The channels have been invaded by *Prionium serattum* (Wilde Palmiet) (Figure 4.14 D). Therefore, the selected site at the bridge was most appropriate, as the channel was straight, had a stable cross-section and was easily accessible for data collection.

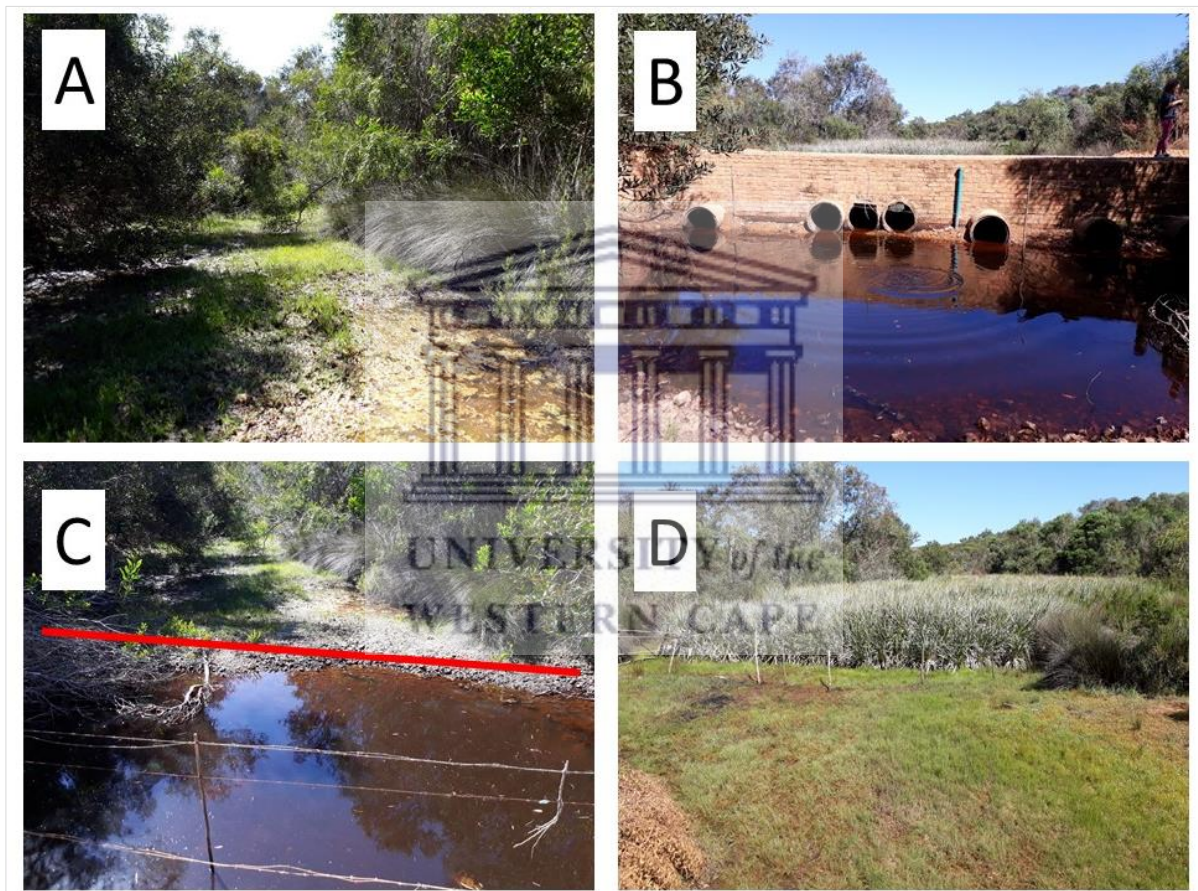


Figure 4.14: Flow monitoring site on the Jan Swartskraal River and the channel bed and bank coverage downstream of the flow monitoring site (A), bridge and stilling well installed (B), cross-section selected for flow measurements (C) and invaded channel and banks upstream of the bridge (D).

The stilling well made of a 75 mm PVC pipe was fixed to the bridge at this site and no gauge plate was installed (Figure 4.14 B). The cross-section where flow measurements were done had

a gravel bed (Figure 4.14 C). Downstream of the selected cross-section the Wilde Palmiet persisted (Figure 4.14 A). The channel bed was underlain by sandy loam soils and the banks were invaded by large *Acacia* species and reeds which aid in bank stabilization (Figure 4.14 A, C). The bankfull stage of this channel was 1.24 m (Figure 4.15). The slope at the cross-section where flow measurements were done was 0.0414 m/m.

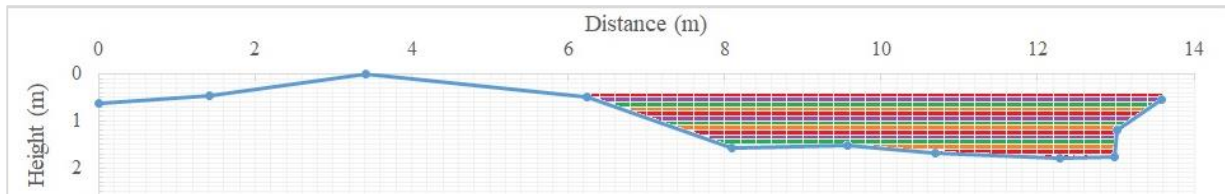


Figure 4.15: Shaded active channel of the cross-section of the Jan Swartskraal flow monitoring site

II) Koue River

The lower part of the Koue River was invaded by alien species and was not accessible. It was not feasible to establish a flow monitoring site on this channel. The flow contributions of this catchment was estimated by subtracting flows of the Jan Swartskraal River from the flows of the Nuwejaars River measured immediately downstream of the Koue and Jan Swartskraal confluence.

III) Nuwejaars River at the Elim Waste Water Treatment Plant

The Nuwejaars river begins at the confluence of the Jan Swartskraal and Koue Rivers. Three river flow monitoring sites were established along the Upper Nuwejaars River. The first of which is a minor tributary which joins the Nuwejaars River 3.8 km downstream of the confluence. This tributary occurs north west of Elim, upstream of the Elim Waste Water Treatment Plant (Figure 4.16). The tributary is referred to as the Elim Waste Water Treatment Plant (EWWTP).

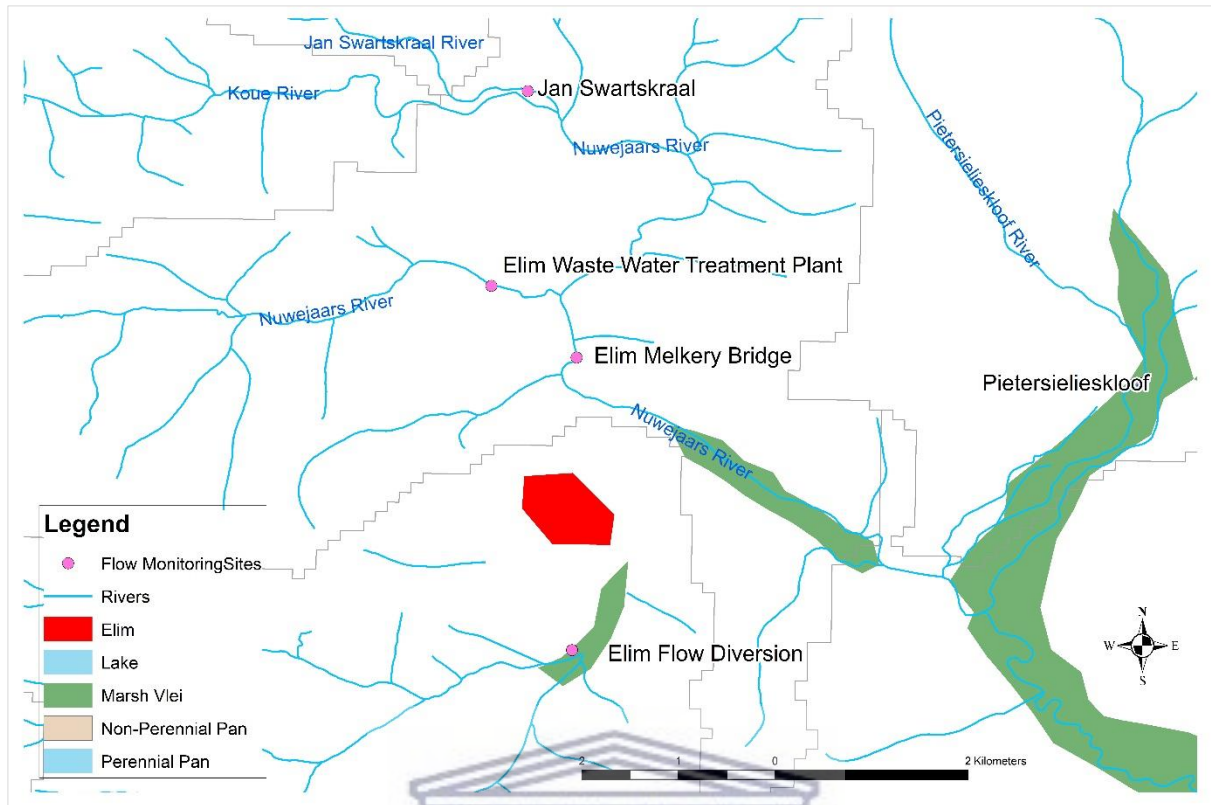


Figure 4.16: Confluence of the Jan Swartskraal and Koue Rivers with the upper tributaries of the Nuwejaars River.

The selection of the EWWTP site was challenging as this area was invaded by dense woody alien vegetation. The banks and bed of the site were covered in large trees and debris of old trees (Figure 4.17 A, B). The bed and bank consisted of sandy loam soil which provided a stable cross-section (Figure 4.17 C, D).



Figure 4.17: Downstream of the Elim Waste Water Treatment Plant flow monitoring site before and after clearing (A, B) and upstream of the site before and after clearing (C, D).

An OTT logger was installed in a PVC stilling well that was driven into the middle of the stream (Figure 4.17). A hand auger was used to drill a 2 m deep hole. The PVC pipe was then driven into this hole and stabilized using a T-bar. There was no gauge plate present at this site, however a depth measurement was taken during each visit at a fixed location against the T-bar. The bankfull stage of this channel was 1.15 m (Figure 4.19). The section circled in red does not form part of the active channel (Figures 4.17 D & 4.19) The slope of the channel at the measuring point was 0.0657 m/m.



Figure 4.18: Installation of the stilling well and a flow measurement being done during one of the peak flows at Elim Water Treatment Plant.

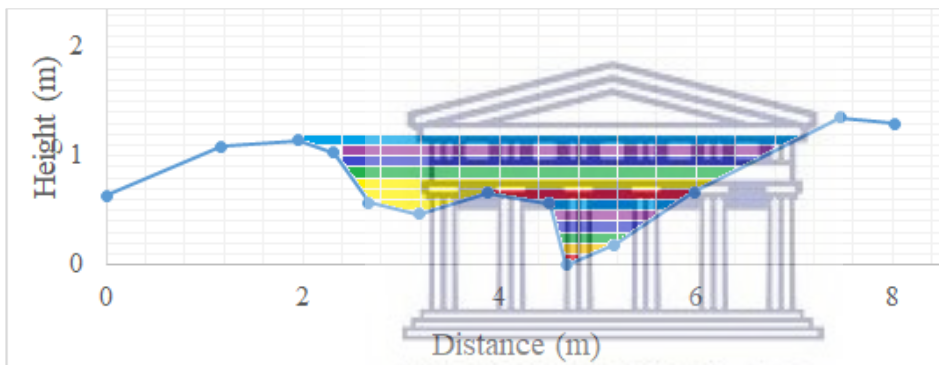


Figure 4.19: Shaded active channel of the cross-section on the upper Nuwejaars River at the Water Treatment Plant flow monitoring site used to estimate Q using Manning's Equation.

IV) Nuwejaars River at the Elim-Boskloof road bridge

The second flow monitoring station established along the Nuwejaars River was at the Elim-Boskloof Road Bridge (herein referred to as the Melkery Bridge) (Figure 4.16). This site is 4.4 km downstream of the Koue – Jan Swartskraal confluence and the EWWTP flow monitoring station.

The Elim-Boskloof road bridge was 2.2 m high and consisted of 2 rows of 24 circular culverts 1 m in diameter (Figure 4.20 A). A Hobo water level logger was placed in a PVC pipe running along the bed and bank (Figure 4.20 D) There was a gauge plate fixed to the bridge.

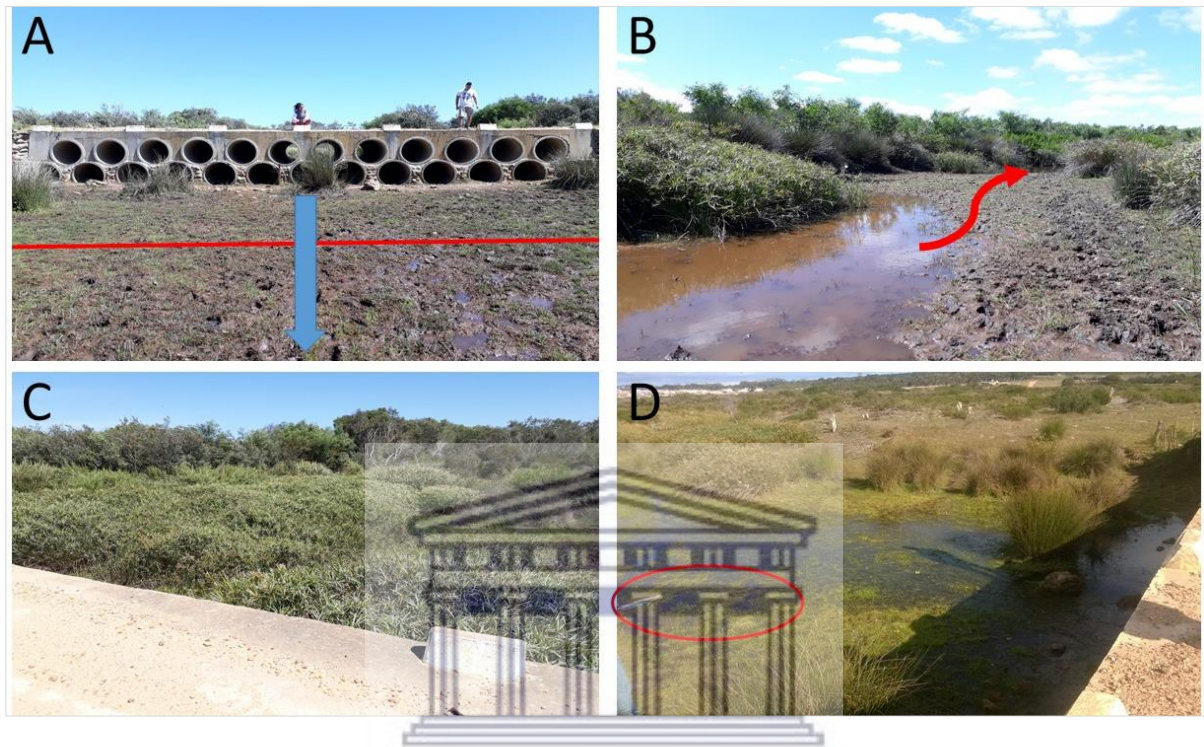


Figure 4.20: The cross-section where flow measurements were conducted on the Nuwejaars River at the Elim-Boskloof Road Bridge (A), Meander and vegetation on banks downstream of the selected cross-section (B), dense vegetation in and around the channel upstream of the bridge (C) and hidden PVC pipe with the logger installed (D).

Flow measurements were done approximately 15 m downstream of the bridge just before the channel starts to meander (Figure 4.20 B). The banks and bed were stable due to grass and reeds which grew across the bed and bank of the channel. The bed material was sandy loam. The area upstream of the bridge was invaded by reeds and alien vegetation (Figure 4.20 C). The bankfull stage was 1.8 m at this site (Figure 4.21). However, flows were too high at bankfull stage to safely conduct flow measurements (Annexure 3). The slope at this station was 0.0875 m/m.

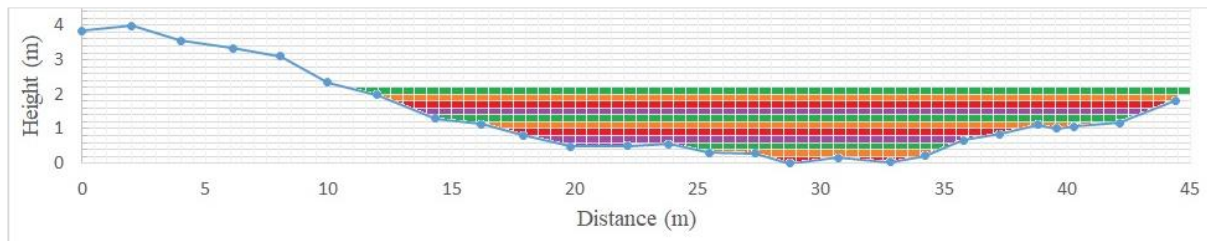
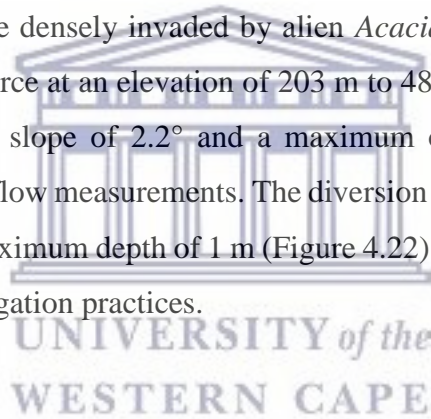


Figure 4.21: Shaded active channel of the cross-section of the Nuwejaars River at the Melkery Bridge flow monitoring station.

V) Nuwejaars River at the Elim Flow Diversion

The third river flow monitoring station established along the Upper Nuwejaars River is referred to as the Nuwejaars River Tributary at the Elim Flow Diversion (herein referred to as the Elim Flow Diversion) (Figure 4.16). This tributary has a source in the undulating plains west of the town of Elim. The banks were densely invaded by alien *Acacia* species. The tributary has a length of 7.22 km from its source at an elevation of 203 m to 48 m at the flow measuring site. The tributary has an average slope of 2.2° and a maximum of 18.2°. The flow diversion provided an ideal location for flow measurements. The diversion channel was made of concrete and was 0.97 m wide and a maximum depth of 1 m (Figure 4.22). It was installed by the people of Elim to divert flows for irrigation practices.



A stilling well was installed at the entrance of the channel and flow measurements were conducted at the same location (Figure 4.22). There was a gauge plate present at this location. The channel upstream of the weir had densely grown reeds and large *Acacia* species were also present along the banks. The composition of the bed and bank was sand, however the banks were stable due to the reeds and trees that surrounded it (Figure 4.22).



Figure 4.22: Flow measuring site along the Upper Nuwejaars River at the Elim Flow Diversion.

VI) Pietersielieskloof River at Farm 299

Due to the removal of alien vegetation and lack of rehabilitation, stream erosion occurs and a large amount of sediment is transported downstream on this river (Figure 4.23 C). The flow monitoring station was established on Farm 299 close to the confluence with the Nuwejaars River.

The bed and bank material were sandy and this river transports high amounts of sediment downstream as reported during a discussion with the farm owner. This was the result of clearing of invasive trees upstream of this location, and excessive erosion which took place in the Palmiet wetlands in the upper parts of the Pietersielieskloof sub-catchment (Figure 4.23 C). As was the case in many of the areas, the bank was densely invaded by alien *Acacia* species (Figure 4.23 A, B).

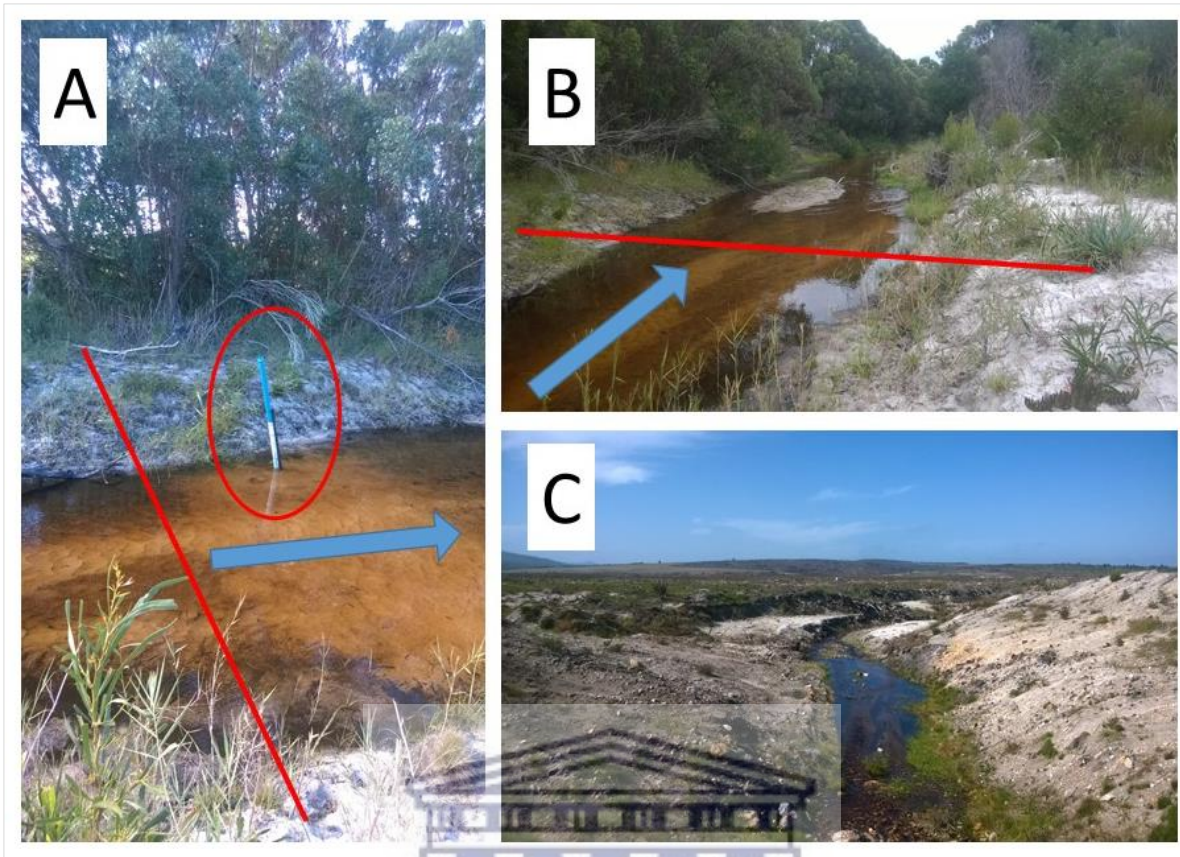


Figure 4.23: Cross-section where flow measurements were conducted and the stilling well installed (A) and cross-section along the straight channel with sandy bed and banks invaded by alien *Acacia* species at the Pietersielieskloof flow monitoring site (B). Erosion of Palmiet wetlands along the Pietersielieskloof River upstream of the flow monitoring site located on Farm 299 (C).

The stilling well was installed by auguring a 2 m deep hole, placing PVC pipe in it and stabilizing it between two T-bars as close to the centre of the stream as possible (Figure 4.23 A). The bankfull discharge occurs at 1.82 m at this site (Figure 4.24). The slope for the Pietersielieskloof monitoring site was 0.0158 m/m.

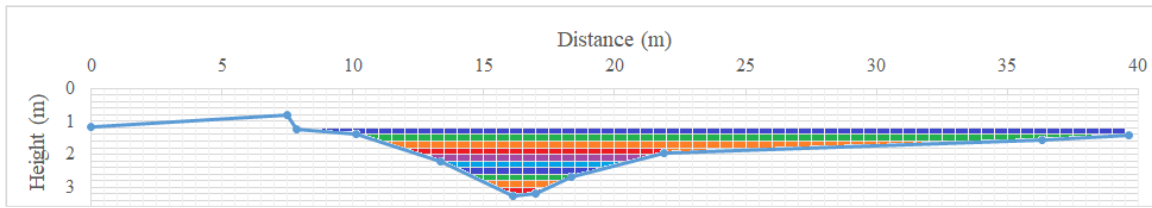


Figure 4.24: Shaded active channel of the cross-section of the Pietersielieskloof River.

VII) Nuwejaars River at Elandsdrift

The Elandsdrift flow monitoring site was established prior to this study on the 17/10/2014 by the Institute for Water Studies at UWC. A blue PVC pipe (75mm in diameter) was fixed to the bridge and secured with a cap, bolt and lock nut (Figure 4.25 A).

The bridge is made up of two concrete culverts each 1.56 m high, while the right culvert is 2.52 m wide and the left is 2.62 m wide (Figure 4.25 B). This location is ideal for flow measurements as the culverts ensured that the cross-sectional area is stable. However, the presence of ponds upstream and downstream of the bridge may affect the measurement of flow due to backflow during high flows (>1.5 m) flows.



Figure 4.25: Stilling well installed at Elandsdrift (A) and the Elandsdrift bridge during the selection of the flow monitoring site in 2014 (B).

VIII) Voëlvlei River at the Elim-Struisbaai road bridge

The Voëlvlei flow monitoring site is located 0.9 km upstream of the Elandsdrift flow measuring site where it converged with the Nuwejaars River. Flow measurements were done at the Elim-Struisbaai Road Bridge downstream of the Voëlvlei Lake (Figure 4.26). The bridge has one culvert, 5.7 m wide and 1.88 m high (Figure 4.26 A). The flow direction at this site depends on the water levels of the Nuwejaars River and the Voëlvlei Lake. Reverse flows occur during rapid increase of flows when the water level of the Nuwejaars River exceeds that of the Voëlvlei Lake.

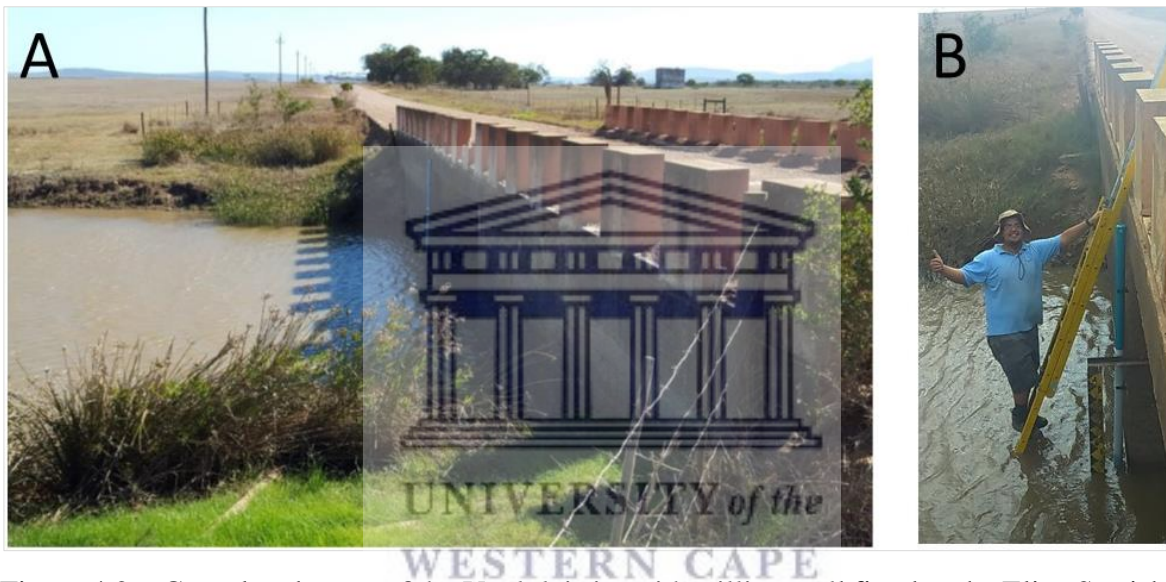


Figure 4.26: Completed setup of the Voëlvlei site with stilling well fixed to the Elim-Struisbaai Road Bridge alongside the gauge plate (A) and installation of the stilling well (B).

IX) Blomkraals River at R43 road bridge

A flow measuring station was established on the Blomkraals River at the R43 Elim-Bredarsdorp Road Bridge. The stilling well was fixed to the 4.7 m high bridge pier. There was no gauge plate at this bridge, however a levelling staff was used to measure water levels at a fixed location, marked with paint close to the stilling well (Figure 4.27 A).

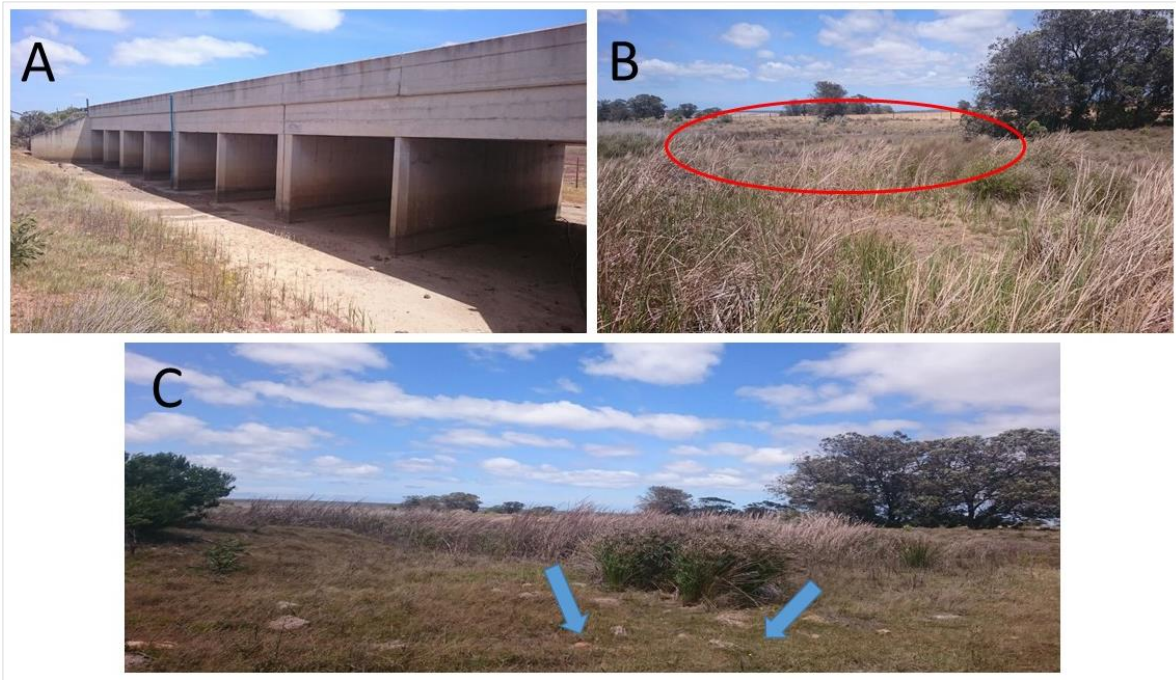


Figure 4.27: Stilling well installed at the Blomkraals site and the culverts used for the initial flow measurements (A), pond upstream of the Blomkraals flow monitoring station which requires flooding before flow occurs through the bridge (B), cross-section of the area where flow measurements were done for the remainder of the study (C).

Approximately 4 m upstream of the cross-section where flows were measured is a dense coverage of reeds and grass (Figure 4.27 A, B). The river bed consisted of grass and reeds underlain by cobbles and stones (Figure 4.27 A, B). The cross-section where flows were measured was 35.5 m upstream of the bridge and upstream of the sharp dip circled in Figure 4.27. The bankfull discharge occurred at 2.24 m (Figure 4.28) and the slope at the flow measuring station was 0.0256 m/m.

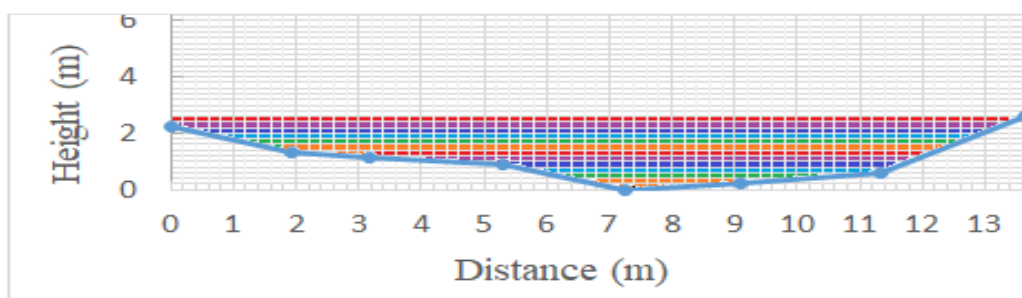


Figure 4.28: Shaded active channel of the cross-section of the Blomkraals River.

4.3.5. Rating curves

The number of discharge measurements done at each of the stations varied due to the frequency of occurrence of flows. Only 4 flow measurements were conducted at the Jan Swartskraal and EWWTP flow monitoring stations as they were dry during the dry season (Table 4.5). The Elandsdrift and Voëlvlei stations have the highest number of measurements as these sites were monitored since 2014.

Table 4.5: Number of discharge measurements done at each of the flow monitoring sites.

Flow Measuring Station	No. of Discharge Measurements
Jan Swartskraal	4
UNJ @ Elim waste water treatment plant	4
UNJ @ Elim-Spanjaardskloof road bridge	7
Pietersielieskloof	5
UNJ @ Elim flow diversion	8
Blomkraals	4
Voëlvlei	13
Nuwejaars @ Elandsdrift	16
Total	61

The rating curve for Elandsdrift was derived using discharge measurements made over 3 years (Figure 4.29). The following rating equation (4.4) was derived from flow measurements made.:

$$Q = 0.0959 \exp^{2.4798H} \quad (4.4)$$

where Q is discharge in m^3/s and H is the stage in metres. It is important to note that Equation 4.4 is only accurate to a maximum of 1.85 m, which was the highest stage at which discharge was measured and should be used with caution when flows exceeded this stage.

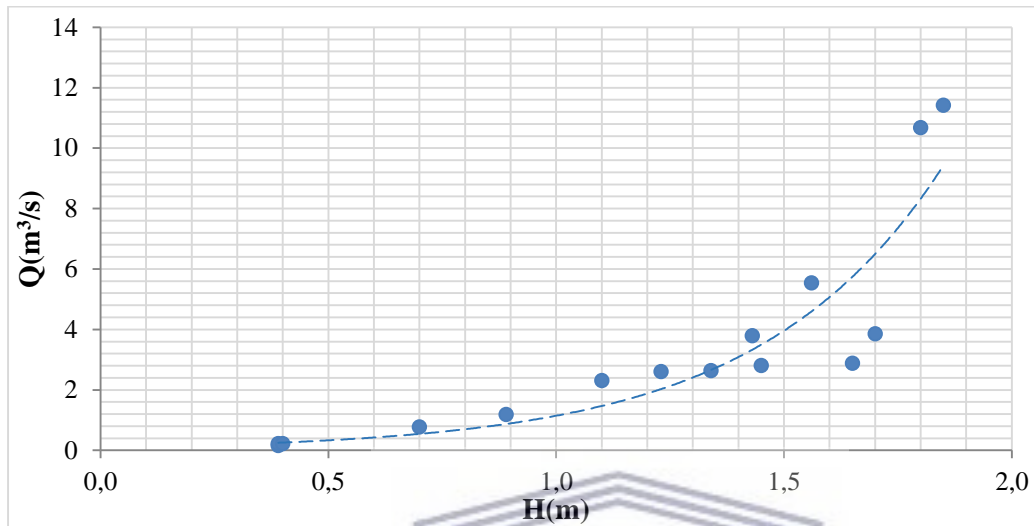


Figure 4.29: Rating curve derived for the Nuwejaars River at Elandsdrift using discharge measurements from 2015 – 2016.

The derivation of the rating curve for Voëlvlei River was problematic due to the occasional occurrence of reverse flows. There are occasions when flows moved from the Nuwejaars River into Voëlvlei. This was due to a sudden increase of water levels along the Nuwejaars River, while at the same time there has not been any rainfall over the Voëlvlei sub-catchment. Thus water levels along the Voëlvlei River will be lower than in the Nuwejaars River.

Table 4.6 shows the discharges measured at the Voëlvlei bridge when reverse flows occurred. The rating curve for Voëlvlei is only applicable when flows occur from Voëlvlei to the Nuwejaars River, and in the absence of reverse flow (Figure 4.30). The following equation may be used to estimate Q with adequate confidence where H does not exceed 2.9 m (Equation 4.5).

$$Q = 0,0303H^{4,414} \quad (4.5)$$

Table 4.6: Occasions when reverse flows occurred from the Nuwejaars River into Voëlvlei

Date	Discharge (m ³ .s)	Stage (m)
29/06/2016	0,1	1,34
13/07/2016	0,078	1,35
27/07/2016	3,681	2,09
25/08/2016	2,401	2,22

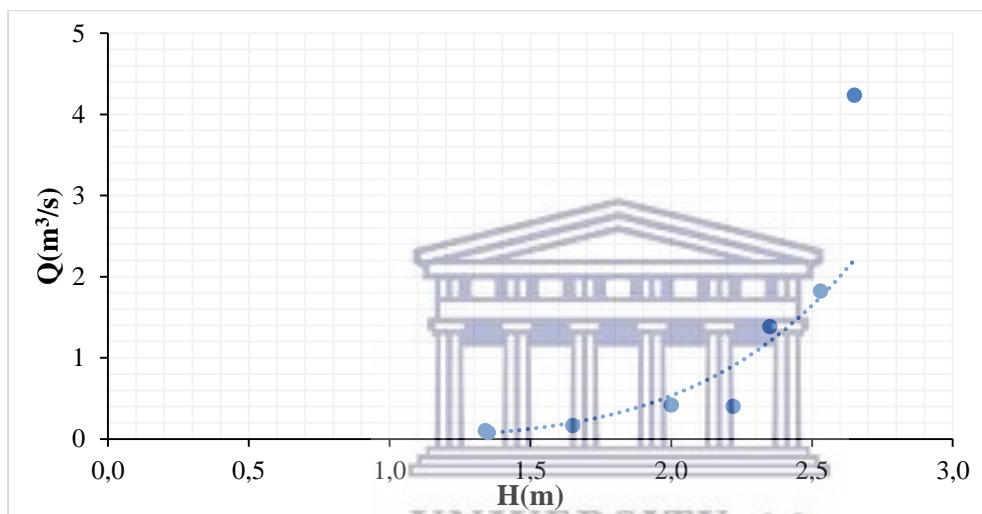


Figure 4.30: Rating curve derived for the Voëlvlei tributary using the discharge measurements from 2015 to 2016.

For the Blomkraals River there were only 4 discharge measurements made. The Manning's equation with a roughness coefficient of $n = 0.15$ and slope of 0.0256° was used to describe the rating curve (Figure 4.31). The 4 discharge measurements were used to improve the estimation of the roughness coefficient. The cross-sectional area and hydraulic radius were estimated from the survey data (Figure 4.28). The Blomkraals rating equation can therefore be used with high confidence as long as H does not exceed 1.5 m (Equation 4.6). The following rating equation was derived for the Blomkraals River:

$$Q = 1.844 H^{3,002} \quad (4.6)$$

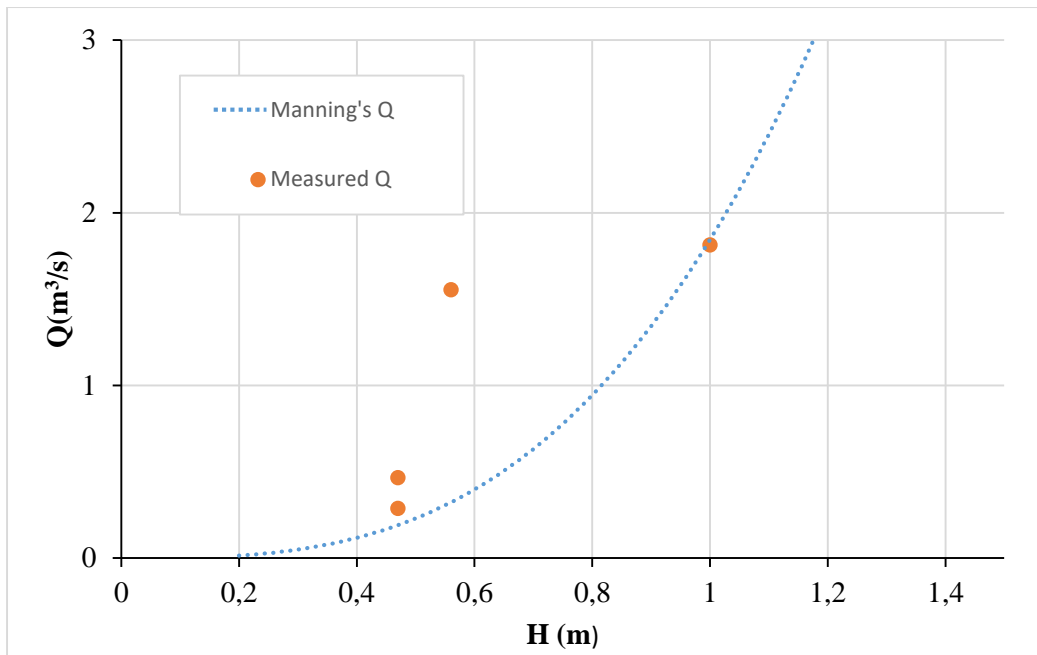


Figure 4.31: The rating curve derived for the Blomkraals River.

For the Melkery Bridge tributary there were 7 discharge measurements made. However, it was not possible to safely measure when flows exceeded 1 m. Two rating curves were used to develop the rating curve for the Melkery Bridge tributary as at very low water levels the flows follow the channel bed and as the water level increases the slope of the water approximates to that of the general surface along this river.

The first rating curve was produced from a stage of 0 m to 1 m, with a slope of 0.00002 m/m (Figure 4.32 A). The second rating curve was produced from a stage of 1 m to 2 m, with a slope of 0.00002 m/m at low stage and 0.0015 m/m at high stage (Figure 4.32 B). A roughness coefficient of $n = 0.045$ was used for both rating curves. The two rating curves were combined and the 7 discharge measurements were used to improve the estimation of the roughness coefficient (Figure 4.32 C). The cross-sectional area and hydraulic radius was estimated from the survey data (Figure 4.21). The discharge for the Nuwejaars River at the Melkery Bridge flow monitoring station can therefore be estimated using the following equations:

$$Q = 1.433H^{1.667} \quad (4.7a)$$

$$Q = 9.165 - 34.955H + 27.559H^2 \quad (4.7b)$$

For water depths between 0 m and 1 m Equation 4.7a was used and for water depths greater than 1 m Equation 4.7b was used. Equations 4.7a and 4.7b can estimate Q based on H with high confidence where $H < 1$ m. However, when H exceeds 1 m this equation should be used with caution.

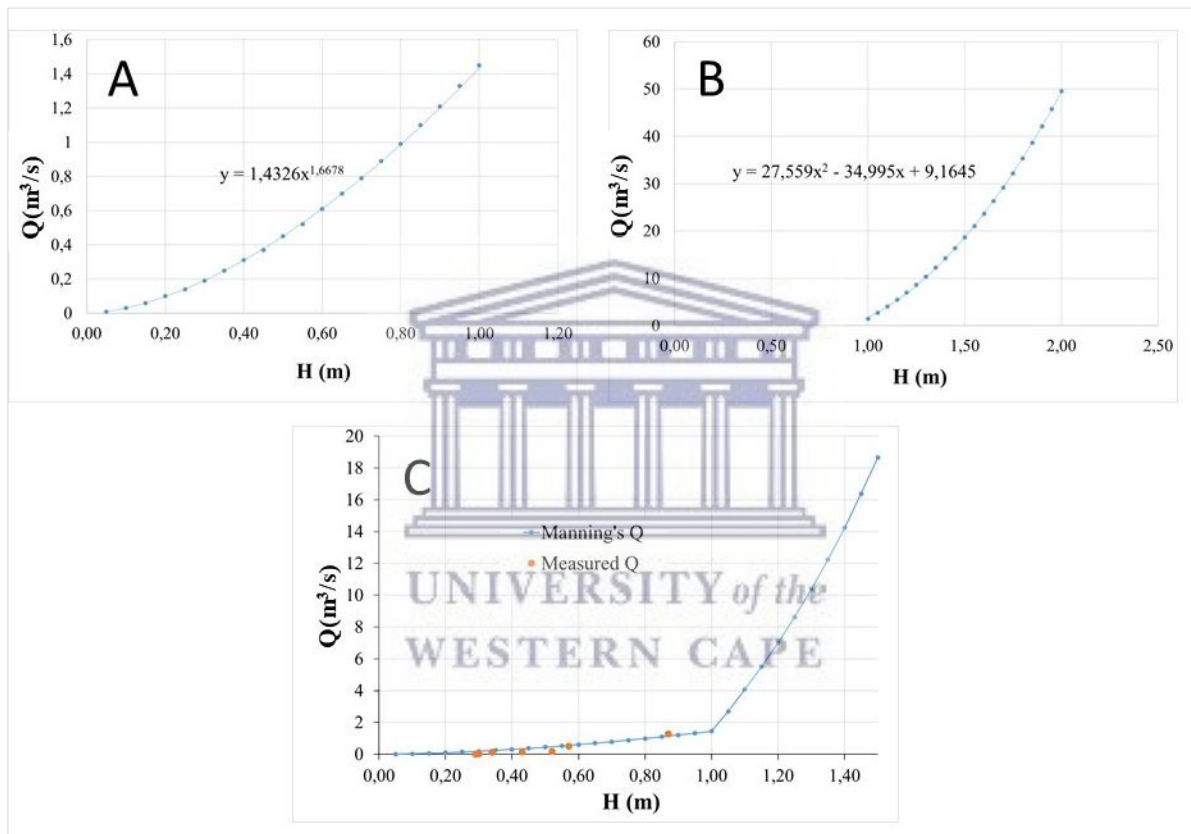


Figure 4.32: Rating curve produced for the Melkery Bridge tributary from 0 m to 1m (A), 1 m to 2m (B) and the combined rating curves with measured discharges (C).

Of the 5 flow measurements done at Pietersielieskloof flow measurement site the highest water level at which discharge Q was measured was 0.25 m. Flows could not be done during peak flows due to accessibility and safety (Annexure 3). The Manning's equation with a roughness coefficient of $n = 0.035$ and slope of 0.0158 m/m was used to derive the rating curve. The roughness coefficient was improved using the 5 discharge measurements (Figure 3.33). The

cross-sectional area and hydraulic radius were estimated from the survey data (Figure 4.24). The following rating equation (Equation 4.8) below was produced and can be used with high confidence. However, it is important to note that the equation will have low confidence in estimating Q when $H > 1,5$ m.

$$Q = 7.4706H^{2.2025} \quad (4.8)$$

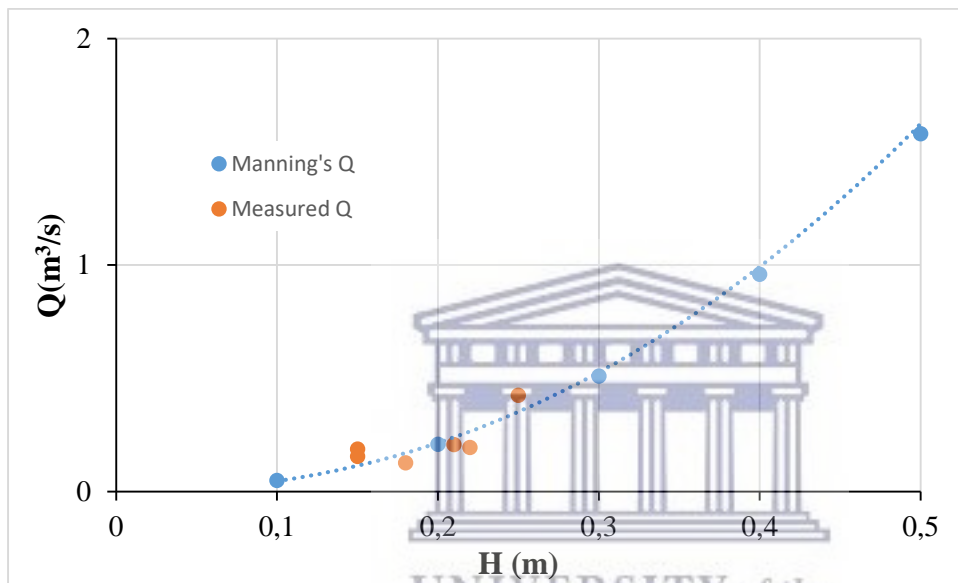


Figure 4.33: Rating curves produced using Manning's equation and the measured Q values for Pietersielieskloof tributary.

The Manning's equation with a roughness coefficient of $n = 0.25$ and slope of 0.0414 m/m was used to derive the rating curve for the Jan Swartskraal tributary. Water levels did not often exceed 0.5 m at this site and when it did, flow measurements could not be done safely (Annexure 3). However, 4 discharge measurements were done at this site and used to improve the estimation of the roughness coefficient (Figure 4.34). The cross-sectional area and hydraulic radius were estimated from the survey data (Figure 4.15). The following rating equation (Equation 4.9) was produced using the measured Q values, with a high confidence in Q estimations when $H > 0,5$ m:

$$Q = 3.0568H^{2.1997} \quad (4.9)$$

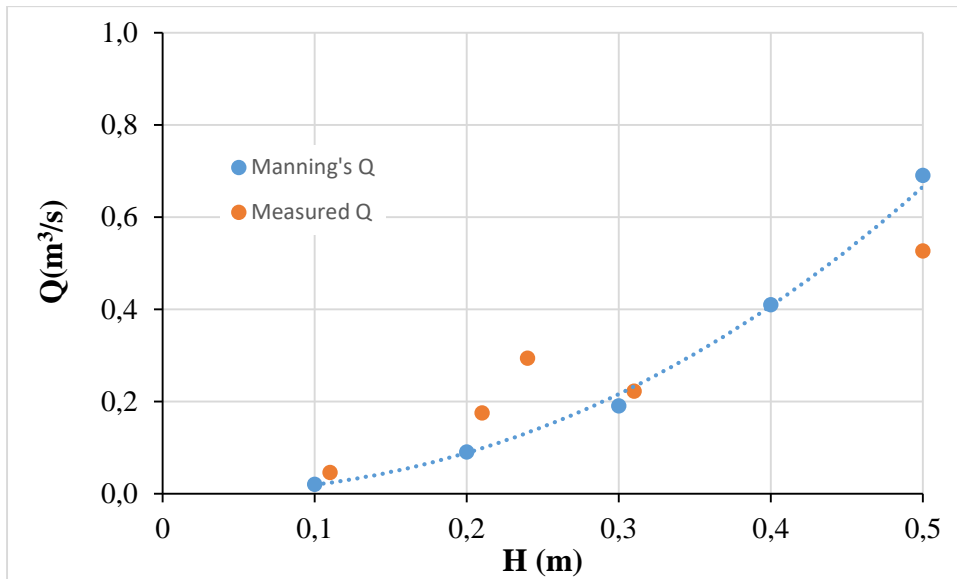


Figure 4.34: Rating curves produced using Manning's equation and the measured Q values for the Jan Swartskraal tributary.

The rating curves derived for the Elim Flow Diversion and the EWWTP tributaries were unreliable and therefore were not used to estimate discharge. At the Elim Flow Diversion the opening and closing of the sluice gate affected the accuracy of the discharge measurements. The discharge of the channel is dependent on the width of the opening of the sluice gate. It was therefore decided that this site would only be used to determine the water level responses of the tributary as there were uncertainties about the duration and width of the opening of the sluice gates.

4.3.6. Daily variations of river water levels

The Elandsdrift flow monitoring station had the longest record of water level data, spanning 795 days from the time it was installed in 2015 (Figure 4.35). The gaps in water level data were due to servicing and removal of the loggers during the dry season, when little to no flow occurred. The only tributaries which had flows throughout the year were the Elim Flow Diversion and Pietersielieskloof tributaries and this will be discussed in more detail further in this chapter (Figure 4.35). Additionally, the loggers were used by multiple students at the same locations and may have been stopped during visits. As flow measurements were only done on

a bi-weekly basis an error such as this resulted in a minimum loss of 2 weeks' worth of data. However, at the time these errors took place, the water levels of all the channels were near zero and by mid-January 2017 all the channels were completely dry (Figures 4.36 and 4.37).

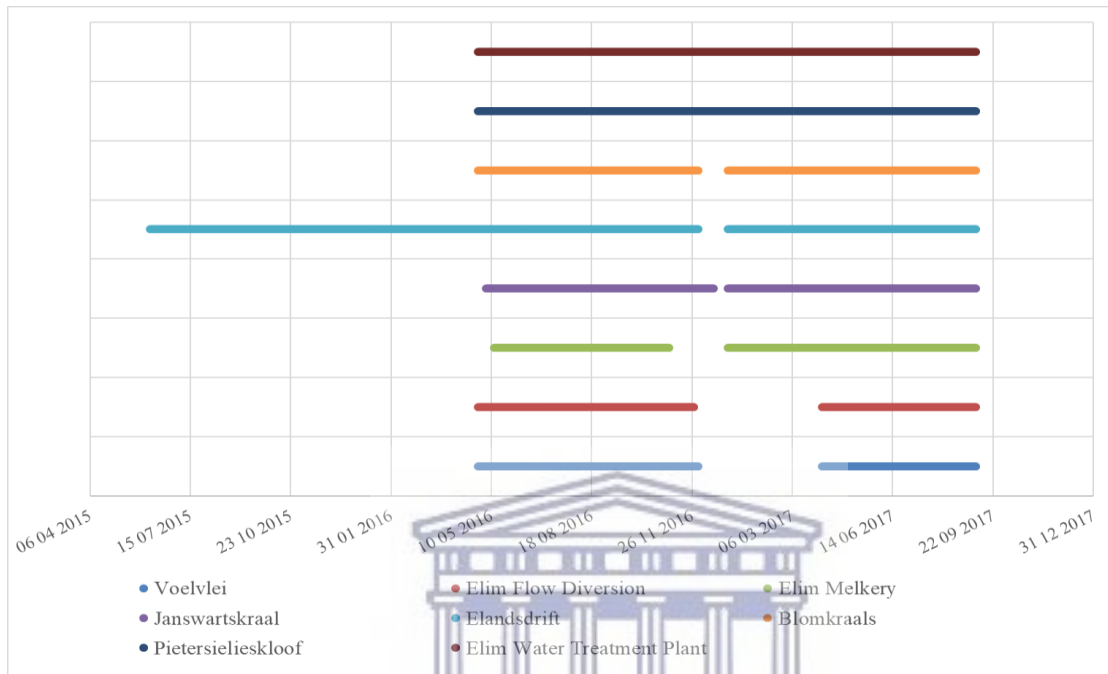


Figure 4.35: The record lengths of collected water level data for all the sites until the 5th September 2017.



Most of the rivers were dry or had no major changes until the 10th June 2016 (Figure 4.36). An immediate increase in water levels of 0.1 m was noted at the Elim Flow Diversion and Pietersielieskloof sites to the rainfall event recorded at Spanjaardskloof of 27 mm/day. However, all the other sites except for the EWWTP showed a delayed response of a few hours to this rainfall event.

The largest rainfall event in 2016 occurred between the 25th and 26th July, 92.2 mm rainfall was recorded at the Moddervlei station within in 24 hr period. It was at this point that the EWWTP had its first response in water level, from 0 m to 1.61 m. The Melkery Bridge tributary peaked at 2.11 m, Elandsdrift at 1.76 m, Blomkraals at 1.37 m, Voelvlei at 1.31 m, Elim Flow Diversion at 0.94 m, Jan Swatskraal at 1.15 m and Pietersielieskloof at 0.82 m (Figure 4.36).

A flow monitoring trip was conducted at the time of this event (Annexure 3) but due to the intensity of flows, many sites could not be accessed as bridges were flooded and the magnitude of flows were too great to measure safely.

The Voëlvlei and Elandsdrift tributaries showed a very similar decline in water level following the major event from the 25th to 26th July. However, the water level at Elandsdrift was always slightly higher during high flows. In addition, when flows reached approximately 0.5 m at the Elandsdrift and Voëlvlei monitoring sites, the water level of the Nuwejaars River at Elandsdrift would be lower than that of the Voëlvlei tributary. The upper tributaries all showed similar responses to the rainfall events (Figure 4.36).

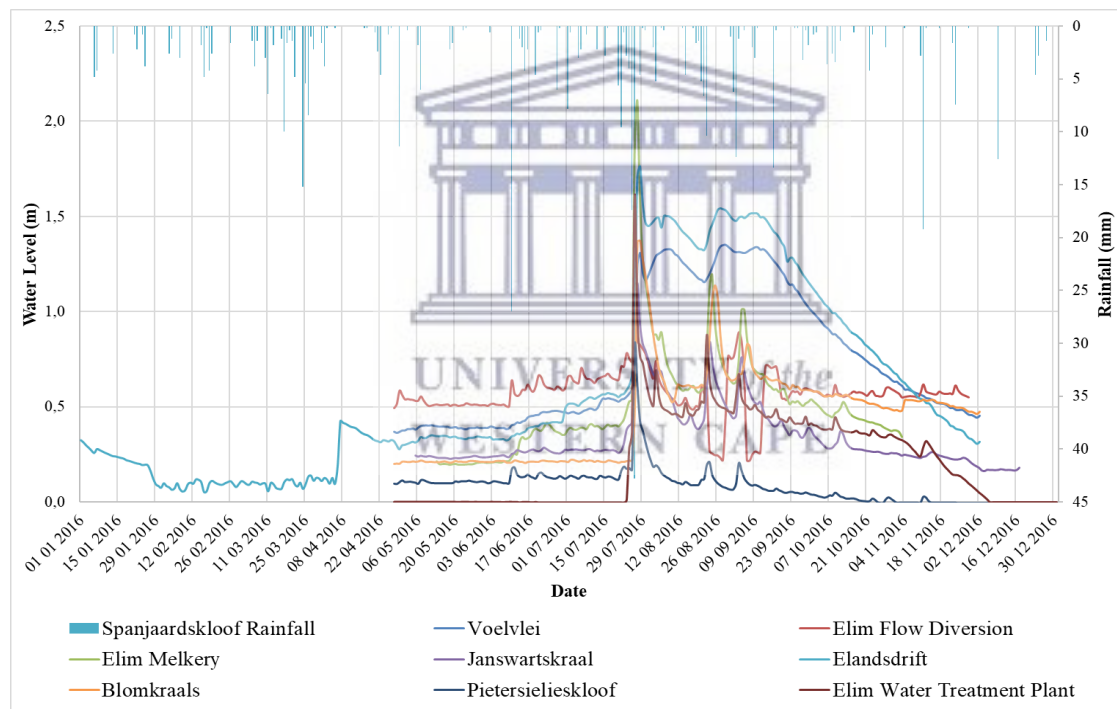


Figure 4.36: Daily variation of water levels for 2016.

From the 6th April 2017 all the streams had water levels less than 0.1 m except for the Elim Flow Diversion which averages at 0.5 m. The first response noticed in the channels occurs after the 7th June when 44 mm/day was recorded at the Spanjaardskloof rain gauge (Figure 4.37). The first major response at Elandsdrift was only noted after the 6th July. The Blomkraals site did not show any response in this year and surprisingly the Elandsdrift site which was the

furthest downstream was the first to respond, while the upper tributaries only responded later. Water levels in the sub-catchments never exceeded 0.5 m up until the 5th September 2017 (Figure 4.37).

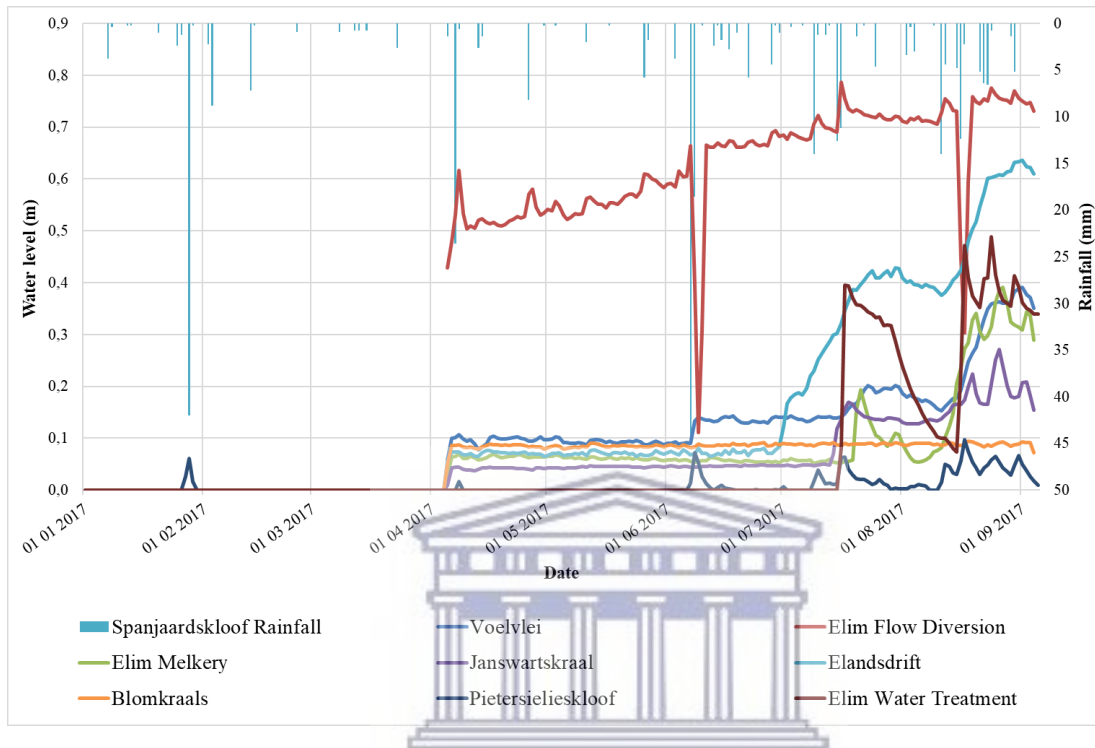


Figure 4.37: Daily variations of water levels from January 2017 to 5th September 2017.

4.3.7. Discharge estimates of sub-catchments

The month with the highest discharge was recorded in August 2016 at the Elandsdrift site. A total of 11.57 Mm³ was recorded for August 2016 with an average of 0.37 Mm³/day at Elandsdrift. However, the maximum daily discharge for 2016 was recorded on the 28th July 2016 at 0.81 Mm³/day (Figure 4.38). The maximum daily discharge in the upper catchment was recorded on the 27th July 2016 at 4.34 Mm³/day at the Melkery Bridge and only reached the Elandsdrift site the next day. The Elandsdrift site showed a gradual decrease in daily discharge from 11.57 Mm³/day for the month of August 2016 to 2.5 Mm³/day in October 2016. On the other hand, the upper tributaries dropped immediately following the major rain event to less than 1 Mm³ per month (Figure 4.38).

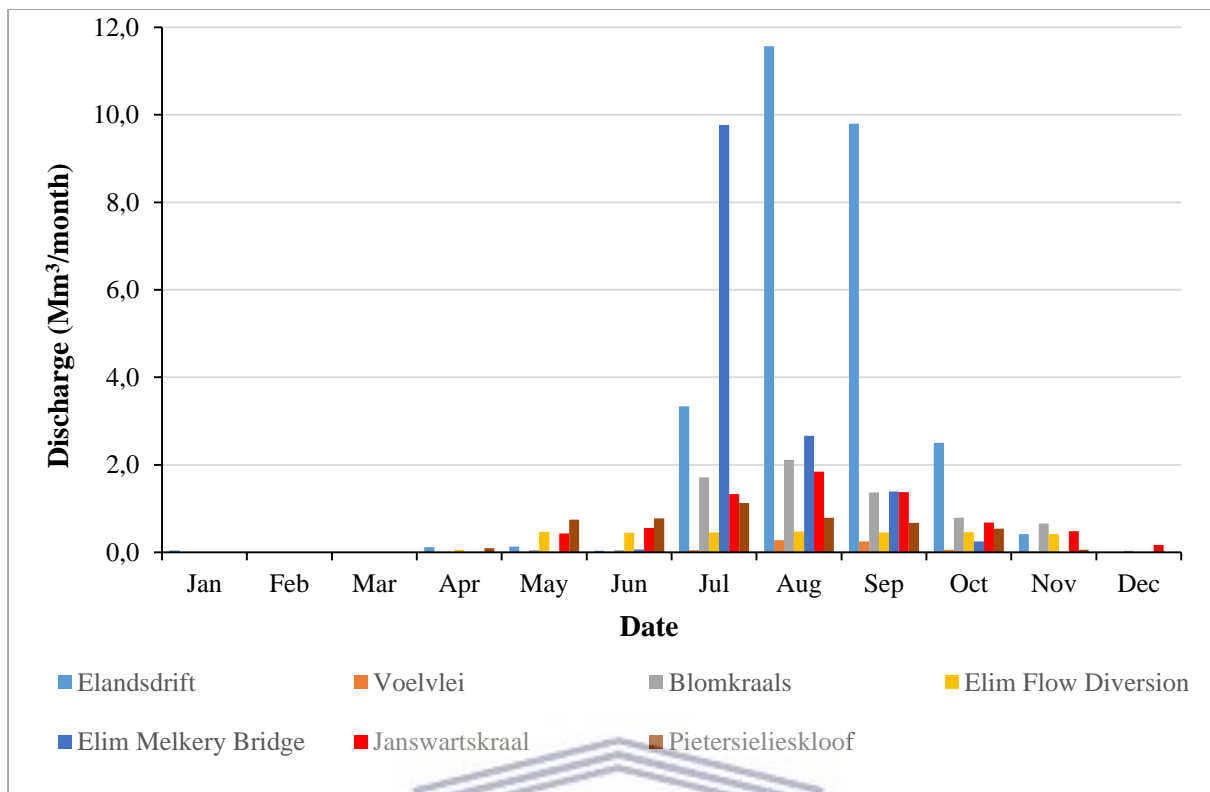


Figure 4.38: Monthly discharge (Mm³/month) of 7 of the flow monitoring sites for 2016

In 2016, 48 % of the annual inflows were recorded at the Melkery Bridge site, 23 % of which was contributed by the Janswarskraal sub-catchment and the other 25 % was split between the Koue sub-catchment and the EWWTP tributary. The total annual discharge recorded at Elandsdrift was 27.97 Mm³/yr and accounted for 94 % of the total inflows which was 29.63 Mm³/yr (Figure 4.39).

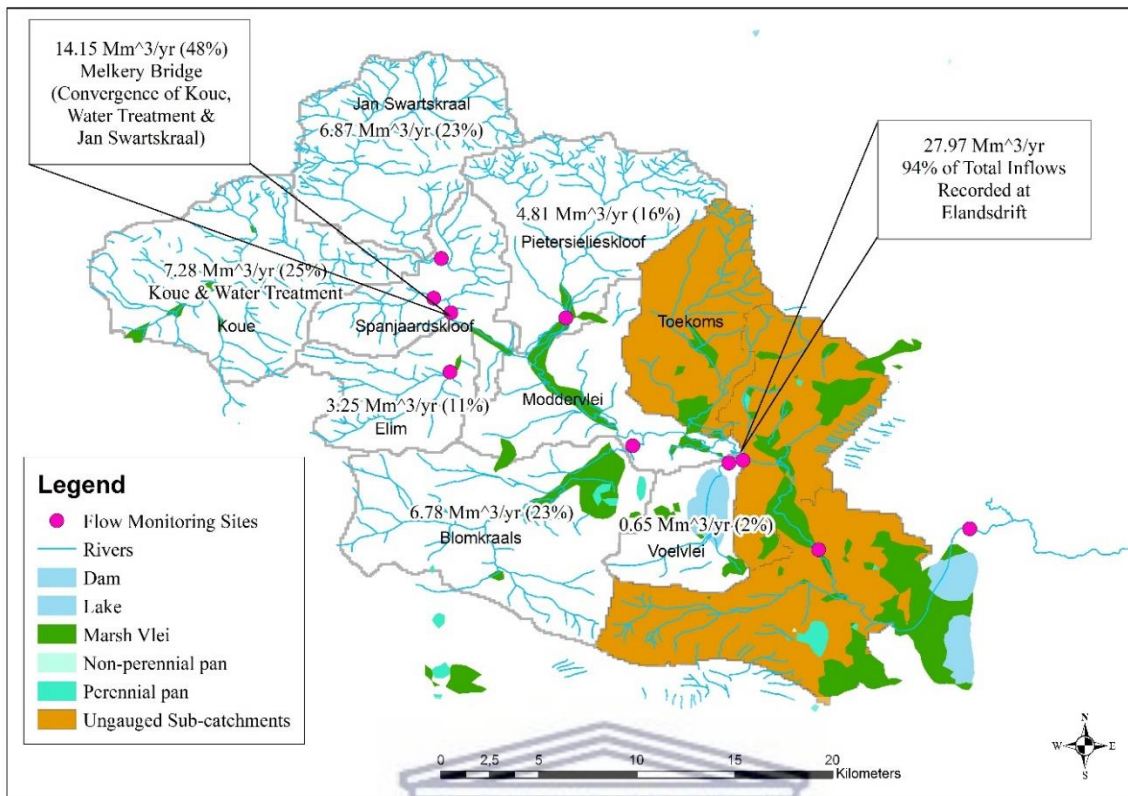


Figure 4.39: Annual contribution to flows from the each of the sub-catchments of the Nuwejaars Catchment for 2016.

From the beginning of 2017 to the 4th September 2017 only 0.68 Mm³ of inflows was measured on the Nuwejaars River at Elandsdrift. An average discharge of 14 000 m³/day was recorded during the month of August 2017 at this site with a total of 0.43 Mm³ for the month (Figure 4.40). There were significantly less flows in 2017 than compared to 2016. The Pietersielieskloof and Elim Flow Diversion sites showed similar average monthly discharges of 0.4 Mm³ per month in comparison to 2016. However, the peak flows were significantly low in 2017 (Figure 4.40). The missing data from the beginning of 2017 to the 5th April 2017 was due to servicing of the equipment (Figure 4.40).

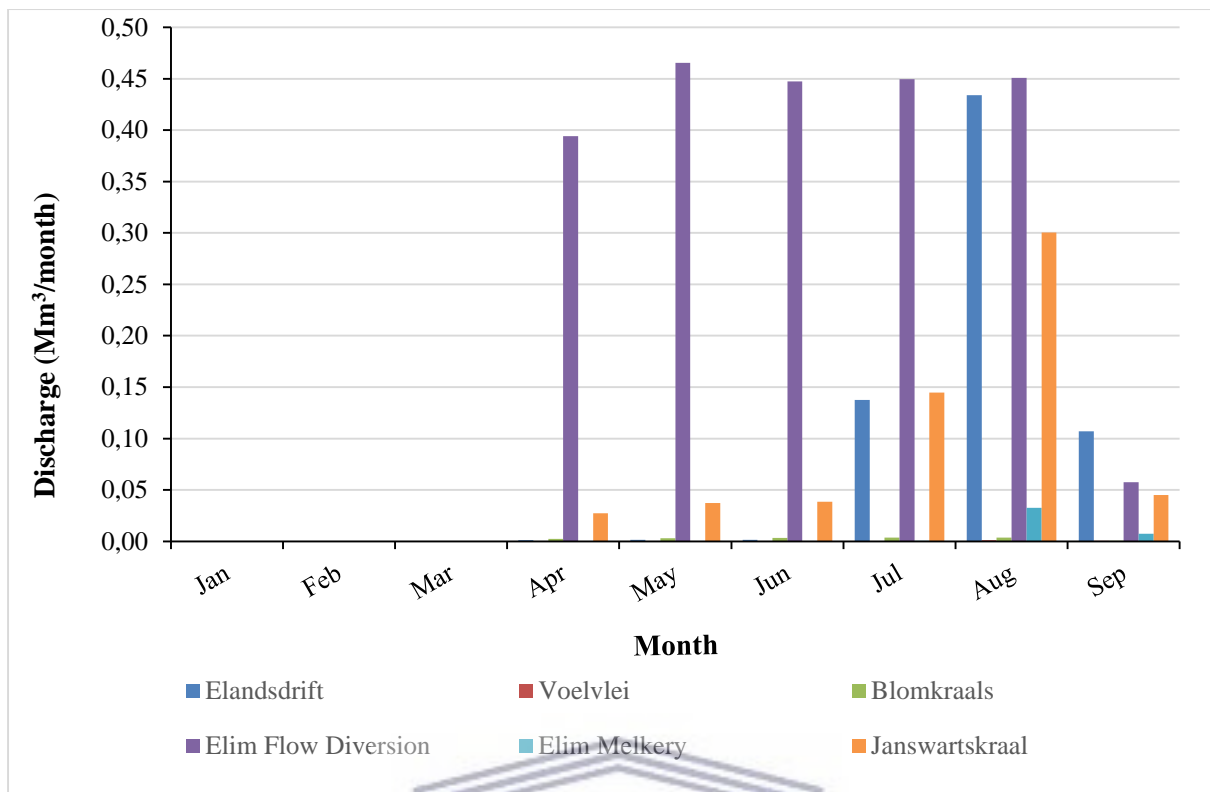


Figure 4.40: Monthly discharge (Mm^3/month) of 6 of the flow monitoring sites from January 2017 to the 4th of September 2017.

The Nuwejaars River at the Elim Flow Diversion tributary contributed 60 % of the inflows estimated during 2017. 0.59 Mm^3 was estimated from the Janswarskraal sub-catchment which accounted for 16 % of the total inflows for 2017. 1.42 Mm^3 of flow was contributed by the Pietersielieskloof sub-catchment and accounted for 38 % of the inflows for 2017 (Figure 4.41). The total inflows at Elandsdrift for 2017 was 0.68 Mm^3 and accounted 18 % of the total inflows from the main tributaries of the Nuwejaars River (Figure 4.41).

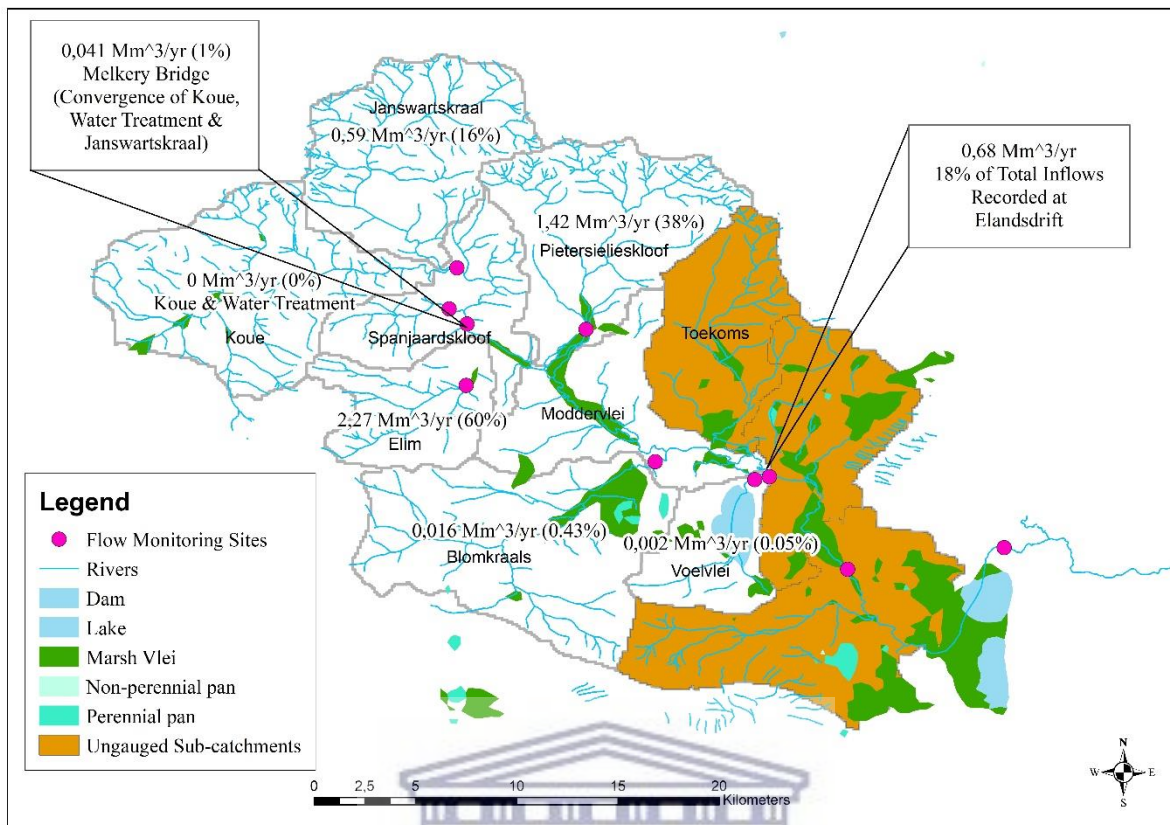


Figure 4.41: Annual contribution to flows from each of the sub-catchments of the Nuwejaars Catchment from January 2017 to the 4th of September 2017.

4.3.8. Sub-catchment responses to rainfall events

In the beginning of the wet season the tributaries showed very little to no response to rainfall events. However, during the first major rainfall event recorded at the Spanjaardskloof station, on the 29th April 2016, the Nuwejaars River at the Elim Flow Diversion showed an increase in water level of 0.1 m after 4 hours (Figure 4.42 A). In addition, this tributary responded similarly to the second event on the 10th June 2016 and responded 4 hours after rainfall occurred. The Pietersielieskloof tributary responded after 14 hours, the Nuwejaars River at the Melkery Bridge showed an increase of 0.1 m 82 hours after rainfall occurred, the Jan Swartskraal tributary responded after 57 hours and the remaining tributaries showed no response (Figure 4.42 B).

During mid wet season the largest event of 2016 occurred on the 25th July 2016. 92.2 mm of rainfall was recorded at the Moddervlei station within in a 22 hr period. The Nuwejaars River at the Elim Flow Diversion showed a more delayed response than in the beginning of the wet season and only responded after 9 hours. The Pietersielieskloof tributary responded similarly to the beginning of the wet season and responded after 14 hours to the event. The Jan Swartskraal tributary and Nuwejaars River at the Melkery Bridge responded quicker during the mid-wet season and responded after 13 hours and 10 hours respectively. The Voëlvei tributary responded after 39 hours and the Blomkraals tributary after 31 hours. The Nuwejaars River flows took 40 hours to reach Elandsdrift (Figure 4.42 C).

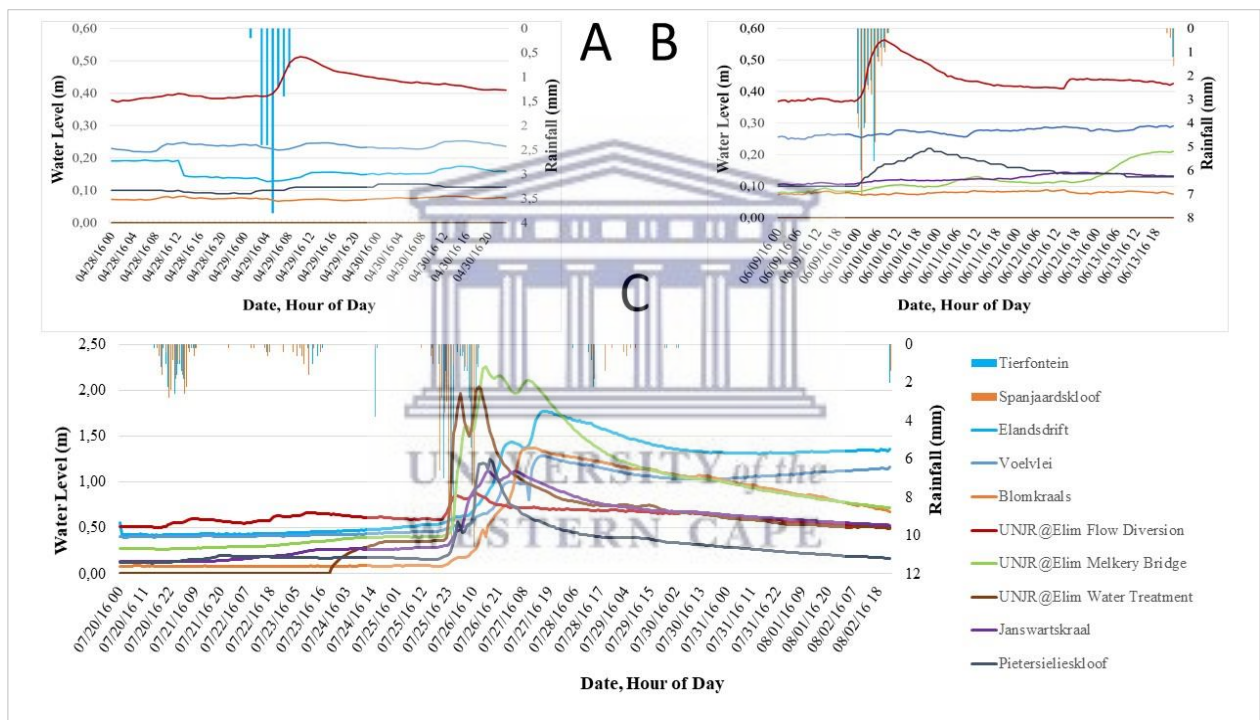


Figure 4.42: Hourly responses of the monitored tributaries to selected rainfall events during the wet season, from the 28th April to 30th April 2016 (A) and from the 9th June to 13th June 2016 (B) prior to the major event which occurred between the 25th and 26th July 2016 (C).

Towards the end of the wet season it took 105 hours for flows from the Melkery Bridge to reach Elandsdrift along the Nuwejaars River. The Blomkraals tributary responded after 82 hours, more than twice the amount of time compared to the response times mid wet season. The Nuwejaars River at the Elim Flow Diversion responded similarly to the beginning of the

wet season, responding after 4 hours. The response times of the Nuwejaars River at the Melkery Bridge, the Jan Swartskraal tributary and Pietersielieskloof tributary more than doubled and responded after 41 hours, 32 hours and 20 hours respectively (Figure 4.43 A).

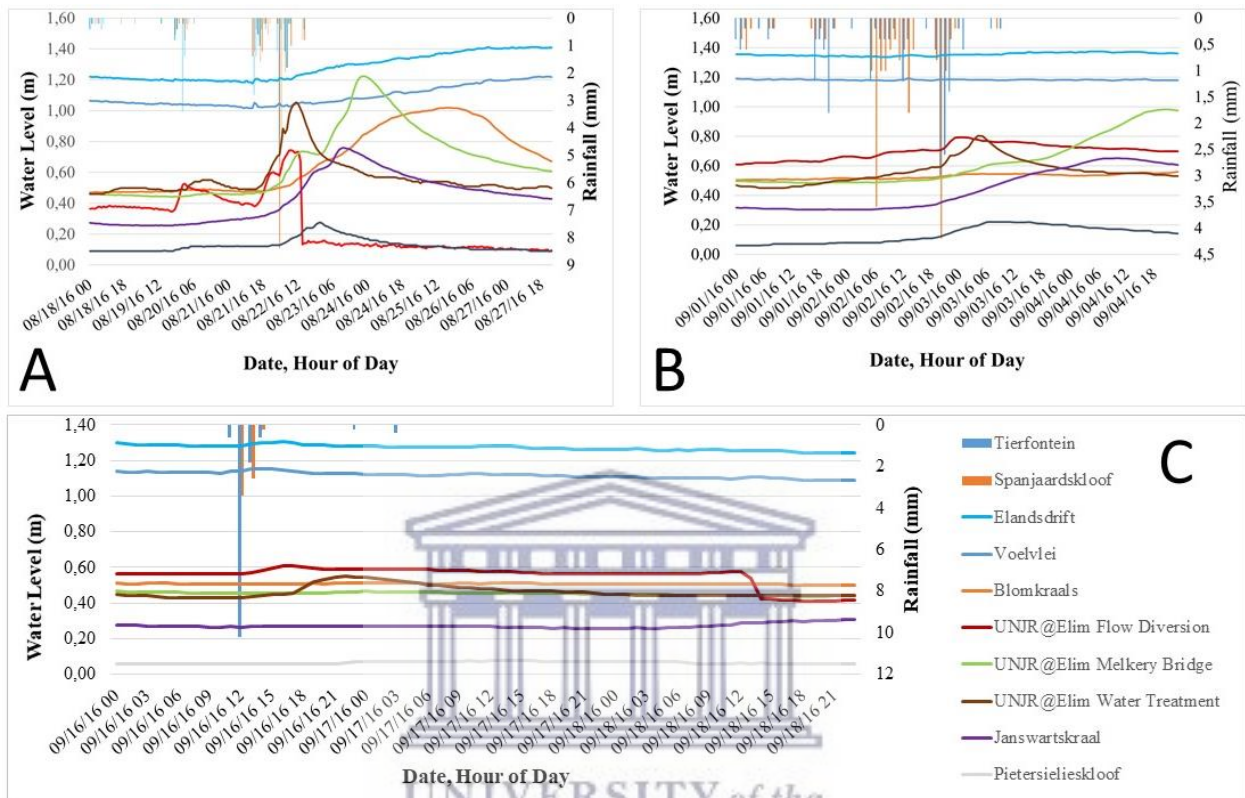


Figure 4.43: Hourly responses of the monitored tributaries to selected rainfall events from mid to the end of the wet season. (A) 18th August to 27th August 2016, (B) from the 1st September to the 4th September 2016 and (C) from the 16th September to the 18th September.

Towards the very end of the wet season there was very little to no response at the Elandsdrift, Voëlvlei and Blomkraals stations. However, there was a response of 0.09 m after 4 hours on the Nuwejaars River at the Elim Flow Diversion, a 0.09 m response at the Pietersielieskloof site after 9 hours and 0.29 m response at the Jan Swartskraal tributary after 34 hours (Figure 4.43 B). This was very similar to the responses at the beginning of the wet season. By late August the Nuwejaars River at the EWWTP was the only tributary to respond with a 0.11 m rise in water level 9 hours after the event (Figure 4.43 C).

4.3.9. Rainfall requirements for flows to occur

Following the dry season in 2016, the Janswatskraal sub-catchment required an average of 150 mm of rainfall before flows were recorded at the Jan Swatskraal tributary. However, 160 mm of rainfall was required for flows to be recorded at the Melkery Bridge tributary. This amounts to an average of 160 mm rainfall between the Spanjaardskloof, Tierfontein and Tussenberg rain gauging stations (Figure 4.44).

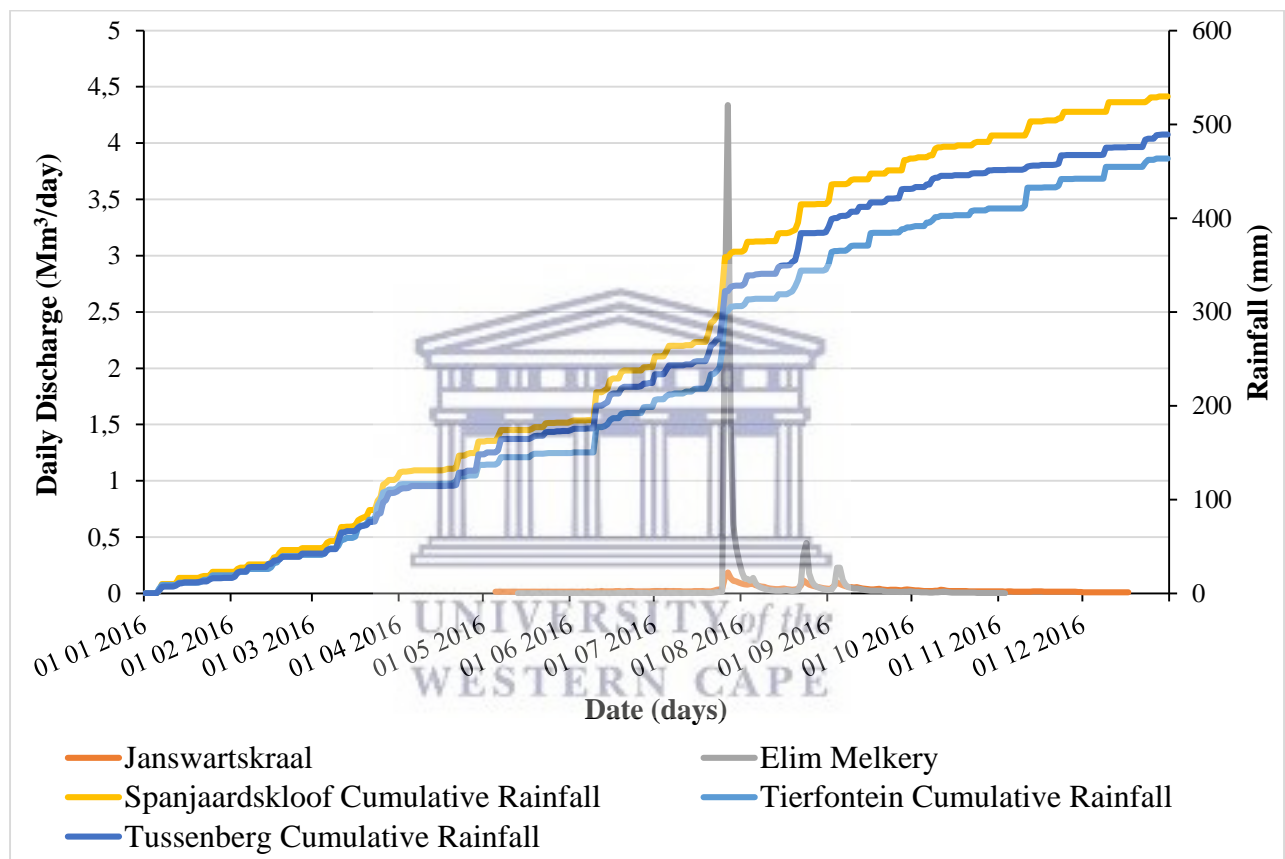


Figure 4.44: Daily discharge of the Janswatskraal and the combined Janswatskraal and Koue sub-catchments (measured at the Melkery Bridge) to the cumulative rainfall received in 2016.

On the other hand, the Pietersielieskloof river flowed throughout the year with an average discharge of 25 346 m³/day during the wet season and 20 861 m³/day towards the dry season. The only peak in discharge was noted in response to the major rainfall event on the 25th July 2016, where the Pietersielieskloof sub-catchment received 90 mm of rainfall in less than 48 hours (Figure 4.45).

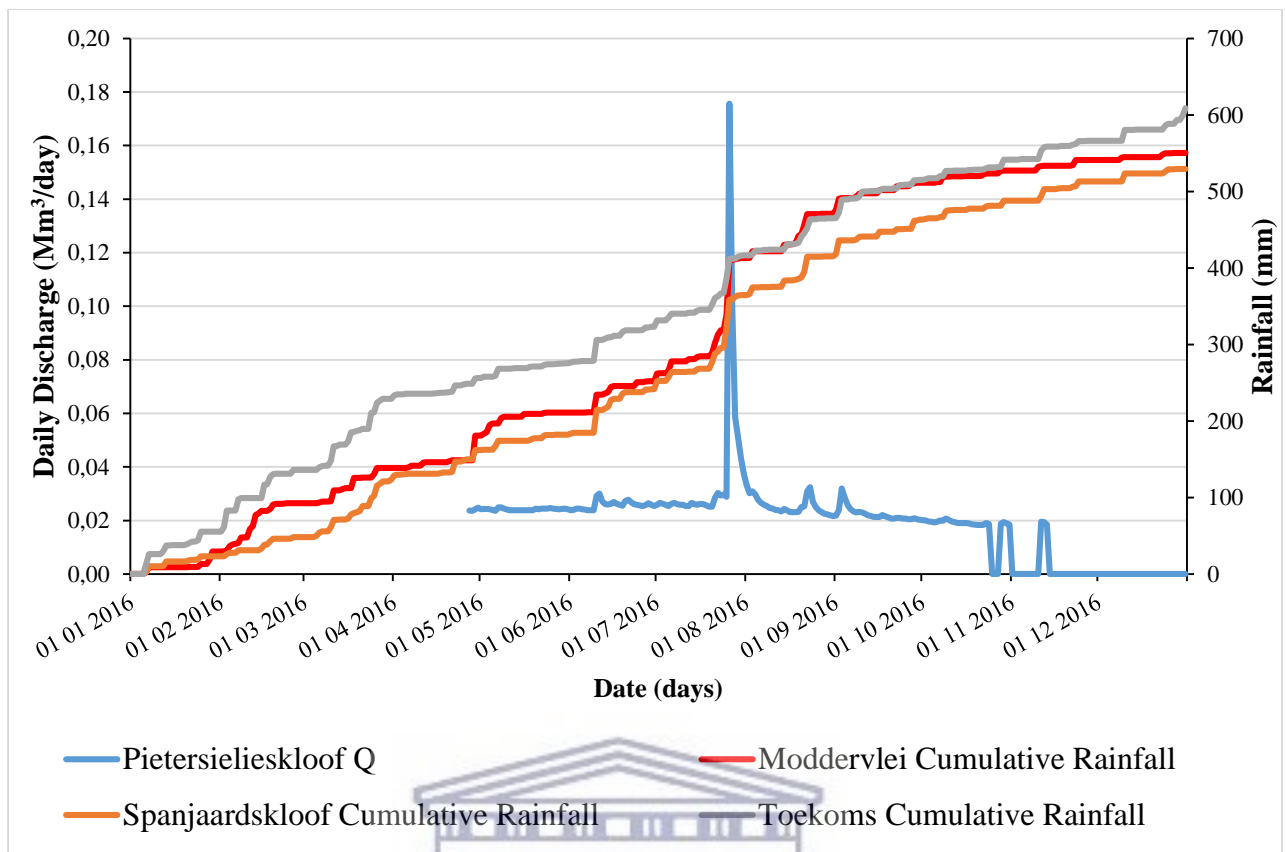


Figure 4.45: Daily discharge of the Pietersielieskloof tributary and the cumulative rainfall received by the sub-catchment in 2016.



During 2016, the Blomkraals sub-catchment required 179 mm of rainfall before flows were recorded at the Elim-Struisbaai road bridge. Whereas the Voëlvlei sub-catchment required only 140 mm of rainfall over the sub-catchment before flows occurred (Figure 4.46). Additionally, the peak discharge of the Blomkraals river to the rainfall event of the 25th July 2016 was 0.42 Mm³. On the other hand, the discharge at Voëlvlei was significantly less at 10 000 m³ during this event (Figure 4.46).

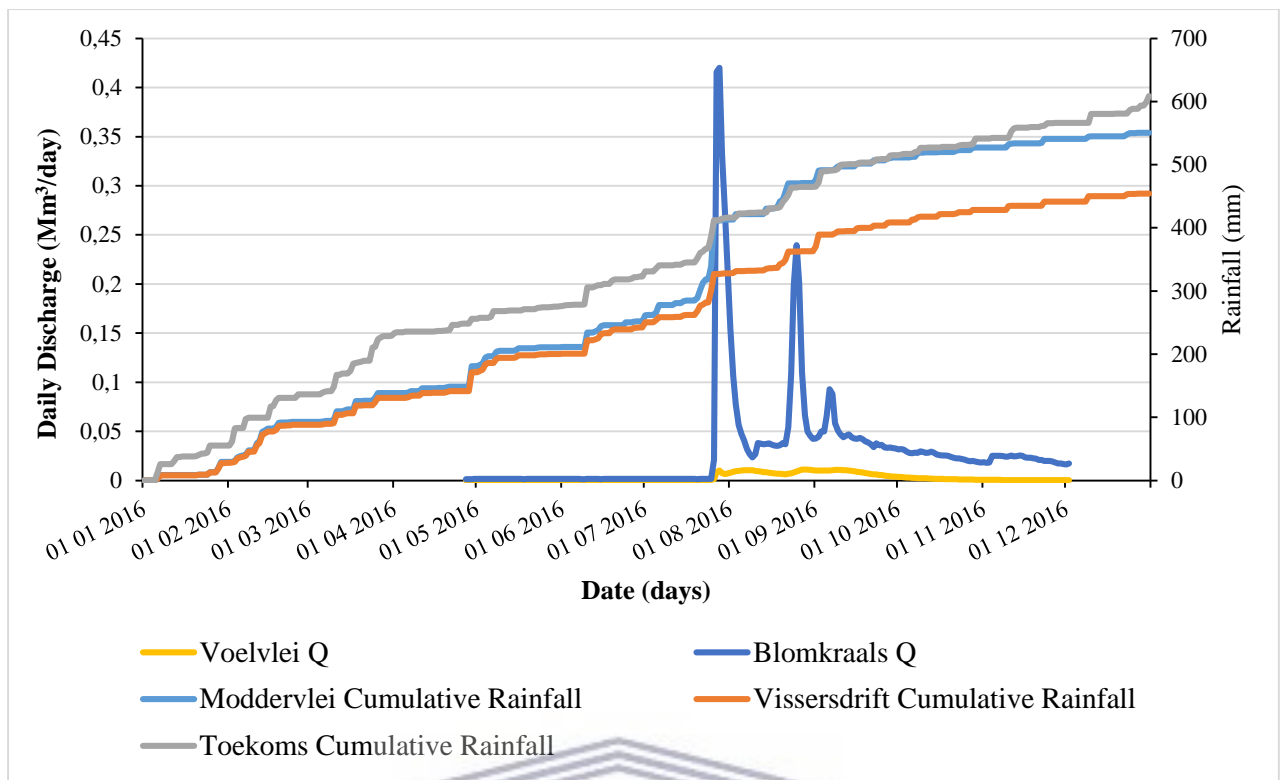
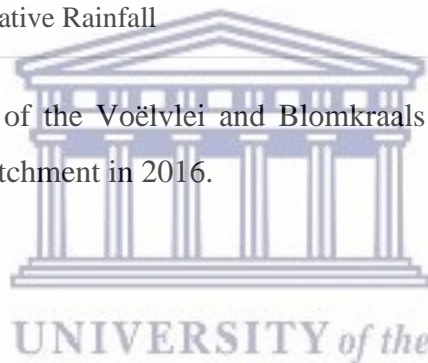


Figure 4.46: Daily discharge of the Voelvlei and Blomkraals tributaries to the cumulative rainfall received by the sub-catchment in 2016.



4.4. Discussion

A similar number of rainy days were recorded in both 2015 and 2017. However, the intensity and duration of these events were much less in 2017 than compared to 2015 and 2016. As flows were only monitored from mid-year 2016 to 2017 the hydrological responses of the sub-catchments were only assessed during this period.

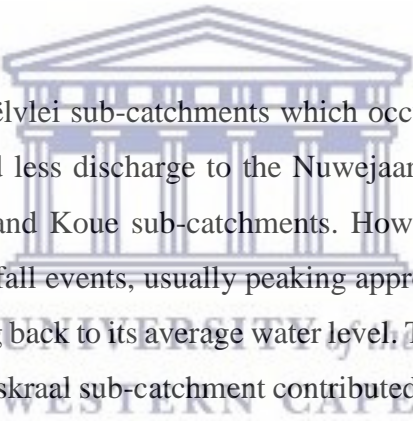
During the wet season most of the rainfall fell over the mountainous Janswarskraal and Pietersielieskloof sub-catchments. Although the Koue and Janswarskraal sub-catchment received less rainfall than the Pietersielieskloof sub-catchment, the annual discharge of these two sub-catchments was more than that of the Pietersielieskloof sub-catchment. This suggested that either there was an influence of groundwater flow from these areas or an overestimation of discharge.

The Pietersielieskloof sub-catchment contributed 11 % of the annual flows to the Nuwejaars River and the Elim sub-catchment contributed 16 % of the annual flows. On the other hand, the mountainous Jan-Swartzkraal and Koue sub-catchments contributed a combined 48 % of the Nuwejaars River inflows. This supports the findings of Blöschl *et al.*, (2013) and WWF-SA, (2013) who noted the importance of mountainous catchments to river flows in Southern Africa. On the other hand, the EWWTP tributary stayed dry and only flowed for a short period of time. This showed a strong reliance on rainfall for flows to occur and attributes to the highly variable nature of the hydrological responses of mountainous catchments noted by Schulze, (2011), Blöschl *et al.*, (2013) and WWF-SA, (2013).

Blöschl *et al.*, (2013) noted that the hydrology of mountainous regions is susceptible to variable precipitation and this may have attributed to the distribution of flows during the 2016 to 2017 period of this study. However, it was clear from the results that the mountainous Jan-Swartzkraal and Koue sub-catchments strongly relied on rainfall during the wet season for flows to occur. In addition, these sub-catchments receded quickly following the wet season and were completely dry by the end of 2016. As reported by locals in the area, the river stops flowing on “nuwejaars dag” or New Year’s Day and was therefore dubbed the Nuwejaars River. However, all the tributaries did not stop flowing at this time as low flows were still recorded on the Pietersielieskloof and Elim Flow Diversion tributaries.

The Pietersielieskloof and Elim Flow Diversion tributaries had flow throughout the period of the study. They were the only two tributaries which had flows during the dry season and throughout the drought in 2017. This provided evidence of an element of groundwater flow and was supported by Blöschl *et al.*, (2013), who noted that flows may be sustained by groundwater discharge during dry seasons in Southern Africa. In addition, during the wet season of 2017, flows were only recorded at the Pietersielieskloof, Jan-Swartzkraal and Elim tributaries. The results therefore suggest a groundwater influence in the Pietersielieskloof, Janswartzkraal and Elim sub-catchments in maintaining or contributing to flows during the wet season. Furthermore, flows were also recorded along the Nuwejaars River at the Elandsdrift site during the 2017 wet season. This suggests an influence of groundwater as most of the tributaries had very little to no flow during the wet season of 2017.

No substantial flows were recorded at the Blomkraals and Voëlvlei tributaries during the drought of 2017. However, the results showed that the Blomkraals and Voëlvlei sub-catchments were dependent on substantial rainfall before flows would occur. This was due to the presence of large wetlands within these sub-catchments and may be due to the presence of dams, filling of pools and the abstraction of water for supply. These findings support the notion of the flood attenuating capabilities of wetlands noted by McCartney, *et al.*, (2013), Kotzé (2000) and Cleaver & Brown (2005). The Blomkraals sub-catchment contributed significantly more discharge to the Nuwejaars River than compared to the Voëlvlei sub-catchment. This was due to the fact that the Voëlvlei tributary would in some cases experience reverse flows. It was noted that during high flows, flow would enter the Voëlvlei lake and once the water level in the lake exceeded that of the Nuwejaars River, flows would return to the Nuwejaars River. However, the Voëlvlei tributary sustained dry season flows for a longer period than compared to the Blomkraals tributary.



The Blomkraals, Elim and Voëlvlei sub-catchments which occur on the undulating plains of the Agulhas region contributed less discharge to the Nuwejaars River than compared to the mountainous Jan-Swartzkraal and Koue sub-catchments. However, the Elim sub-catchment responded more rapidly to rainfall events, usually peaking approximately 4 hours following a rainfall event and then returning back to its average water level. The Koue sub-catchment being bigger in size than the Janswartzkraal sub-catchment contributed more runoff to the Nuwejaars River. In addition, peak flows would reach the Melkery Bridge site before reaching the Janswartzkraal site, which was further upstream. This may have been due to the EWWTP tributary which quickly responds to rainfall, contributions from the Koue tributary or groundwater discharge which may reach the Melkery Bridge site.

The Nuwejaars River at Elandsdrift when compared to the Melkery Bridge site showed a more delayed receding of daily discharge. The upper tributaries showed quick and high peaks of daily discharge in response to rainfall events and quickly receded following these major events. However, the Elandsdrift site showed a delayed and much slower drop in daily discharge. This may have been due to the presence of wetlands in the lower regions which stored water temporarily, groundwater discharge which occurred further downstream or the temporary storage of water in ponds and lakes such as the Voëlvlei lake. As noted by Bullock &

McCartney (1996), Cleaver & Brown (2005) and McCartney, *et al.* (2013), the presence of wetlands has the ability to reduce high flows and maintain river flows during the dry season. This substantiates the need to improve knowledge of the functioning of wetlands in the area and will be further discussed in Chapter 5 of this paper.



5. INFLUENCE OF THE NUWEJAARS WETLAND ON RIVER FLOWS

5.1 Introduction

The Nuwejaars River passes through an 8.5 km long and 0.9 km wide floodplain wetland. The wetland is fed by multiple valley-bottom wetlands (Nel, *et al.*, 2011; Mills, 2018). Improved knowledge is required on the hydrological functioning of the wetland. There are several factors to consider when assessing the flood attenuating properties of wetlands. These factors include the climate of the wetland, topography of the wetland, wetland size and shape, presence of vegetation, location in the catchment, sources of flows, the hydrological flow regimes and the soil properties (Kotzé, 2000; McCartney, *et al.*, 2013). This chapter addresses the second objective of this study and is aimed at determining the effect of the Nuwejaars Wetland on flows of the Nuwejaars River.

5.2 Methods

Prior to this study the Nuwejaars Wetland was classified using the hydrogeomorphic approach to level 4a of the National Wetland Classification System (Nel, *et al.*, 2011; Mills, 2018). The focus of this chapter was therefore solely on assessing the factors which affect the flood attenuation of the wetland. The topography, shape and size and presence of vegetation of the wetland were determined using remotely sensed data and field surveys. The flow regimes and climatic conditions were discussed in Chapter 4 and will be further discussed in this chapter. The source of flows was determined using stable isotope analysis and the soil properties were assessed using in situ soil samples and surveys within the wetland. The collected data was used to develop a conceptual model of the wetland on flows.

5.2.1. Wetland morphology

The wetland shape and size was determined using a wetland delineation data provided by NGI and Nel, *et al.*, (2011). Nel, *et al.*, (2011), identified inland water areas of the Agulhas region and classified them based on wetland types. In addition, GPS coordinates and elevation data were collected along several transects across the wetland using a Leica Zeno 15 DGPS with an accuracy between 10 cm and 50 cm.

A NDWI using Sentinel imagery was used to determine the presence of pools within the wetland. Sentinel imagery has a 10 m spatial range and therefore only pools larger than 100 m² were identified. An image from the 16th of June 2016 (when the wetland was reasonably dry) was compared to an image from the 4th of August 2016 (when the wetland was inundated) to determine the spatial variation of pools within the wetland. Pools were identified using the NDWI produced during the dry (16th June 2016) and the wet season (4th August 2016) and digitized to estimate the area and volume of each pool. The NDWI identifies water or moist soils with values close to or equal to 1, bare soil = 0 and vegetation and cultivated land as negative values. The combination of the volume of pools and the transects of the wetlands were then used to estimate the maximum storage capacity of the wetland.

5.2.2. Determination of soil texture and infiltration rates

In situ soil samples were collected along transects using the auguring method in order to determine the variation of soil types throughout the wetland. 100 cm³ surface samples were taken using a handheld auger and a 100 cm³ subsurface soil sample was then taken at or near a depth of 1 m. Infiltration rates were measured at each location along the transects using a mini-disk infiltrometer model S (Decagon Devices, Inc.).

The infiltration rates were determined using the New-Minidisk-Infiltrometer-Macro-V.4 software developed by Gaylon Campbell which uses hydraulic conductivity to estimate the infiltration rate. In order to determine the soil type or texture the Settling Tube Analysis Method was used. This process requires 20 g of oven dry soil to be treated with Hydrochloric Acid (HCl) and Hydrogen Peroxide (H₂O₂) to remove organic matter. The soil is then placed in a 1 000 ml settling tube filled with water and 10cc dispersion solution (Annexure 5). The cylinder was shaken and a 25 ml sample was taken after 32 seconds and 8 hours respectively. The sample taken after 32 seconds contained silt and clay, whereas the 8 hr sample contained only clay (Annexure 5). These samples are dried in the oven and weighed. The sand, silt and clay percentages were then calculated.

5.2.3. Spatial distribution of wetland vegetation

Notes and pictures were taken of the various types of vegetation within the wetland during the morphological surveying above. The notes and pictures along with GPS coordinates were used to determine the spatial distribution of vegetation throughout the wetland. Google Earth Pro imagery from the 5th August 2017 was used to digitize the spatial distribution of vegetation throughout the wetland and species were identified during the surveys.

5.2.4. Wetland flow regimes and water sources

It was important to understand the wetland flow regime including the water source of the wetland. Water source analysis was therefore imperative to understand whether the inundation was due to over spilling of the Nuwejaars River, high water table or a combination of the two. The daily discharge of the Jan Swartskraal, Pietersielieskloof, Nuwejaars River at the Melkery Bridge, Voëlvlei and Blomkraals tributaries entering the wetland and outflows at Elandsdrift were determined in Chapter 4 and used here. The water sources were determined by installing 4 rainfall isotope collectors at the Vissersdrift, Toekoms, Spanjaardskloof and Tierfontein stations (Figure 4.1). The rainfall collectors consisted of a 75 mm PVC pipe placed inside a larger white PVC pipe and sealed with Styrofoam to keep the sample cool. The lid was sealed with a rubber ring and a table tennis ball was placed in the funnel to prevent further evaporation (Annexure 4).

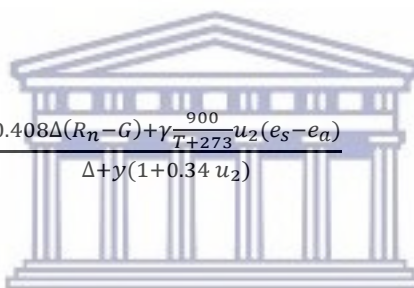
A 50 ml water sample was taken at each of these 4 rainfall isotope samplers on a monthly basis. In addition, a 50 ml water sample was taken from each of the flow monitoring sites except for the Nuwejaars River at the Melkery Bridge as this combined flows from the Koue and Jan Swartskraal tributaries. A sample was also taken from the Nuwejaars River within the wetland 100 m upstream of the Moddervlei weather station (Figure 4.1). The samples were stored on ice, placed in a cooler-box and placed in the fridge in the lab. A handheld Martini pH 50 and EC 52 meter were used to measure the pH and EC of each of the samples once in the lab.

The LGR DLT-100 liquid water isotope analyser was used to determine the $\delta^{18}\text{O}$ and $\delta^2\text{H}$ values of the collected water samples. The isotope analyser uses the Off-Axis Integrated Cavity

Output Spectroscopy (OA-ICOS) method to analyse water samples and determine the $\delta^{18}\text{O}$ and $\delta^2\text{H}$ values. The $\delta^{18}\text{O}$ and $\delta^2\text{H}$ values, EC and pH values of the rainfall samples and river samples are then compared in order to determine whether or not the water was sourced directly from the rainfall event or groundwater. However, there were no boreholes in the area during the time of this study and it was therefore not possible to obtain a groundwater sample.

5.2.5. Wetland climatic conditions

The daily rainfall estimates obtained in Chapter 4 for the Moddervlei station were used for the Nuwejaars Wetland as an input for the water balance of the wetland. The FAO Penman-Monteith (Equation 5.1) method was used to estimate evapotranspiration for the wetland as weather data is readily available from the automatic weather station installed within the wetland (Allen, *et al.*, 1998; Blight, 2002; Zribi *et al.*, 2011; Schwerdtfeger *et al.*, 2014).



$$ET_o = \frac{0.408\Delta(R_n - G) + \gamma \frac{900}{T + 273} u_2 (e_s - e_a)}{\Delta + \gamma(1 + 0.34 u_2)} \quad (5.1)$$

where: ET_o = reference ET rate ($\text{mm}\cdot\text{d}^{-1}$)

R_n = net radiation ($\text{MJ}\cdot\text{m}^{-2}\cdot\text{d}^{-1}$)

G = soil heat flux density ($\text{MJ}\cdot\text{m}^{-2}\cdot\text{d}^{-1}$)

T = mean daily air temperature @ 2m height ($^{\circ}\text{C}$)

u_2 = wind speed @ 2m height ($\text{m}\cdot\text{s}^{-1}$)

e_s = saturation vapour pressure (kPa)

e_a = actual vapour pressure (kPa)

$e_s - e_a$ = saturation vapour pressure deficit (kPa)

Δ = slope of saturation vapor curve ($\text{kPa } ^{\circ}\text{C}^{-1}$)

γ = psychrometric constant ($\text{kPa } ^{\circ}\text{C}^{-1}$)

5.2.6. Conceptual model of the floodplain wetland

A conceptual model adapted from Schulze and Pike (2004) was used to estimate the effect of the Nuwejaars River on the flows of the Nuwejaars River (Figure 5.1). A water budget was used to account for the exchanges between the atmosphere and the wetland. The foundation of this concept is based on Equation 5.2 below (U.S. EPA, 2008).

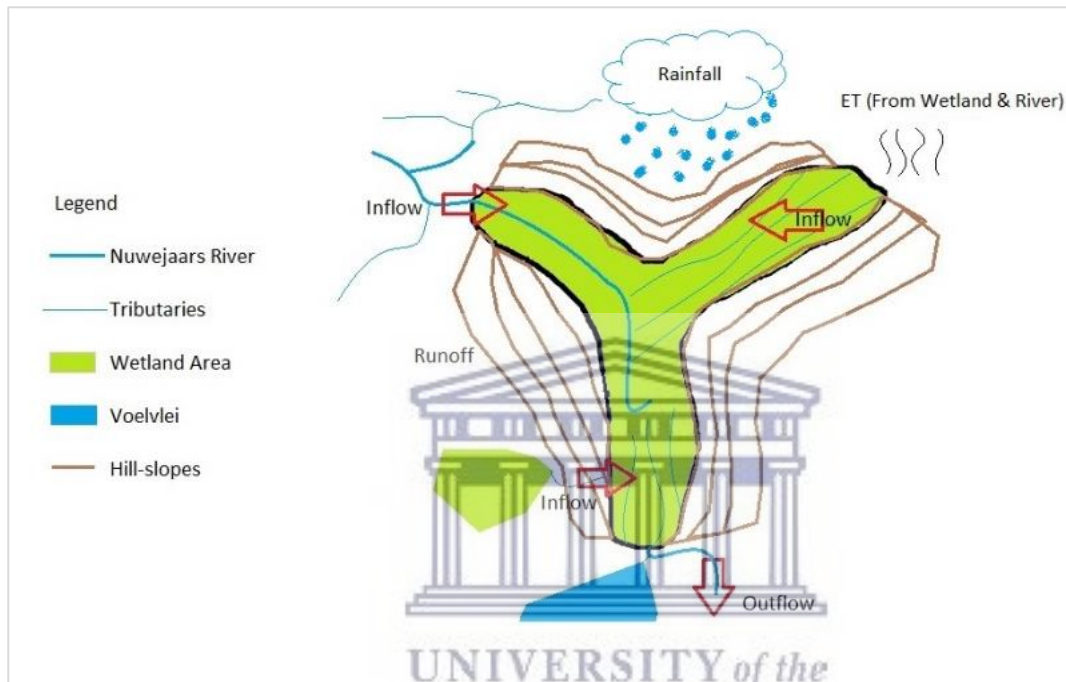


Figure 5.1: Diagrammatic representation of the conceptual model adapted from Schulze and Pike, (2004).

$$\Delta S = I(t) - O(t) = \frac{\Delta S}{\Delta t} \quad (5.2)$$

where: ΔS = Change in wetland storage

$I(t)$ = Inflows

$O(t)$ = Outflows

Δt = Time

Inflows include the sum of precipitation directly into the wetland (P), surface runoff from the surrounding areas (R), groundwater discharge also from surrounding areas (GW_D) or interflow, overbank flow and surface water flow (Q_{in}) (U.S. EPA., 2008).

Outflows include the sum of evapotranspiration (ET), groundwater recharge (GW_R) and surface water flow out of the wetland (Q_{out}) (U.S. EPA., 2008). ΔS can therefore be calculated using the following equation (Equation 5.3):

$$\Delta S = \frac{(P+R+GW_D+Q_{in})-(ET+GW_R+Q_{out})}{A} \quad (5.3)$$

P and ET were estimated using the data from the weather station installed within the wetland. R, Q_{in} and Q_{out} were estimated using the river flow data collected in Chapter 4. GW was neglected due to time constraints and a lack of boreholes or piezometers in the area. However, the soil characteristics and wetland survey were used to estimate the influence of groundwater.

5.2.7. Modelling of the Nuwejaars Wetland

A modified version of the Flex-topo model adapted from Savenije (2010) was used to predict the effects of the Nuwejaars Wetland on the flows of the Nuwejaars River. Six parameter estimations were required for the conceptualization of the wetland (Savenije, 2010). The parameters include two thresholds for the subsurface reservoir (S_{max} and S_{min}), interception threshold (D_w), wilting point (WP) and groundwater recharge (R) (Figure 5.2).

S_{max} is the maximum storage of the wetland before overland flow occurs. S_{min} is the minimum storage required in the wetland for discharge to occur downstream of the wetland (Figure 5.2). D_w is the interception threshold for P, which simulates the interception of rainfall by vegetation within the wetland. WP is a standard subsurface storage always present in the wetland and cannot be removed from the soil by vegetation, recharge or ET (Savenije, 2010) (Figure 5.2).

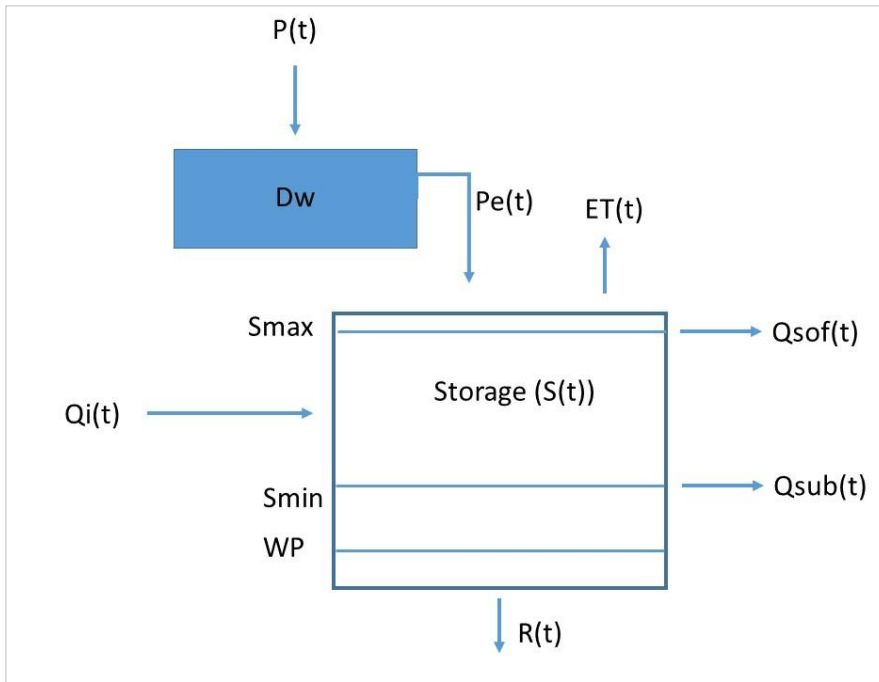


Figure 5.2: Diagrammatic representation of the conceptual model adapted from Savenije (2010).

The predicted outflow or simulated discharge ($Q_{sim}(t)$) was predicted by summing the saturation excess overland flows ($Q_{sof}(t)$) and the subsurface flow ($Q_{sub}(t)$). The simulated discharge can therefore be estimated using the following equation (Equation 5.4):

$$Q_{sim}(t) = Q_{sof}(t) + Q_{sub}(t) \quad (5.4)$$

The saturation excess overland flows are estimated using the following equation (5.5):

$$Q_{sof}(t) = C_w \cdot P_e(t) \quad (5.5)$$

Where $Q_{sof}(t)$ is the saturation overland flow (m^3/day) C_w is the runoff coefficient and $P_e(t)$ is the effective rainfall (m^3/day).

Precipitation is the first input of the surface reservoir and is added to the wetland when the interception threshold is exceeded. Flow only occurs when S_{\max} and S_{\min} is exceeded. The precipitation accounted for in this model is not the effective precipitation (Wolski, *et al.*, 2006; Fenicia, *et al.*, 2008). However, the Flex-topo model approach was used to estimate interception loss of rainfall and calculated as follows (Savenije, 2010) (Equation 5.6):

$$P_e(t) = \max(P(t) - Dw; 0) \quad (5.6)$$

Where: $P_e(t)$ = Effective rainfall (m^3/day)

$P(t)$ = Rainfall (m^3/day)

Dw = Interception threshold (m^3)

The final threshold S_{\max} is flow that occurs as saturation excess overland flow (SOF). A runoff coefficient (C_w) is given to the subsurface reservoir in order to estimate SOF (Fenicia *et al.*, 2008) and is given as follows (Equation 5.7):

$$C_w = 1 - \left(1 - \frac{S(t)}{S_{\max}}\right)^\beta \quad (5.7)$$

Where C_w is the Runoff coefficient, $S(t)$ is the storage in subsurface reservoir (m^3), S_{\max} is the maximum storage threshold in subsurface reservoir (m^3), and β is a constant.

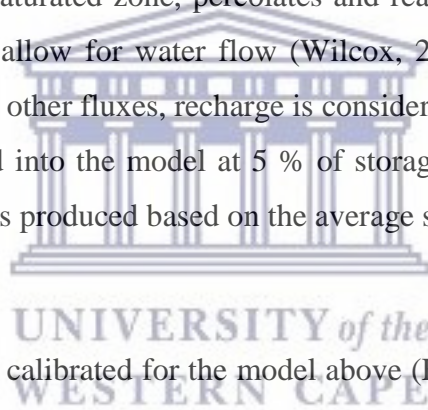
The other inputs of the reservoir are surface water inflows (Q_i). The sum of the inflows from the Nuwejaars River at the Melkery Bridge, the Pietersielieskloof River, Voëlvlei and Blomkraals tributaries are used to estimate Q_i . The third process involved in the surface reservoir is ET and was estimated using the Penman Monteith method. The last process involved in the surface reservoir is infiltration (K). Infiltration rates vary across various soil types. However, an average daily infiltration rate was applied to the model and was estimated during the soil characterization of the wetland.

S_{\min} was estimated using the wetland area and soil depth. The flow that occurs at S_{\min} is regarded as subsurface flow (Q_{sub}) and is given by the following equation 5.8:

$$Q_{\text{sub}}(t) = \alpha(S_{(t)} - S_{\min})^\beta \quad (5.8)$$

Where Q_{sub} is the subsurface flow (m^3/day), $S_{(t)}$ is the storage of the subsurface reservoir (m^3), S_{\min} is the minimum storage threshold (m^3), and α and β are constants.

The final process accounted for in the subsurface reservoir is Recharge (R). Recharge occurs when water infiltrates the unsaturated zone, percolates and reaches the saturated zone. Clay and loam soils do not easily allow for water flow (Wilcox, 2010). Some flow may occur, however, in comparison to the other fluxes, recharge is considered to be small. An estimate of the recharge was incorporated into the model at 5 % of storage based on (Xu, *et al.*, 2001; DWAF, 2004). This estimate is produced based on the average soil type of the wetland.



Several parameters need to be calibrated for the model above (Equation 5.4). The parameters include D_w , WP , R , S_{\min} , S_{\max} , α and β . A trial and error approach was used to calibrate the parameters. Firstly, the storage parameters S_{\min} and S_{\max} were estimated using the wetland area, soil depths and presence of pools. α and β are curve fitting parameters and were estimated in order to minimise the correlation between observed and simulated flows. The following objective function was used to minimise the root mean square error and correlation coefficient between the observed and simulated flows (Equation 5.9).

$$\text{minimise } \sum_{i=1}^n (Q_{\text{obs}}(t) - Q_{\text{sim}}(t))^2 \quad (5.9)$$

Where, $Q_{\text{obs}}(t)$ is the observed discharge (m^3/day) and $Q_{\text{sim}}(t)$ is the simulated flow (m^3/day). The predicted outflow was validated using regression analysis and the Root Mean Square Error

(RMSE) method. The output is a coefficient of determination which is an r^2 value that ranges from 0 to 1. The correlation coefficient has an r value which ranges from -1 to 1.

5.3 Results

5.3.1. Wetland morphology

The Nuwejaars Wetland being classified as a flood plain wetland is relatively flat. It is 12 km in length and 0.9 km at its widest section (Figure 5.3). The Nuwejaars River is confined to one channel at the beginning of the wetland for 3 km with a few meanders. In addition, the tributary from the Elim Flow Diversion converges with the Nuwejaars River at this point (Figure 5.3). In transects 1 to 3 the Nuwejaars River was not deeper than 1 m with very few meanders (Figures 5.3 & 5.4).

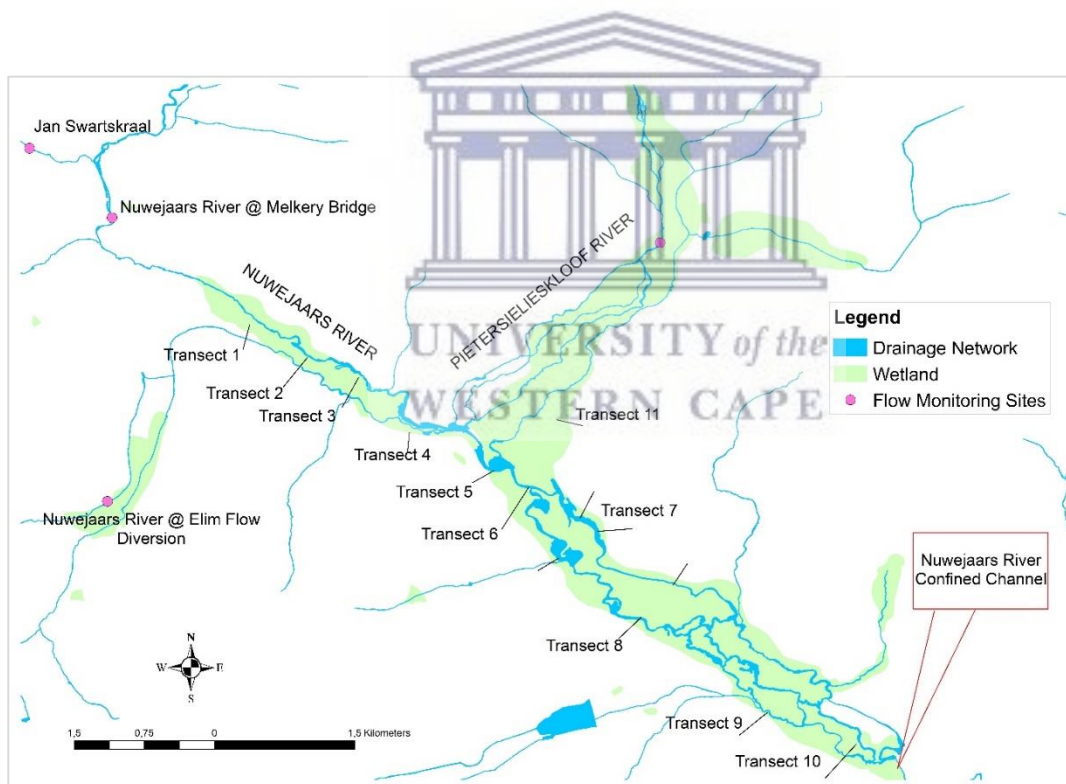


Figure 5.3: Drainage network of the Nuwejaars Wetland and the locations at which transects were conducted

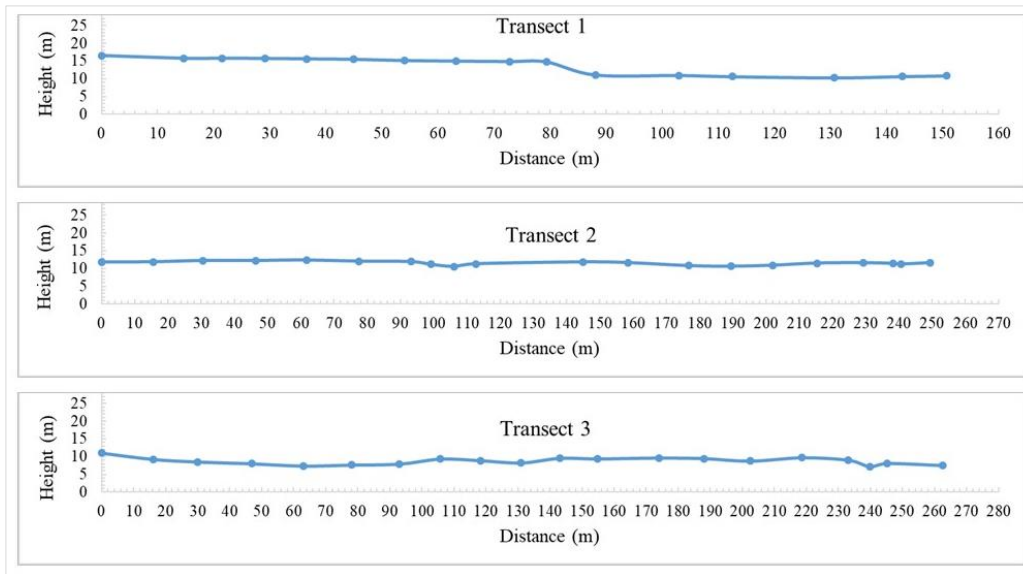


Figure 5.4: Transects 1 to 3 of the upper section of the Nuwejaars Wetland.

Large pools and ox bow lakes were formed in the middle of the wetland (Figure 5.5). The Nuwejaars River ranged from 8 m to 57 m in the area of the Zoetendal vineyard and was too deep to wade (Figure 5.5). The floodplain is relatively flat throughout the middle section of the wetland (Figure 5.6). However, transects 4 and 5 could not be completed as the Nuwejaars River was too deep to wade. The Nuwejaars River meanders through the middle section of the wetland and the remence of old oxbow lakes and current oxbowlakes were present in the middle of the wetland (Figure 5.7).

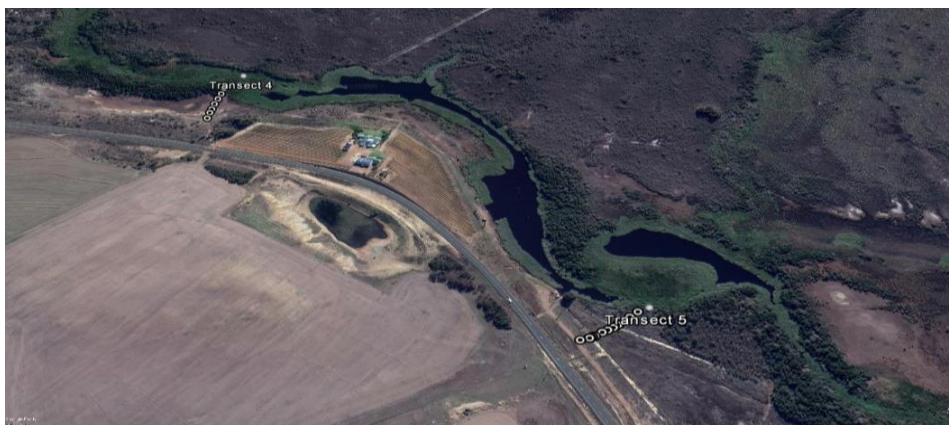


Figure 5.5: Meandering of the Nuwejaars River at the Zoetendal Vineyard. (Source: Google Earth Pro – 05/18/2017)

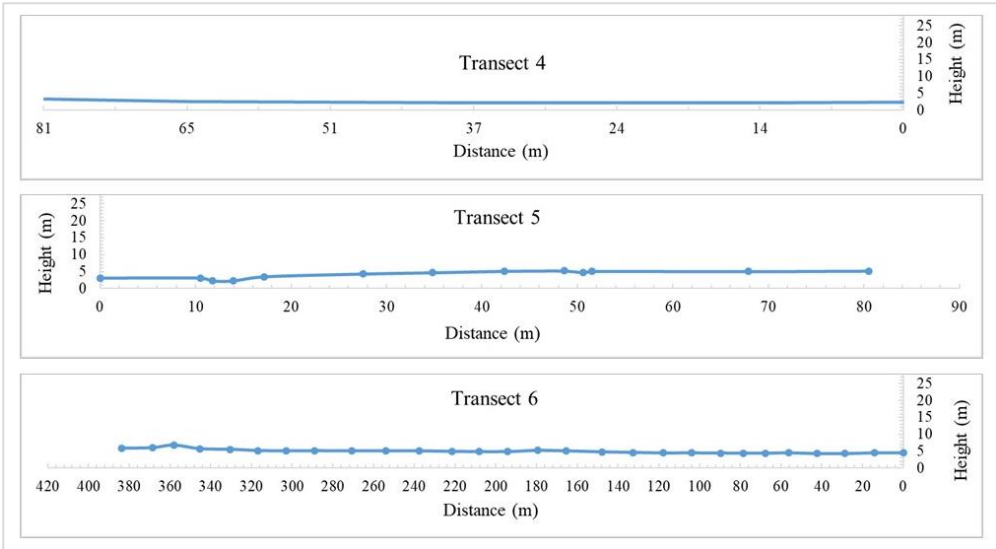


Figure 5.6: Transects 4 to 6 of the middle section of the Nuwejaars Wetland.

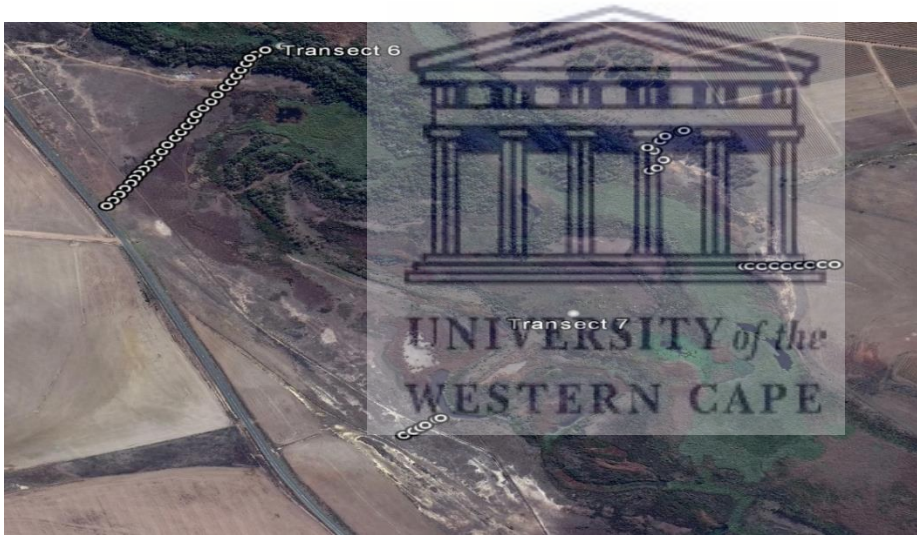


Figure 5.7: Meandering and oxbow lakes in the middle section of the Nuwejaars Wetland. (Source: Google Earth Pro – 05/18/2017)

The Nuwejaars River begins to disperse between transect 6 and 7 and flow is no longer constricted to a single channel and diffuse flow occurs (Figures 5.3 & 5.7). Multiple channels are present in transect 10 towards the end of the wetland (Figure 5.8). However, downstream of transect 10 the Nuwejaars River is confined to one channel and continues downstream towards the Elandsdrift flow monitoring site (Figure 5.3).

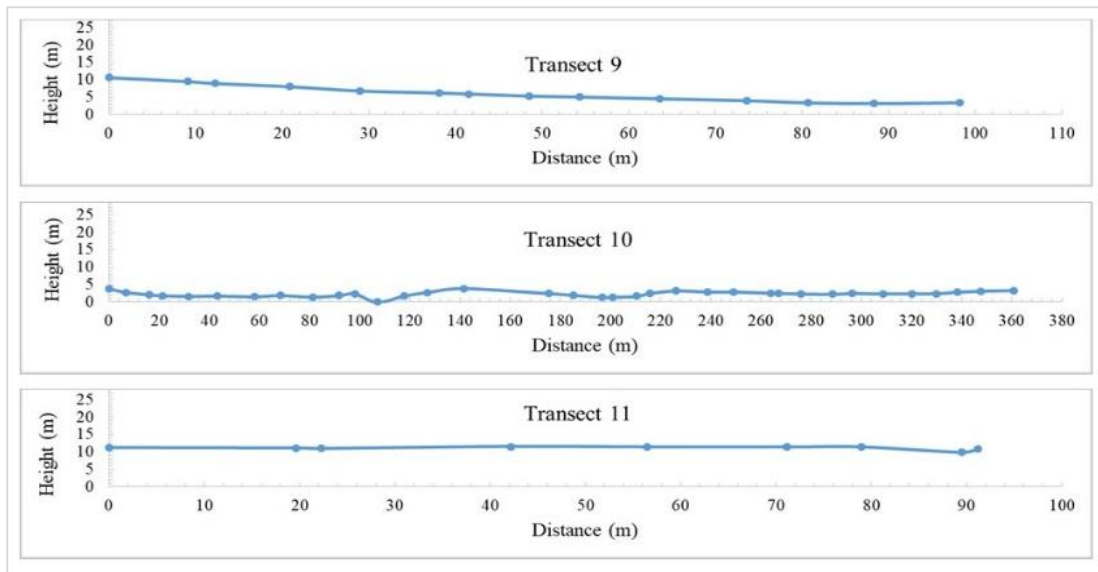
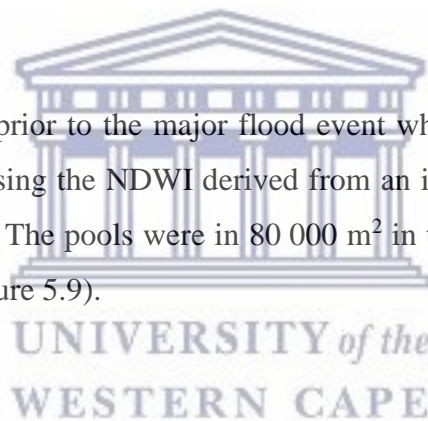


Figure 5.8: Transects 9 and 10 of the lower section of the Nuwejaars Wetland and transect 11 along the Pietersielieskloof's convergence with the wetland.

There were 11 pools present prior to the major flood event which occurred on the 25th July 2016. Pools were identified using the NDWI derived from an image before (16th June 2016) and during (4th August 2016). The pools were in 80 000 m² in total and grew to a total of 19 pools 104 611 m² in total (Figure 5.9).



A maximum depth of 2 m was used to estimate the volume of the pools based on observations during the surveying of the wetland (Table 5.1). The maximum of 2 m was selected as the pools identified during the survey did not exceed this depth and the maximum storage therefore may not exceed 2 m. In addition, this would include the water present in a 2 m soil column and therefore accounts for water stored in the soil column.

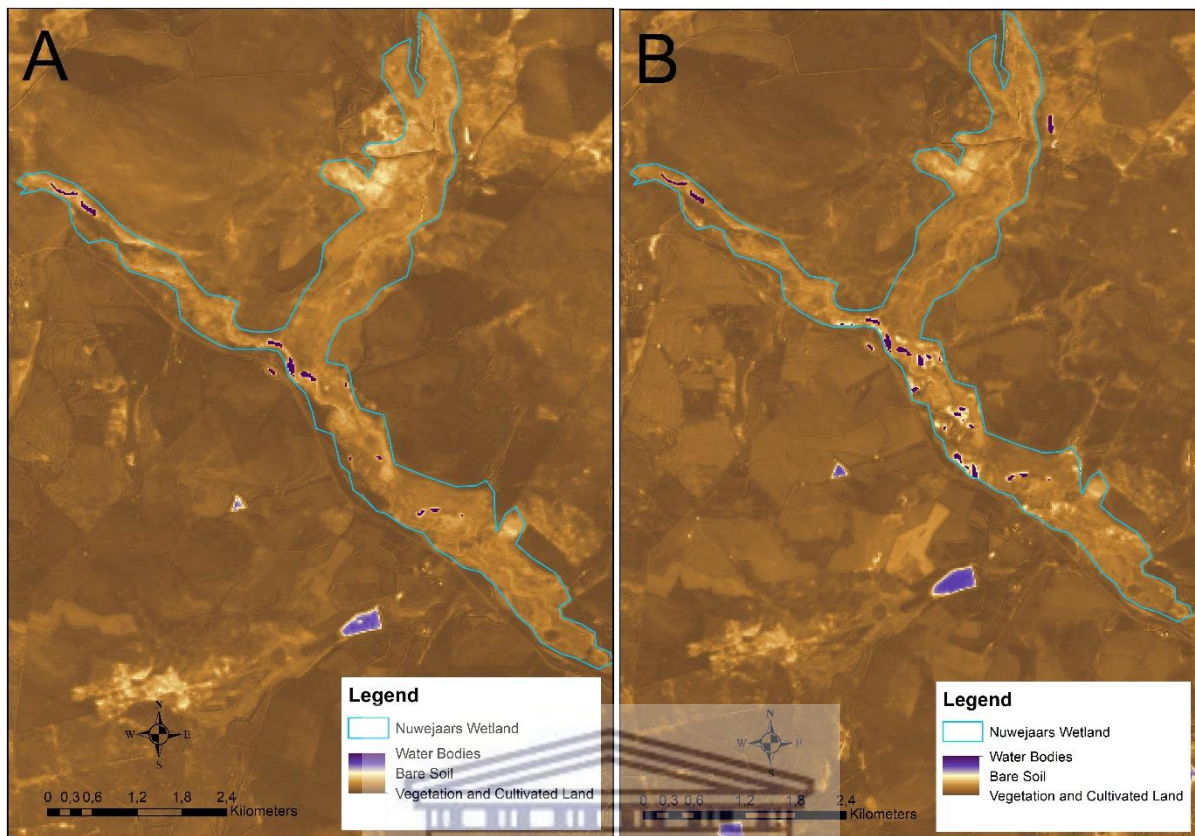


Figure 5.9: Spatial distribution of pools before (A) and after (B) the major rainfall event that occurred on the 25th July 2016. Derived using NDWI

Table 5.1: Volume of the wetland, pools within the wetland and the amount of water required to fill the pools

Storage Area	Volume (Mm ³)
Wetland	6.5
11 Pools before peak	0.16
19 Pools after peak	0.21
Water required to fill pools	0.049
Maximum Storage of Wetland	6.55

5.3.2. Wetland soil characteristics

Most of the wetland's surface soil was classified as sandy loam, followed by loam soil type (Figure 5.10). The average clay percentage across the wetland was 10 %, 60 % sand and 30 % silt. The average infiltration rate was 55 mm/day for the surface of the Nuwejaars Wetland. Infiltration rates were higher in the southern parts of the wetland with more sandy loam soils. On the other hand, the middle of the wetland had lower infiltration rates and more loamy sand and loamy soils (Figure 5.10).

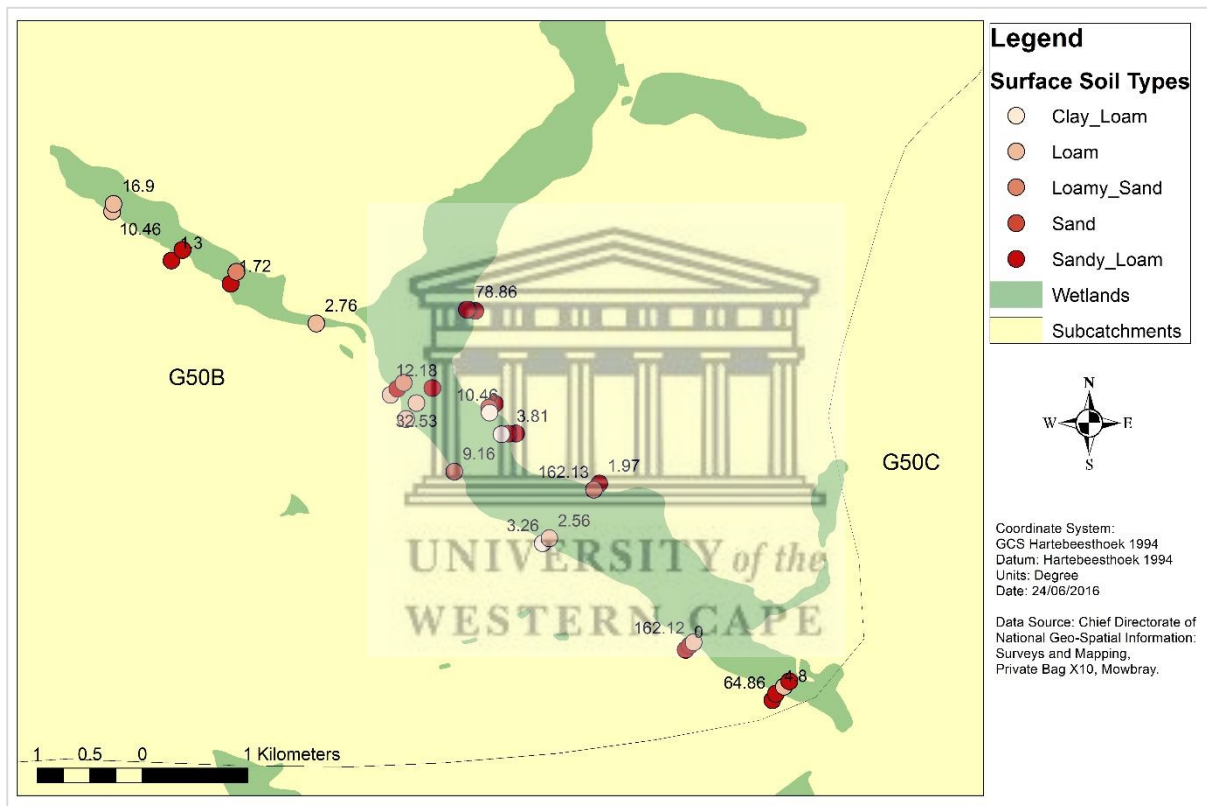


Figure 5.10: The spatial distribution of surface soil types across the Nuwejaars Wetland and infiltration rate estimates in mm/day.

Most of the wetlands sub-surface soil was loamy sand and sandy loam (Figure 5.11). The average clay percentage was higher in the sub-surface at 13 % than compared to the surface samples. There was a layer of clay soil at approximately 0.5 m depth in majority of the wetland. Which was most likely resulted in the increase in clay percentage with depth (Figure 5.11). The average infiltration in the sub-surface of the wetland was 43 mm/day.

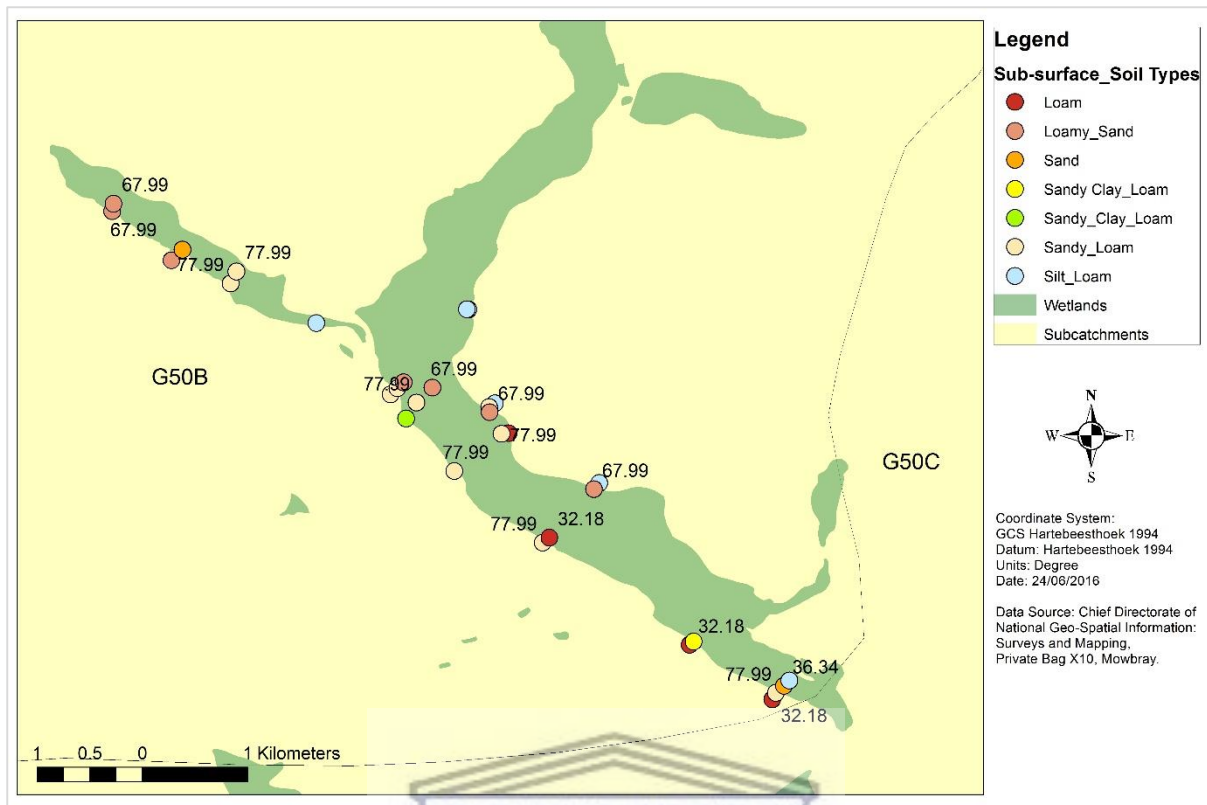


Figure 5.11: The spatial distribution of sub-surface soil types across the Nuwejaars Wetland and infiltration rate estimates in mm/day.

5.3.3. Wetland vegetation

The beginning of the wetland for the first 3 km is densely invaded by *Acacia longifolia* and *Acacia mearnsii* increasing in density towards transect 4. The invasions spread across the floodplain and along the Nuwejaars River itself (Figure 5.12). The Pietersielieskloof tributary had been densely invaded by *Acacia longifolia* and *Acacia mearnsii*, the density of the invasions decreased as the tributary converged with the Nuwejaars River (Figure 5.12).

At the convergence of the Pietersielieskloof tributary and the Nuwejaars River large pools were formed and were surrounded by Wilde Palmiet and aquatic reeds (Annexure 6 C & D). 100 m downstream of the Zoetendal vineyard the floodplain was covered in reeds, grasses and salt marsh. The banks of the river were densely invaded by *Acacia longifolia* and *Acacia mearnsii* throughout the middle of the wetland (Annexure 6 A & B). This continued for 1.8 km, upstream of transect 8 (Figure 5.12).

Downstream of transect 8 the floodplain is covered in reeds and grasses, while the difusse channels are covered in Wilde Palmiet and aquatic reeds (Figure 5.12). This continues up to transect 9, where the end of the wetland is sparsely invaded by *Acacia longifolia* and *Acacia mearnsi* between various reeds, grasses and salt marsh (Figure 5.12).

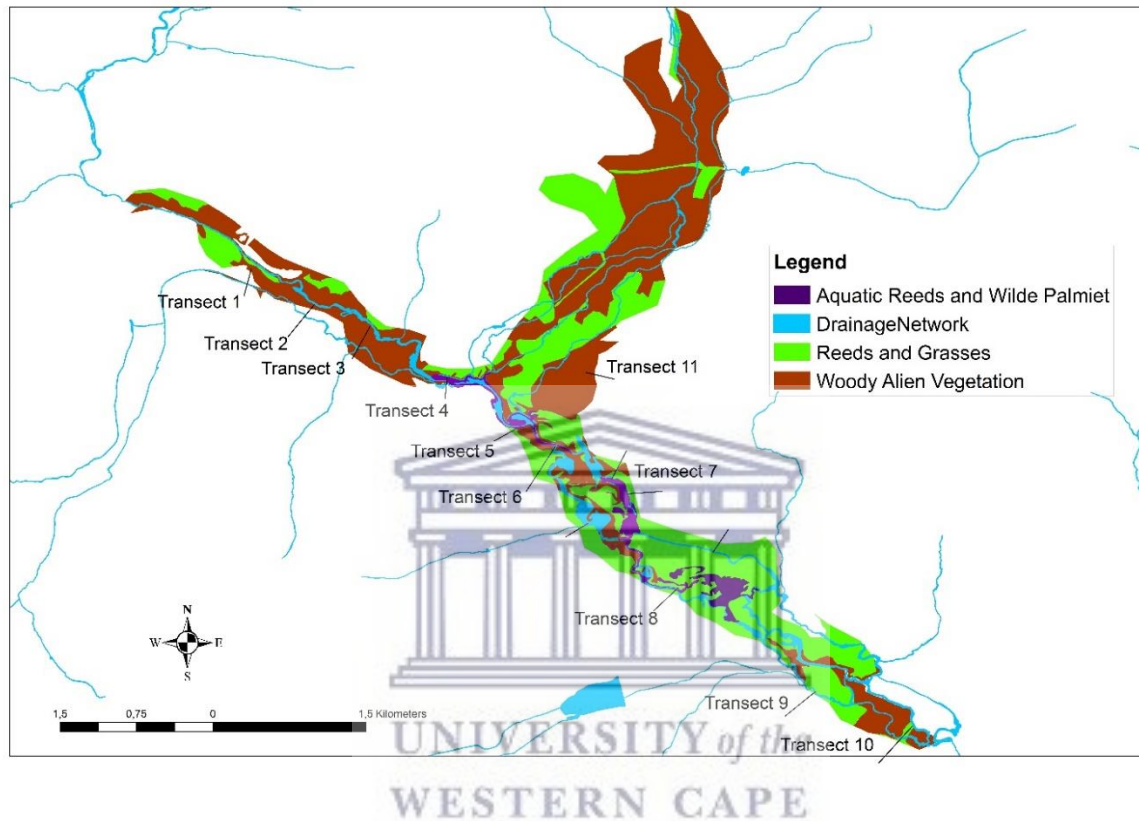


Figure 5.12: Spatial distribution of vegetation in the Nuwejaars Wetland and the locations at which cross-sections and soil samples were collected.

5.3.4. Spatio-temporal variation of water quality

In June 2016, there was an increase in EC and decrease in pH from the upper tributaries and rainfall samples to the Elandsdrift site (Figure 5.13 A). An average EC of 0.46 mS/m and pH of 6.92 was recorded for the samples. The EC at Elandsdrift was 0.82 mS/m in July and was only slightly higher than the EC recorded within the Nuwejaars Wetland at the Moddervlei sample point.

Similarly, in July 2016 the Blomkraals and Elandsdrift sites have the highest EC and lowest pH. However, the EC was significantly lower at Elandsdrift when compared to that of Blomkraals (Figure 5.13 B). The average EC was 0.8 mS/m with an average pH of 6.71. The sample taken from the Nuwejaars River at Moddervlei was 50 m downstream of the Zoetendal Vineyard. At this point the pH was slightly more acidic than in the upper tributaries and rainfall samples and the EC was slightly higher (Figure 5.13 B).

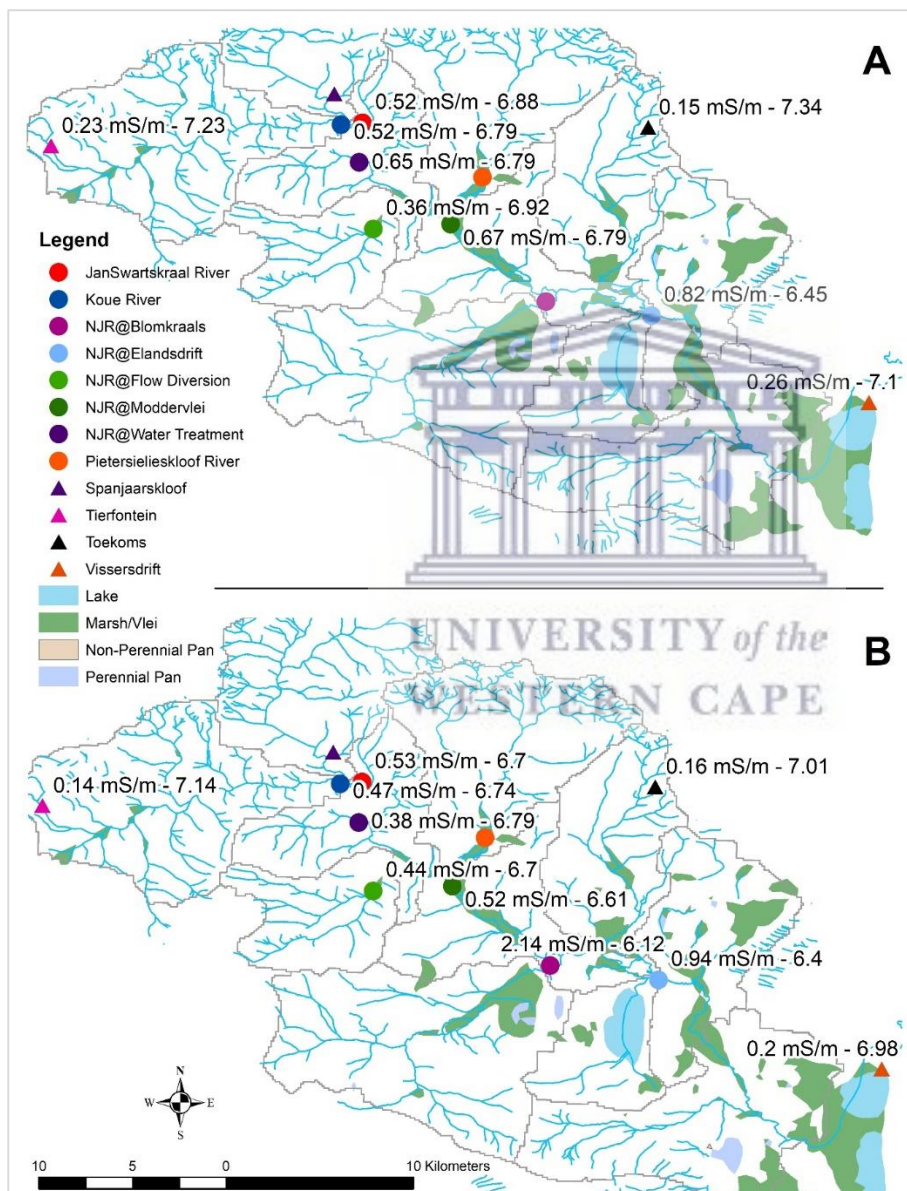
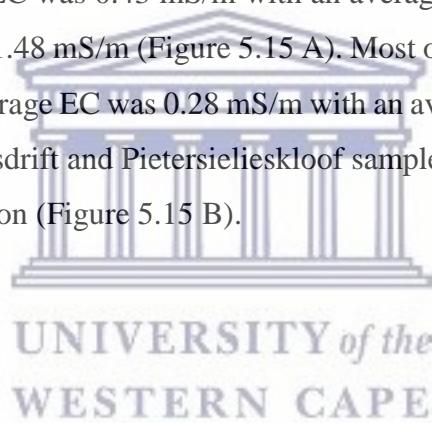


Figure 5.13: Variation of electrical conductivity (EC) and pH of river water along the Nuwejaars River and tributaries in June 2016 (A) and July 2016 (B). At each location EC value is separated from pH by “-”.

In August 2016 the Blomkraals, Elandsdrift and the sample collected at Water Treatment had the highest EC. The pH for all the sites were similar for August following the flooding which occurred in late July (Figure 5.14 A). The average EC was 0.68 mS/m with an average pH of 7.14. However, the water was more acidic within the wetland and at the Elandsdrift site.

Likewise, in September 2016, the Blomkraals, Elandsdrift and Water Treatment samples had the highest EC and lowest pH. The average EC was 0.58 mS/m with an average pH of 7.65. In addition, there was a decrease in EC from the Blomkraals tributary to the Nuwejaars River at Elandsdrift (Figure 5.14 B). The pH along the Nuwejaars River decreased from the tributaries of the Nuwejaars River towards the Elandsdrift monitoring site.

In October 2016 the average EC was 0.43 mS/m with an average pH of 7.38. The Elandsdrift sample had the highest EC of 1.48 mS/m (Figure 5.15 A). Most of the tributaries were near dry in November 2016 and the average EC was 0.28 mS/m with an average pH of 7.42. The highest EC was recorded in the Elandsdrift and Pietersielieskloof samples and was significantly lower than compared to the wet season (Figure 5.15 B).



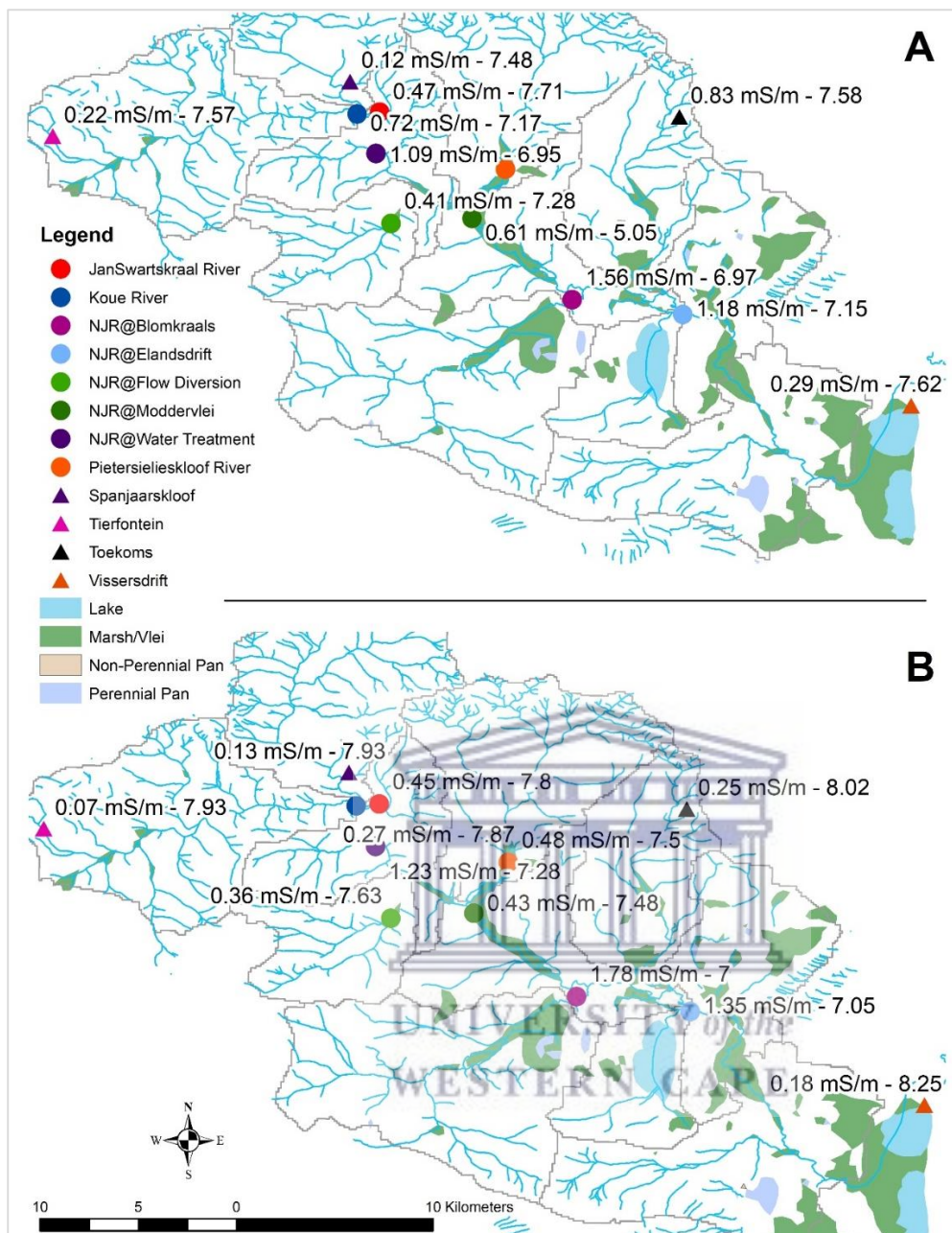


Figure 5.14: Variation of electrical conductivity (EC) and pH of river water along the Nuwejaars River and tributaries in August 2016 (A) and September 2016 (B). At each location EC value is separated from pH by “-”.

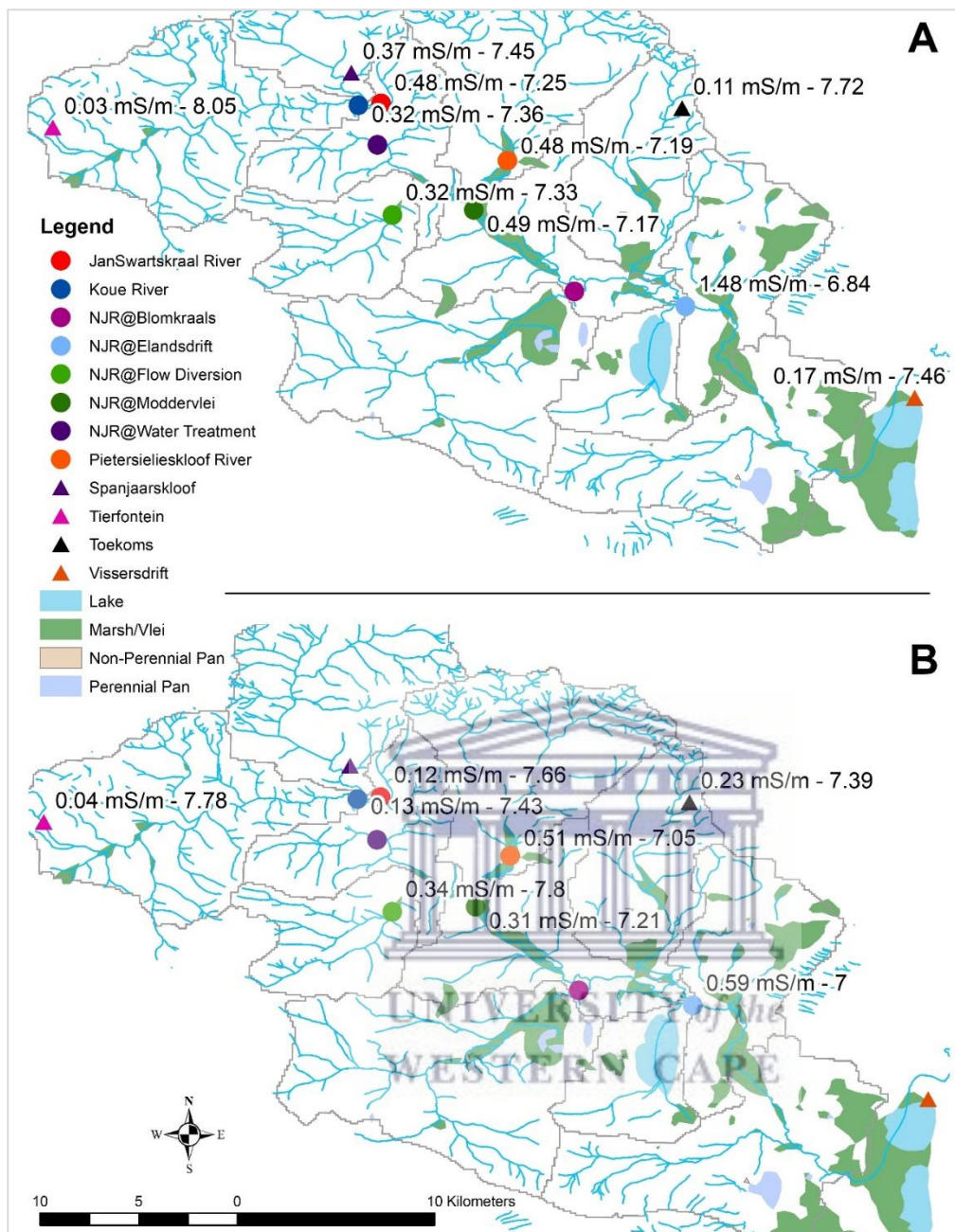


Figure 5.15: Variation of electrical conductivity (EC) and pH of river water along the Nuwejaars River and tributaries in October 2016 (A) and November 2016 (B). At each location EC value is separated from pH by “-”.

5.3.5. Wetland climatic conditions

The Nuwejaars wetland being in a Mediterranean climate had its highest air temperatures from November to March where the average monthly air temperature exceeded 25 °C. On the hand,

during the winter months of June to August monthly averages did not exceed 20 °C (Figure 5.16). The windiest month was June with an average wind speed of 57 m.s (Figure 5.16).

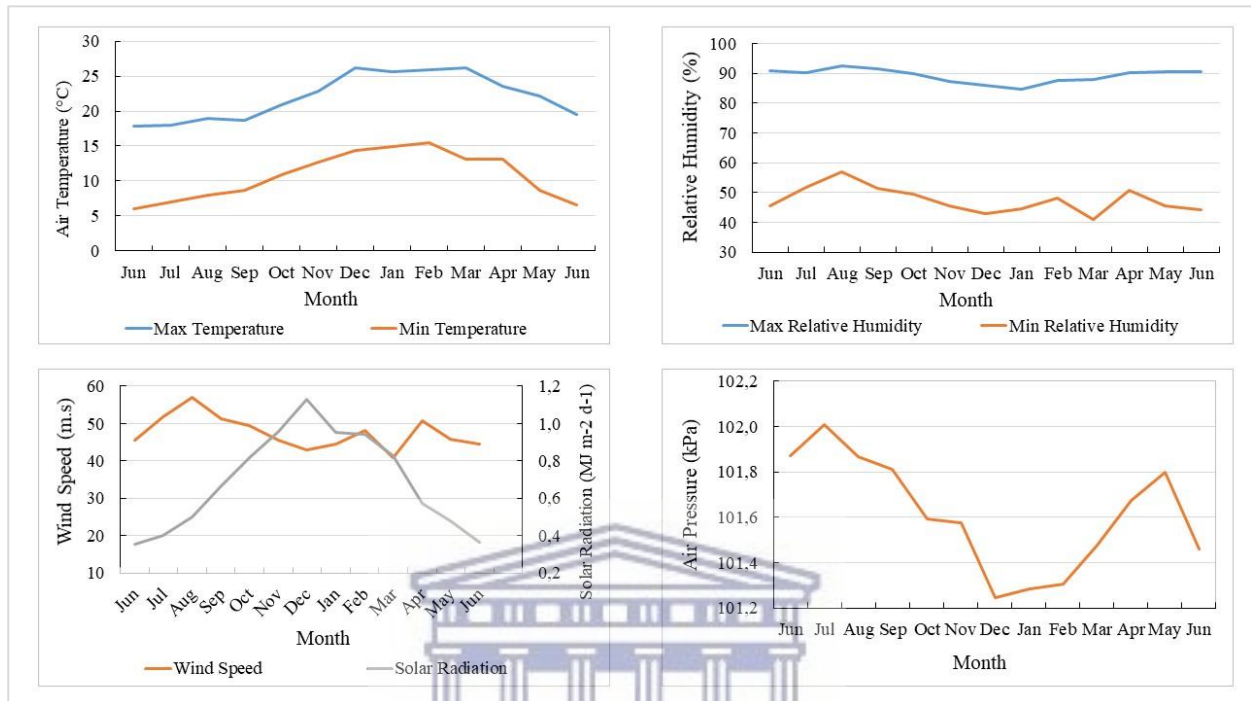


Figure 5.16: Average monthly maximum and minimum air temperatures, maximum and minimum relative humidity, wind speed, solar radiation and air pressure measured at the Moddervlei weather station from the 16th June 2016 to 16th June 2017.

The average ET estimated using the Penman-Monteith method was 4.12 mm/day at the Moddervlei station. The maximum ET was 11.08 mm/day recorded on the 18th of January 2017 (Figure 5.17). This is during the warmer and windier months in the catchment and it is therefore expected. Most of the rainfall fell over the wetland during the wet season of July to August of 2016 (Figure 5.17).

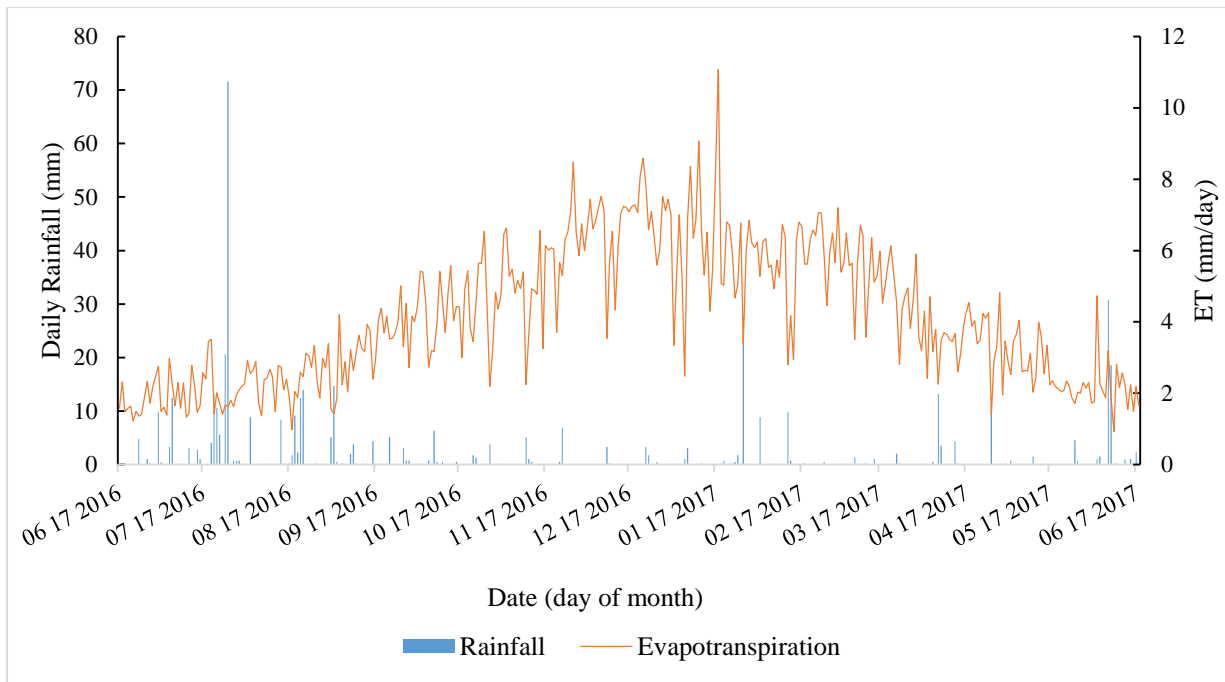


Figure 5.17: Daily rainfall recorded at the Moddervlei station and the daily ET estimated using the Penman-Monteith method from the 16th June 2016 to the 16th June 2017.

5.3.6. Spatio-temporal variations of flows through the wetland

The Nuwejaars River at Elandsdrift showed very little to no response to rainfall during the early stages of the wet season (Figure 5.18). The first notable response at Elandsdrift was recorded following the major rainfall event which occurred on the 25th July 2016. The Nuwejaars water levels at Elandsdrift rose from 0.5 m to 1.8 m and from 0.5 m to 2.1 m at the Melkery Bridge (Figure 5.18). Water levels at the Melkery Bridge showed a steady decline towards the end of the wet season and only responded to 2 major rainfall events. However, the Elandsdrift water levels were maintained towards the end of the wet season and slowly declined towards the dry season (Figure 5.18)

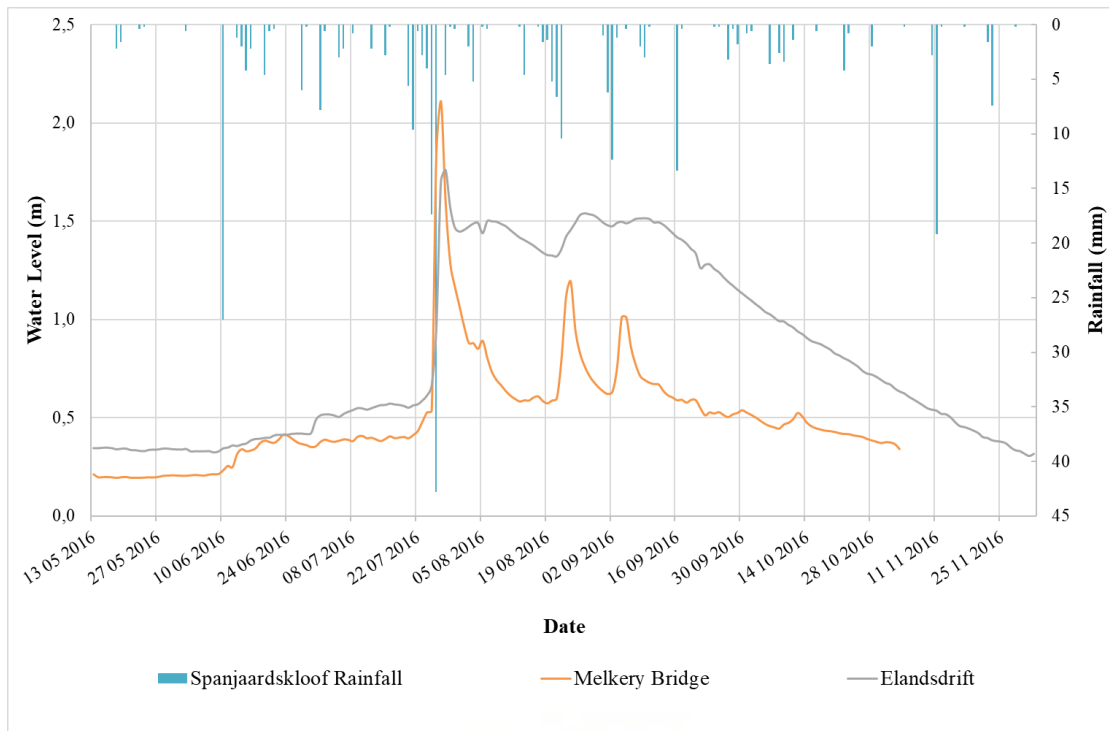


Figure 5.18: Daily water level responses of the Nuwejaars River at the Elim Melkery Bridge (inflow to the wetland) and Elandsdrift (wetland outflow) to rainfall recorded at the Spanjaardskloof station, from the 13th May 2016 to 2nd December 2016.

On the 1st July 2016, during the early stages of the wet season, 10 mm rainfall was recorded at the Spanjaardskloof weather station. The Nuwejaars River at Elandsdrift and Melkery Bridge did not respond to this event (Figure 5.19). The average discharge at Elandsdrift was 0.07 m³.s and 0.01 m³.s at the Melkery Bridge.

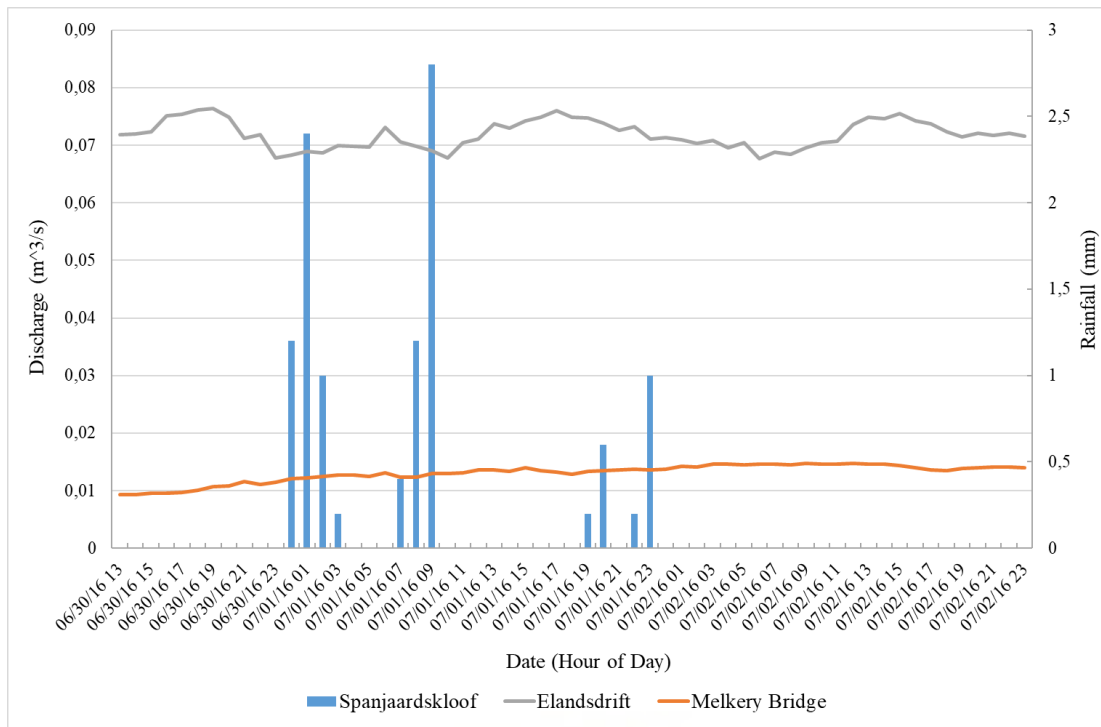


Figure 5.19: Average hourly discharge of the Nuwejaars River at the Melkery Bridge (upstream of the wetland) vs the outflow of the wetland at Elandsdrift in response to a selected rainfall event during the early stages of the wet season.

During mid-wet season, the major rainfall event on the 25th of July 2016, started at 16h00, a total of 63 mm of rainfall fell at an average rainfall intensity of 3.31 mm/hr. The peak flow reached the Melkery Bridge 23 hours after the start of the rainfall event with a peak flow of 70.63 m³.s. It took a further 27 hours for the peak at the Elandsdrift site which had a peak flow of 9.65 m³.s (Figure 5.20). The wetland therefore reduced peak flows by 60.98 m³.s. An average discharge of 3.45 m³.s maintained at the Elandsdrift site following the peak flow. However, by 21h00 on the 30th July the discharge of the Melkery Bridge had dropped below that of Elandsdrift and continued to drop to 0.84 m³.s (Figure 5.20).

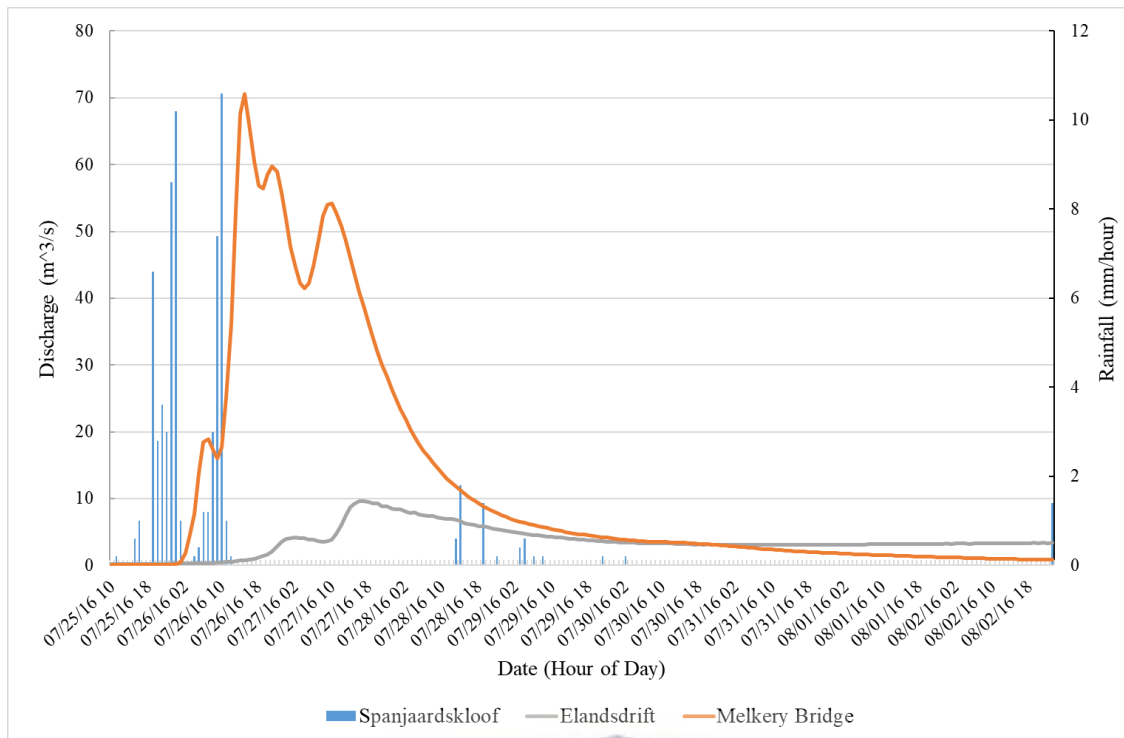


Figure 5.20: Average hourly discharge of the Nuwejaars River at the Melkery Bridge (upstream of the wetland) vs the outflow of the wetland at Elandsdrift in response to the major rainfall event on the 25th July 2016 mid-wet season.

Towards the end of the wet season, 21 mm rainfall was recorded at the Spanjaardskloof station between the 1st and 2nd September 2016. The Nuwejaars River at the Melkery Bridge responded after 49 hours to this event and no response was recorded at Elandsdrift (Figure 5.21). The peak discharge on the Nuwejaars River at the Melkery Bridge was 2.8 m³.s, while an average discharge of 3.4 m³.s was maintained at Elandsdrift (Figure 5.21).

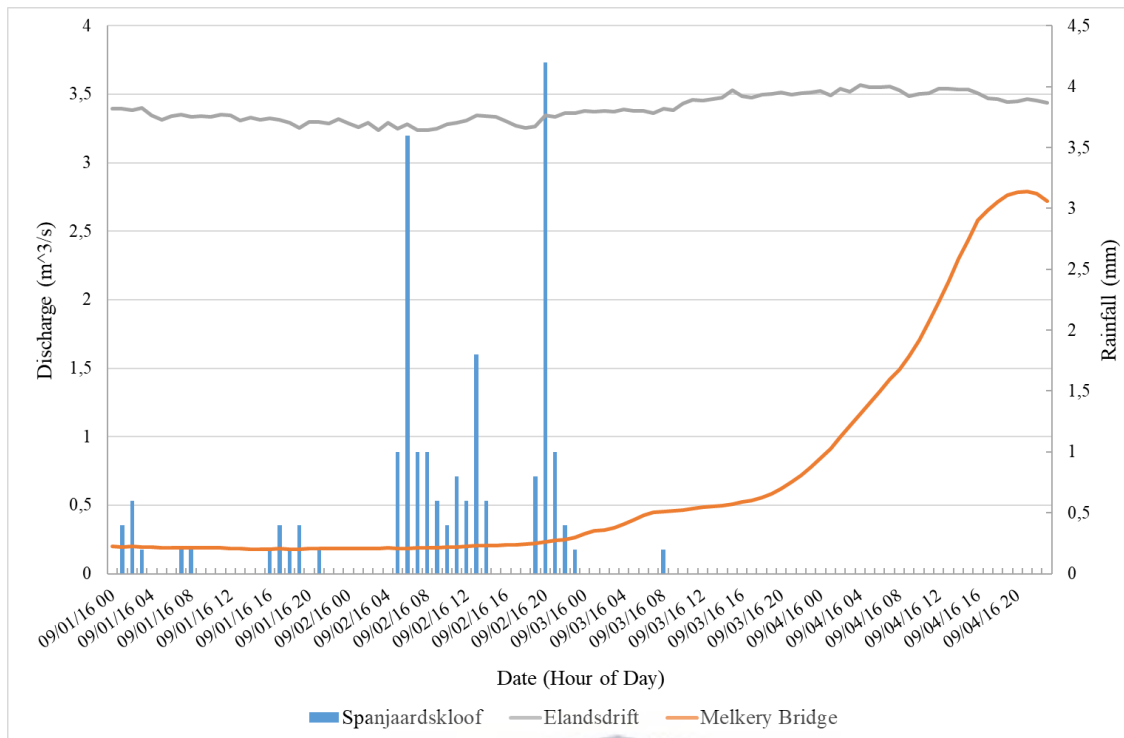


Figure 5.21: Average hourly discharge of the Nuwejaars River at the Melkery Bridge (upstream of the wetland) vs the outflow of the wetland at Elandsdrift in response to a selected rainfall event during the end of the wet season.



The Global Meteoric Water Line for (GMWL) for the Western Cape is defined by the equation (5.10) (Saayman, *et al.*, 2003):

$$\delta^2H = 6.1 \delta^{18}O + 8.6 \quad (5.10)$$

In June 2016, there was a distinct difference between the rainfall samples and the river samples. The river samples had an average δ^2H % of -12.94 and $\delta^{18}O$ % of -4.02 while the rainfall samples had an average δ^2H % of -22.43 and $\delta^{18}O$ % of -5.22 (Figure 5.22).

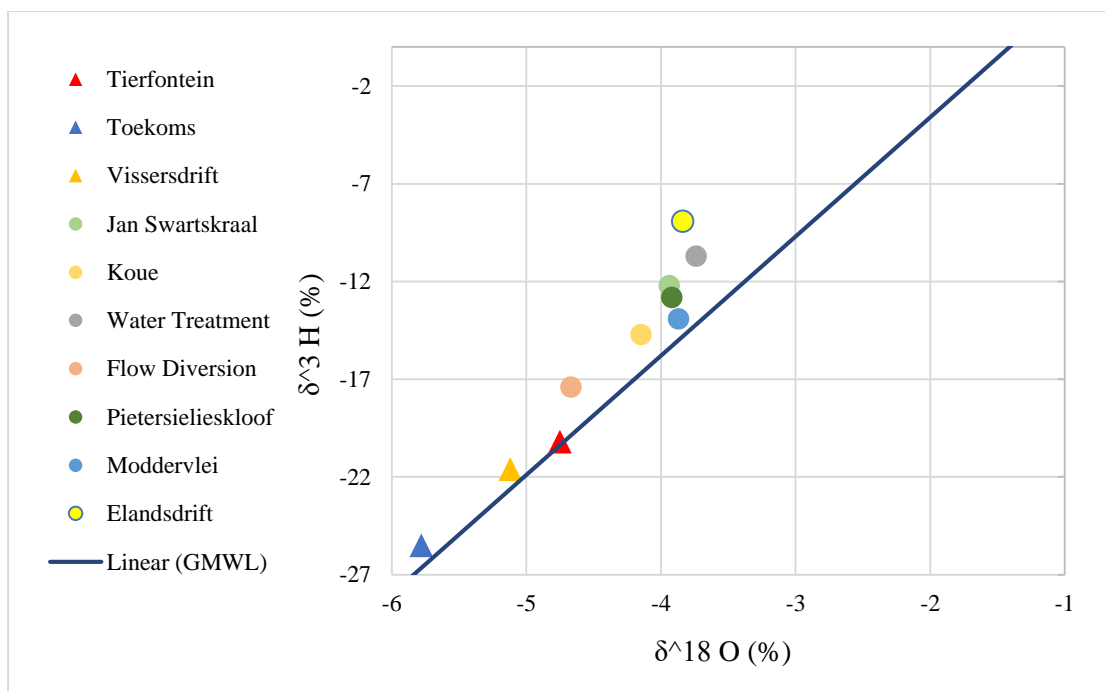


Figure 5.22: Isotopic results of the rainfall water samples (triangles) and river water samples (circles) collected in June 2016.

There was a strong correlation between the isotopic signatures of the rainfall and river samples for July 2016 (Figure 5.23). The river samples had an average $\delta^2\text{H}$ % of -46.15 and $\delta^{18}\text{O}$ % of -7.96 while the rainfall samples had an average $\delta^2\text{H}$ % of -53.9 and $\delta^{18}\text{O}$ % of -9.03 (Figure 5.23). The rivers responded quickly to rainfall during the wet season and therefore a strong relationship between the isotopic signatures was expected.

Similarly, for August 2016 the isotopic signatures of the rainfall and river samples showed a strong correlation (Figure 5.24). The river samples had an average $\delta^2\text{H}$ % of -17.16 and $\delta^{18}\text{O}$ % of -4.79 while the rainfall samples had an average $\delta^2\text{H}$ % of -22.7 and $\delta^{18}\text{O}$ % of -5.48 (Figure 5.24). The samples for August 2016 were taken following the major rainfall event on the 25th July 2016 and a strong relationship between the rainfall and river isotopic signatures is therefore expected.

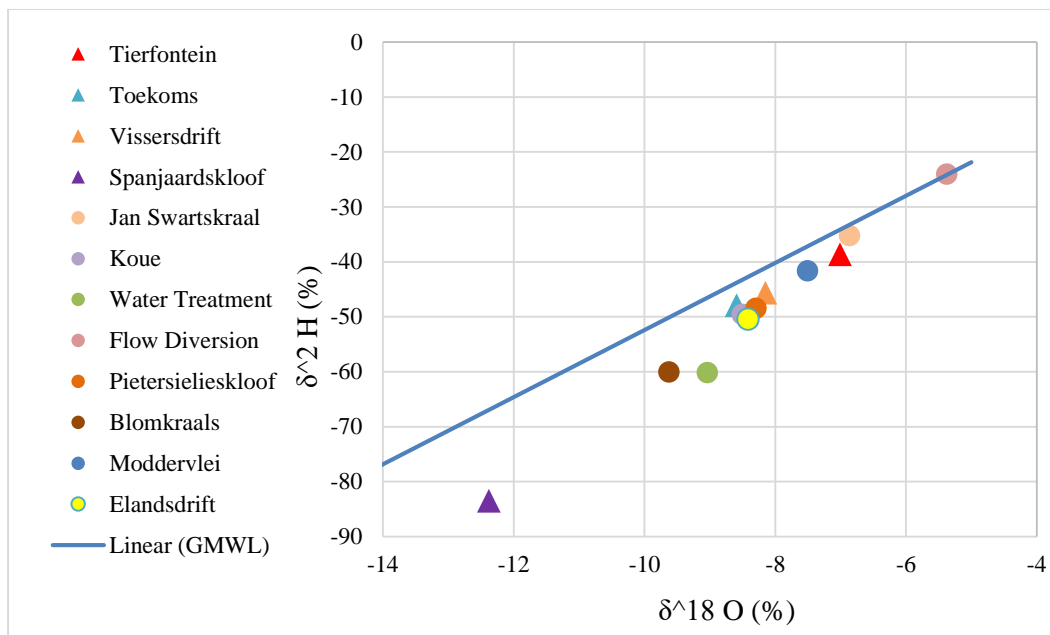


Figure 5.23: Isotopic results of the rainfall water samples (triangles) and river water samples (circles) collected in July 2016.

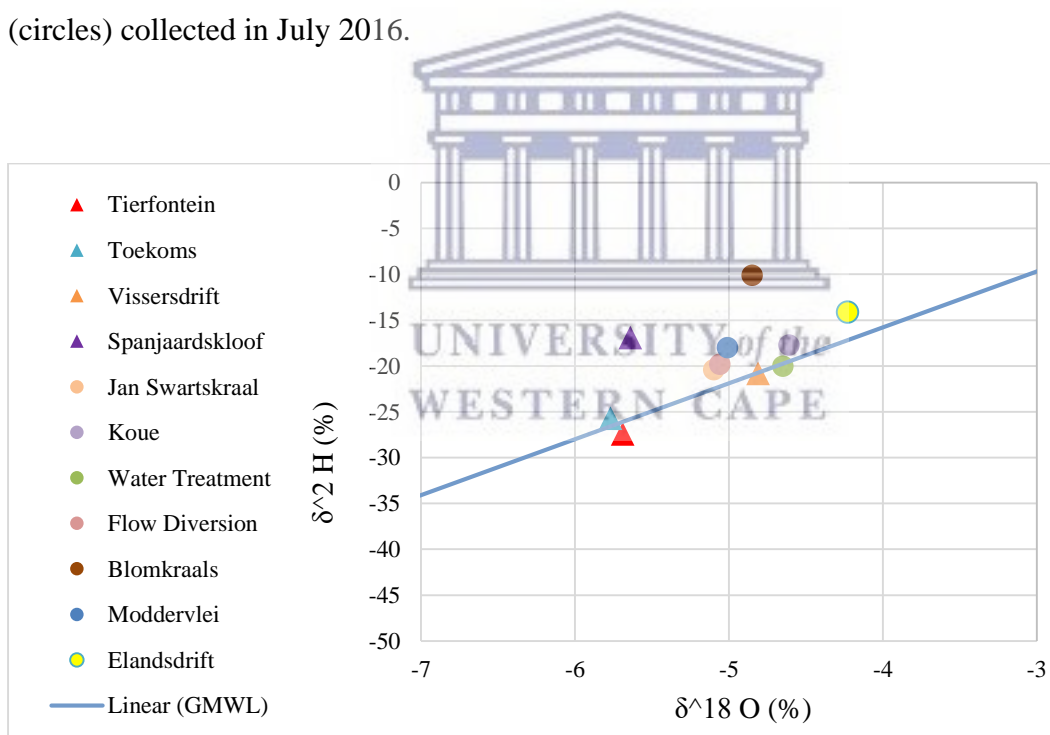


Figure 5.24: Isotopic results of the rainfall water samples (triangles) and river water samples (circles) collected in August 2016.

Towards the end of the wet season the isotopic signatures of the rivers were lower than that of the rainfall samples, with the exception of Elandsdrift and Blomkraals river samples (Figure 5.25). However, the Elandsdrift and Blomkraals samples are collected further downstream of

the wetland and are therefore more susceptible to evaporation and the influence of groundwater. The river samples for September 2016 had an average $\delta^2\text{H}$ % of -14.49 and $\delta^{18}\text{O}$ % of -4.34 while the rainfall samples had an average $\delta^2\text{H}$ % of -0.53 and $\delta^{18}\text{O}$ % of -3.5 (Figure 5.25)

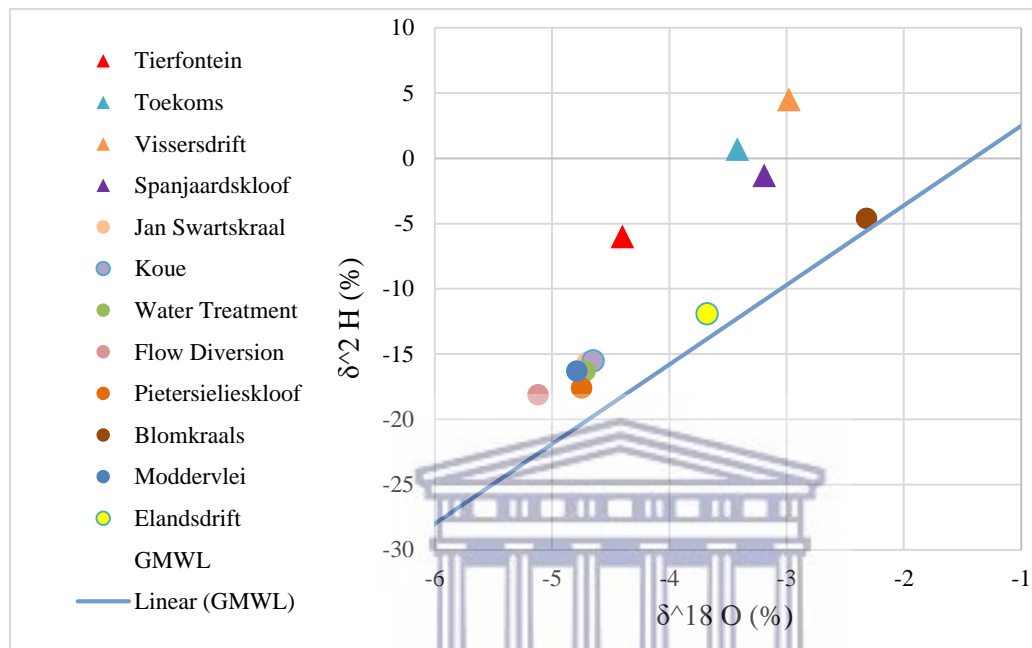


Figure 5.25: Isotopic results of the rainfall water samples (triangles) and river water samples (circles) collected in September 2016.

5.3.7. Predicting the wetland response to inflows

S_{\min} for the wetland was estimated at 0.75 Mm^3 , S_{\max} was estimated at 7 Mm^3 , α was estimated at 463.41 and β at 0.422 with an average Recharge estimated at 5 % of the daily inflows as recommended by Xu *et al.*, (2001) and DWAF, (2004). The relationship between the measured and predicted outflows of the wetland was good, with an R^2 value of 0.65 and a root mean square error of 0.13. The predicted total discharge for the 1-year cycle from the 17th June 2016 to 17th June 2017 was 21.4 Mm^3 , while the measured discharge was 27.7 Mm^3 (Figure 5.26 and Table 5.2). The predicted discharge for the cycle was 6.4 Mm^3 less than the observed discharge (Table 5.2). The effects of the wetland on flows can clearly be seen by the 2-day lag following the major rainfall event of the 25th July 2016 (Figure 5.26).

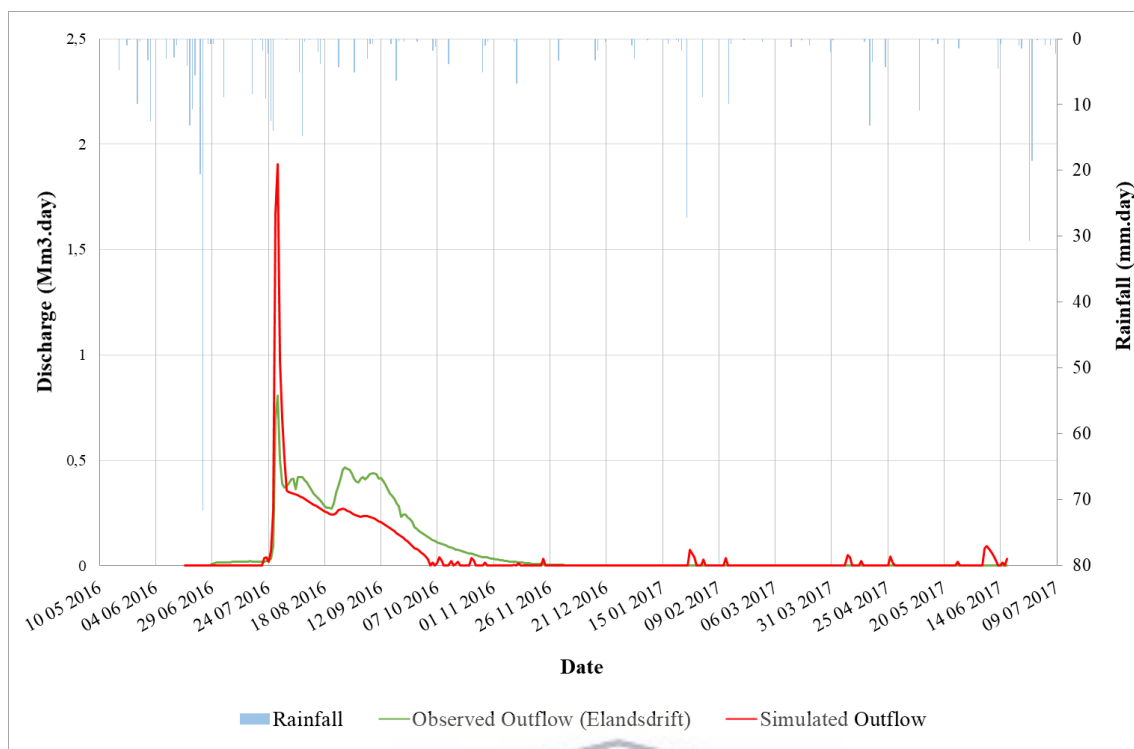


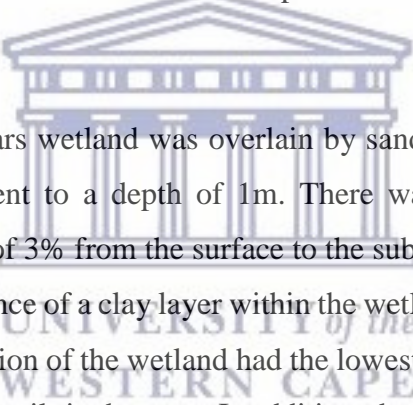
Figure 5.26: The predicted daily discharge at Elandsdrift estimated using the water balance vs the measured daily discharge at Elandsdrift from 17th June 2016 to the 17th June 2017.

Table 5.2: The volume and percentage of inflows and outflows of the Nuwejaars Wetland and the measured vs predicted outflow from the 17th June 2016 to 17th June 2017.

	Water (Mm ³)	Percentage
Rainfall	3.1	10 % of inflows
River Flows	28.9	90 % of inflows
Rainfall + River Flows	32.0	100 %
ET (outflow)	10.1	46 % of outflows
Inflows - ET	21.9	
Measured Outflow	27.7	
Predicted Outflow	21.5	

5.4 Discussion

The morphology of the Nuwejaars wetland is characteristic of a floodplain wetland. As described by Ollis, *et al.*, (2013), a floodplain wetland is characteristically formed by an alluvial river, flat surfaces along the margin of the river and terraces which are not generally active. Ollis, *et al.*, (2013), reported that floodplain wetlands are characterized by geomorphological features such as point bars, scroll bars, oxbow lakes and levees. The presence of oxbow lakes within the wetland is evident from the results, and large pools which temporarily store water are found throughout the wetland. The concentration of pools was highest in the middle section of the wetland, with less pools present towards the end. In addition, the largest pool of water was located near the middle of the wetland at the confluence of the Nuwejaars and Pietersielieskloof Rivers. The results of morphological surveys support the classification of the Nuwejaars wetland as a floodplain wetland.



For the most part, the Nuwejaars wetland was overlain by sandy-loam and loamy-sand soils with an increase in clay content to a depth of 1m. There was a notable increase of clay percentage in the soil samples of 3% from the surface to the sub-surface. As noted by Bullock & McCartney (1996), the presence of a clay layer within the wetland affects the water retention of the wetland. The middle section of the wetland had the lowest infiltration rates as a result of higher clay content found in the soils in that area. In addition, the soil data showed characteristic deposition as a result of occasional flooding of the wetland. Thus, substantiating the alluvial nature of the wetland and supporting the notion of Ollis, *et al.*, (2013). The alluvial nature of the wetland promotes the growth of vegetation and therefore contributes to the flood attenuating capabilities of the wetland. As noted by McCartney *et al.*, (2013) wetlands are usually highly vegetated and therefore aid in reducing flow velocities.

The deposition of these soils aid in the growth of vegetation. Unfortunately, this promotes the growth of alien species such as *Acacia longifolia*, which are commonly found in and around the Nuwejaars wetland. Although these trees are considered to be alien and have negative impacts on the environment, due to their abilities to abstract large amounts of water (Rowntree, 1991; Le Maitre & Versefeld, 2000; Kotzé *et al.*, 2010), they improve the flood attenuation of

the wetland by reducing the magnitude of floods and removing water via transpiration. In addition, they are located mostly in the floodplain of the Nuwejaars River (Figure 5.12) and therefore aid in stabilizing the banks of the river and protecting the wetland from surface scour and erosion. On the other hand, they pose a threat to natural vegetation such as the Wilde Palmiet and *Cyperus spp.* (various species of sedge) which thrive in wetland environments.

The presence of Wilde Palmiet within a wetland, aids in its flood attenuation as they have the ability to slow flows and in most cases result in ponding of water (Annexure 6). The presence of Wilde Palmiet within the Nuwejaars wetland may have contributed to the formation of pools, such as the large pool in the middle of the wetland (Annexure 6 D). In addition, the presence of the Palmiet and woody alien vegetation aid in the formation of oxbow lakes and may result in diffuse flow which occurs within the wetland.

Ollis, *et al.*, (2013) noted that, water flow through floodplain wetlands are predominantly horizontal, in and out of the wetland and occurs through diffuse surface and or sub-surface flow. Furthermore, Ollis, *et al.*, (2013) noted that temporary storage of water may occur within depressions of the wetland, thus making it vulnerable to infiltration and ET. This was substantiated in this study, as flows were stored in depressions along the floodplain of the wetland following the flood on the 25th July 2016 (Annexure 6). In addition, diffuse flow is evident from the middle of the wetland towards the end, where the channel dissipates, and only becomes a fixed to a single channel towards the end of the wetland.

In addition, the results of the isotope data show that the wetland is strongly influenced by surface runoff from the surrounding areas and tributaries. However, there is an influence of groundwater which is not accounted for. There is a decrease in EC from the water quality samples taken along the Nuwejaars River at Blomkraals to the sample taken at Elandsdrift. This may be the result of the wetland, which acts as a filter and therefore may help improve the water quality further downstream. These results clearly show the storage and filtration capabilities of the wetland. However, it is more important to understand to what extent flows are reduced, rather than whether or not the process occurs. It was therefore important to assess the effect of the wetland on the magnitude of flows in addition to its storage capabilities.

The effect of the Nuwejaars wetland on the magnitude of the flows of the Nuwejaars River is evident from the sustained flows of the Nuwejaars River at Elandsdrift following the wet season. The distinct difference in the magnitude of the flows measured along the Nuwejaars River at the Melkery Bridge and Elandsdrift clearly indicate a decrease in the magnitude of flows (Figure 5.20). The wetland reduced flows by an average of 6.2 m³/s between the Melkery Bridge and the Elandsdrift site. These findings substantiate the findings noted by McCartney, *et al.*, (2013) on the flood attenuating capabilities of floodplain wetlands and their importance in maintaining dry season flows. Although monitoring the flood attenuation of the wetland was time consuming it proved to be effective and therefore needed to be further assessed by attempting to model this process.

The Flex-topo model approach used for the Nuwejaars wetland performed well. Considering that only a year cycle of data was used a R² value of 0.65 and a root mean square error of 0.13 is considered to be good. However, the model overestimates the initial peak flow and underestimates peak flows following the major event on 25th July 2016. This may be the result of groundwater recharge being underestimated. Furthermore, the simulated outflows following the wet season are lower than the measured outflow and may be the result of overestimated ET. The measured annual discharge of 27.7 Mm³ at Elandsdrift was 5.8 Mm³ more than the difference between the inflows and the measured outflows (ET). These results support the need to further assess the groundwater recharge and ET measurements of the wetland.

Due to the time constraints and limited data associated with an ungauged catchment it was expected for the model to perform reasonably well. With a longer set of hydrological data and improved assessment of the groundwater processes the model should perform substantially better. It can then be used for flood predictions in the area and therefore improve management and planning of water resources within the Heuningnes Catchment. Furthermore, modelling and studying this wetland under the stressed conditions of the drought which occurred over the 2016-2017 was an eye-opener to the consequences we may face if our water resources are not managed correctly.

6. CONCLUSION AND RECOMMENDATIONS

The mountainous Janswartzkraal and Koue sub-catchments of the Nuwejaars Catchment responded quickly to rainfall events and showed a strong reliance on rainfall for runoff to occur. These two sub-catchments contributed 48% of the Nuwejaars River flows and substantiates the finding of Blöschl *et al.*, (2013) and WWF-SA, (2013) who noted the importance of mountainous headwater catchments to flow contributions in South Africa. These mountainous sub-catchments stop flowing during the dry season, around new year's day and during the drought period experienced in 2017 have very little to no flow. This further substantiates the reliance of mountainous headwater catchments on rainfall.

The Elim and Pietersielieskloof sub-catchments contributed substantially less flows to the Nuwejaars River, when compared to the Janswartzkraal and Koue sub-catchments. Interestingly, flows occurred in the Elim and Pietersielieskloof sub-catchments during the dry season when the Janswartzkraal and Koue sub-catchments showed very little to no flow. This provided evidence of a groundwater influence in the Elim and Pietersielieskloof sub-catchments. The influence of groundwater in the Elim and Pietersielieskloof sub-catchments was further substantiated by the fact that these were the only tributaries which had flows during the drought in 2017. Flows were recorded along the Nuwejaars River at Elandsdrift during the drought in 2017. This site was the furthest downstream and as very little to no flows occurred in the upper sub-catchments, these flows may be the result of groundwater discharge downstream of the Nuwejaars wetland.

On the other hand, no substantial flows were recorded at the Blomkraals and Voëlvlei tributaries during the drought of 2017. Unlike the Janswartzkraal and Koue sub-catchments, the Blomkraals and Voëlvlei sub-catchments occurred in the undulating plains of the Agulhas region and as a result require substantially more rainfall before flows occurred. However, due to the presence of large wetlands within the Voëlvlei and Blomkraals sub-catchments, flows were sustained for a longer period than compared to the mountainous Janswartzkraal and Koue sub-catchments following the wet season. These findings support the notion of the collective effect of multiple interlinked wetlands on flood attenuation at a catchment scale noted by McCartney, *et al.*, (2013), Kotzé (2000) and Cleaver & Brown (2005).

The presence of the multiple channelled valley-bottom wetlands which lead to floodplain wetlands in the flatter areas of the Agulhas region had a great effect on the flows of the Nuwejaars River. It was found that the Nuwejaars wetland reduced the magnitude of flows by temporarily storing water following a flood and then slowly releasing the water throughout the dry season. This lasts until approximately the 1st of January 2016. From the results it was evident that the Nuwejaars wetland reduced the magnitude of floods by an average of 6.2 m³/s, increased travel times by 27 hours and temporarily stored flows. Therefore, supporting the findings of McCartney, *et al.*, (2013), Kotzé (2000) and Cleaver & Brown (2005) on the flood attenuating capabilities of wetlands.

The results clearly showed evidence of the flood attenuating capabilities of the Nuwejaars wetland on the flows of the Nuwejaars River and warranted further investigation for modelling purposes. The Flex-topo model proved to be effective in modelling the effects of the Nuwejaars wetland on the flows of the Nuwejaars River. Considering that only a year cycle of hydrological data was used, a R² value of 0.65 and a root mean square error of 0.13 is considered to be good. However, continued monitoring and data collection is imperative to more accurately model and understand the collective effects of these wetlands on river flows.

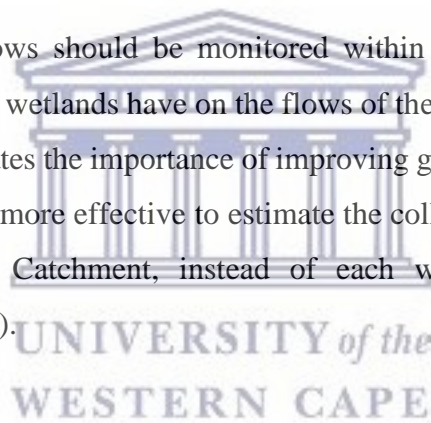
A study such as this is strongly reliant on long term hydrological data to accurately model the process. A particular challenge during this study was the drought which occurred during 2017 as the study was reliant on flows to occur. The initiation and maintenance of a river flow monitoring system was quite challenging and manually monitoring flows can be quite a challenge. With 13 flow monitoring sites and several weather stations to visit, bi-weekly field trips for 2 days seem to be the most feasible and effective. It took approximately 45 mins per site for flow measurements and downloading of data. During high flows many sites could not be accurately measured as it was not safe to enter the channel or even possible to access the site due to flooded bridges. This had a major impact on the data as it was not possible to measure peak flows and in turn affects the accuracy of the rating curves.

The lack of groundwater data was a concern as this was neglected from the study. However, the water balance did reveal that further investigation in this area was required. The in situ soil

sampling conducted provided an idea of the wetland soils in the area. However, various parts of the wetland were inaccessible and therefore could not be characterized. In addition, the depth of the pools and depressions present in the wetland could not be accurately measured during the wetland survey, due to the depth of the Nuwejaars River itself. The soil infiltration tests were conducted when the wetland was dry. Soils may be hydrophobic during this period and may result in infiltration rates that are lower than expected.

It is recommended that monitoring of flows at these sites are maintained for a longer period of time in order to improve the accuracy of the river flow estimates. The installation of a weir would help accurately assess flows. In addition, accessibility should be a key factor when determining the use of sites for flow measurements specifically during high flows.

Furthermore, groundwater flows should be monitored within this area in order to further understand the influence these wetlands have on the flows of the Nuwejaars River. The deficit in the water balance substantiates the importance of improving groundwater monitoring in this system. In addition, it may be more effective to estimate the collective effects of the wetlands on flows in the Nuwejaars Catchment, instead of each wetland individually, as was recommended by Kotzé (2000).



In conclusion, the Nuwejaars Catchment plays host to multiple hydrological processes which work together. The steeper mountainous sub-catchments show a more rapid short-term response to rainfall and contribute more flows directly to the Nuwejaars River than compared to the flatter sub-catchments. The topography of the lower lying sub-catchments plays host to multiple wetlands, pools and dams which aid in flood attenuation and the slow release of flows. The presence of these wetlands are imperative to maintaining dry season flows and reduce the magnitude of peak flows or floods during the wet season. The Nuwejaars wetland did in fact reduce the magnitude of peak flows and maintain the dry season flows of the Nuwejaars River and substantiates the collective effect of wetlands on flood attenuation.

7. REFERENCES

Allen, R.G., Pereira, L.S., Raes, D., Smith, M. (1998). Crop evapotranspiration - Guidelines for computing crop water requirements - FAO Irrigation and drainage paper 56. FAO – Food and Agriculture Organization of the United Nations Rome. Available at: https://appgeodb.nancy.inra.fr/biljou/pdf/Allen_FAO1998.pdf

Ameli, A. A., & Creed, I. F. (2017). Quantifying hydrologic connectivity of wetlands to surface water systems. *Hydrology and Earth System Sciences*, 21(3), 1791–1808. Available at: <https://doi.org/10.5194/hess-21-1791-2017>

Arcement, G.J. & Schneider, V.R. (1984). Guide for Selecting Manning’s Roughness Coefficients for Natural Channels and Flood Plains. U.S. Department of Transportation. Report No.: FHWA – TS – 84 – 204, pp. 1-62. Available at: <https://www.fhwa.dot.gov/bridge/wsp2339.pdf>

Asadi, A. (2013). The Comparison of Lumped and Distributed Models for Estimating Flood Hydrograph (Study Area : Kabkian Basin). *Quest Journal, Journal of Electronics and Communication Engineering Research*, 1(2), 7–13.

Azizi, Z., Najafi, A. & Sohrabi, H., (2008). Forest Canopy Density Estimating , Using Satellite Images. *The International Archives of Photogrammetry, Remote Sensing and Spatial Information Sciences*. 37(Part B8), pp. 1127-1130. Available at: http://www.isprs.org/proceedings/XXXVII/congress/8_pdf/11_WG-VIII-11/21.pdf.

Bartley, R., Keen, R.J., Hawdon, A.A., Disher, M.G., Kinsey-Henderson, A.E., Hairsine, P.B. (2006). Measuring rates of bank erosion and channel change in northern Australia: a case study from the Daintree River catchment. CSIRO Land and Water Science Report, Report No.: 43/06, pp.1-51. Available at: <http://www.clw.csiro.au/publications/science/2006/sr43-06.pdf>.

Bengtson, M.L. & Padmanabhan, G. (1999). A Review of Models for Investigating the Influence of Wetlands on Flooding. International Joint Commission Red River Task Force North Dakota State Water Commission Minnesota Department of Natural Resources, Division of Waters. Available from: <https://www.ndsu.edu/wrri/Publications/A%20Review%20of%20models.pdf>

Bickerton, I.B. (1984). Estuaries of the Cape. Estuaries of the World. Council for Scientific and Industrial Research, Report number: 25, pp.1–63. Available at: http://fred.csir.co.za/project/CAPE_Estuaries/documents/Heuningnes%20EMP%20draft.pdf.

Blight, G. E. (2002). Measuring evaporation from soil surfaces for environmental and geotechnical purposes. *Water SA*, 28(4), 381–394. Available at: <http://doi.org/10.4314/wsa.v28i4.4911>

Blöschl, G., Sivapalan, M., Wagener, T., Viglione, A. & Savenije, H. (2013). *Runoff Prediction in Ungauged Basins: Synthesis across Processes, Places and Scales*. Cambridge University Press. The Edinburgh Building, Cambridge CB2 8RU, United Kingdom. pp 465.

Brauer, C. C., Teuling, A. J., F. Torfs, P. J. J., & Uijlenhoet, R. (2014). The Wageningen Lowland Runoff Simulator (WALRUS): A lumped rainfall-runoff model for catchments with shallow groundwater. *Geoscientific Model Development*, 7(5), 2313–2332. <https://doi.org/10.5194/gmd-7-2313-2014>

Brirhet, H., & Benaabidate, L. (2016). Comparison of Two Hydrological Models (Lumped and Distributed) Over A Pilot Area of the Issen Watershed in the Souss Basin, Morocco.

European Scientific Journal, 12(18), 347–358. Available at:

<https://doi.org/10.19044/esj.2016.v12n18p347>

Bullock, A., and McCartney, M. (1996). Wetland and river flow interactions in Zimbabwe. *Tropical Hydrology: Geoscience and Tool for Developing*, 238(238), 305–321.

Cleaver, G. & Brown, L.R. (2005). Wetland Restoration: Nuwejaars, Heuningnes, Kars and Ratel Wetland and River Systems: Information Status Quo Report and Recommendations. Report to the Department of Agriculture, Project No.: AGR100239/0001.

Dilts, T.E., Yang, J. & Weisberg, P.J., 2010. Mapping Riparian Vegetation with Lidar Data. *ArcUser*, (Winter 2010), pp.18–21. Available at:

<http://www.esri.com/news/arcuser/0110/files/mapping-with-lidar.pdf>.

Doña, C., Chang, N. Bin, Caselles, V., Sanchez, J. M., Perez-Planells, L., Bisquert, M. del M., Camacho, A. (2016). Monitoring hydrological patterns of temporary lakes using remote sensing and machine learning models: Case study of La Mancha Humeda Biosphere Reserve in Central Spain. *Remote Sensing*, 8(8). Available at: <http://doi.org/10.3390/rs8080618>.

Du, Y., Zhang, Y., Ling, F., Wang, Q., Li, W., & Li, X. (2016). Water bodies' mapping from Sentinel-2 imagery with Modified Normalized Difference Water Index at 10-m Spatial Resolution Produced by Sharpening the SWIR Band. *Remote Sensing*, 8(354). Available at: <http://doi.org/10.3390/rs8040354>

Department of Water Affairs and Forestry (DWAF). (2004). 'Guidelines for Groundwater Management in Water Management Areas, South Africa. *Integrated Water Resources Management*. 2(Implementation).

Fenicia, F., Savenije, H. H. G., Matgen, P., & Pfister, L. (2008). Understanding catchment behavior through stepwise model concept improvement. *Water Resources Research*, 44(1), 1–13. Available at: <http://doi.org/10.1029/2006WR005563>

Gholami, V. & Khaleghi, M.R., (2013). The impact of vegetation on the bank erosion (case study: The haraz river). *Soil and Water Research*, 8(4), pp.158–164.

Holmes, P.M. et al., (2008). Guidelines for improved management of riparian zones invaded by alien plants in South Africa. *South African Journal of Botany*, 74(3), pp.538–552. Available at: <http://linkinghub.elsevier.com/retrieve/pii/S0254629908001749>.

Huang, C., Yang, L., Wylie, B. & Homer, C. (2001). A Strategy for Estimating Tree Canopy Density Using Landsat 7 ETM+ and High Resolution Images over Large Areas. *U.S. Geological Survey*, Available at: http://landcover.usgs.gov/pdf/canopy_density.pdf.

King, J.M., Scheepers, A.C.T., Fisher, R.C., Reinecke, M.K. & Smith, L.B. (2003). River rehabilitation: literature review, case studies and emerging principles. Water Research Commission, WRC No.: 1161/1/03. Available at: <http://www.wrc.org.za/Knowledge%20Hub%20Documents/Research%20Reports/1161-1-03.pdf>.

Knighton, D. (1984). *Fluvial Forms and Processes*. Edward Arnold Limited Publishers. 41 Bedford Square, London WC1D 3DQ. pp 44-189.

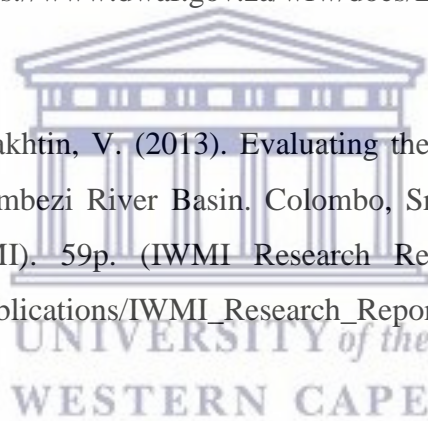
Kotzé, D., (2000). The Contribution of Wetlands to the Attenuation of Floods. *Mondi Wetlands Programme*. Available at: [http://www.wetland.org.za/ckfinder/userfiles/files/3_8-Scientific info_wetlands & flood research paper.pdf](http://www.wetland.org.za/ckfinder/userfiles/files/3_8-Scientific_info_wetlands_&_flood_research_paper.pdf).

Kotzé, I., Beukes, H., van den Berg, E. & Newby, T. (2010). National Invasive Alien Plant Survey. Agricultural Research Council, Report No.: GW/A/2010/21, pp.1-45. Available at: http://bgis.sanbi.org/EDRR/NationSurvey_IPAs.pdf.

Kraaij, T., Hanekom, N., Russell, I.A. & Randall, R.M. (2009). Agulhas National Park-State of Knowledge. South African National Parks. pp.1-51. Available at: http://www.sanparks.co.za/docs/conservation/scientific/coastal/Agulhas/ANP_SOK_Mar2009.pdf.

Le Maitre, D.C., Versefeld, D.B. & Chapman, R.A. 2000. The impact of invading alien plants on surface water resources in South Africa : A preliminary assessment. *Water SA.*, 26(3), pp.397–408. Available at: <https://www.dwaf.gov.za/wfw/docs/LeMaitreetal,2000.pdf>.

McCartney, M.; Cai, X.; Smakhtin, V. (2013). Evaluating the flow regulating functions of natural ecosystems in the Zambezi River Basin. Colombo, Sri Lanka: International Water Management Institute (IWMI). 59p. (IWMI Research Report 148). Available from: http://www.iwmi.cgiar.org/Publications/IWMI_Research_Reports/PDF/PUB148/RR148.pdf



McFeeters, S.K. (1996). The use of the Normalized Difference Water Index (NDWI) in the delineation of open water features. *International Journal of Remote Sensing*, 17, 1425–1432. Available at: <https://doi.org/10.1080/01431169608948714>

McFeeters, S. K. (2013). Using the normalized difference water index (NDWI) within a geographic information system to detect swimming pools for mosquito abatement: A practical approach. *Remote Sensing*, 5(7), 3544–3561. Available at: <http://doi.org/10.3390/rs5073544>

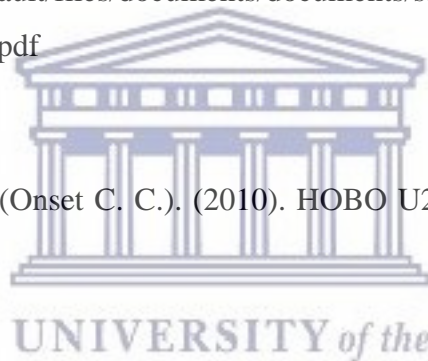
Mills, A., & Hunter, R. (2018). Restoration of wetlands on the Agulhas Plain is unlikely to generate peat. *South African Journal of Science*, 114(1–2), 3–5. Available at: <http://doi.org/10.17159/sajs.2018/a0252>

Morisawa, M. (1985). *Rivers, Forms and Processes*. Edited by Clayton, K.M. Longman Group Limited Publishes. Longman House, Burnt Mill, Harlow, Essex, CM20 2JE, England. Chapters 5-6, pp. 54-89.

Nel, J. L., Murray, K. M., Maherry, A. M., Petersen, C. P., Roux, D. J., Driver, A., ... Nienaber, S. (2011). Technical Report for the National Freshwater Ecosystem Priority Areas Project, (1801), 150.

Ollis, D.J., Snaddon, C.D., Job, N.M. & Mbona, N. (2013). Classification System for Wetlands and other Aquatic Ecosystems in South Africa. User Manual: Inland Systems. SANBI Biodiversity Series 22. South African National Biodiversity Institute, Pretoria. Available from: <http://www.sanbi.org/sites/default/files/documents/documents/sanbi-biodiversity-series-wetlands-classification-no-22.pdf>

Onset Computer Corporation (Onset C. C.), (2010). HOB0 U20L Water Logger (U20L-0x) Manual. Onset C. C. Bourne.



OTT Hydromet. (2011). OTT Orpheus Mini Ground Water Data Logger. OTT Hydromet. Germany.

Penna, D., Stenni, B., Šanda, M., Wrede, S., Bogaard, T. A., Gobbi, A., ... Chárová, Z. (2010). On the reproducibility and repeatability of laser absorption spectroscopy measurements for $\delta^2\text{H}$ and $\delta^{18}\text{O}$ isotopic analysis. *Hydrology and Earth System Sciences*, 14(8), 1551–1566. Available at: <http://doi.org/10.5194/hess-14-1551-2010>

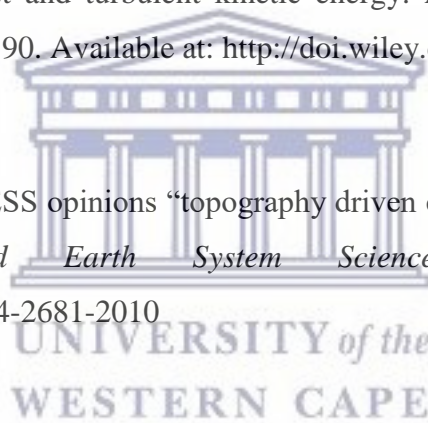
Piegay, H. et al., (1997). Bank erosion management based on geomorphological, ecological and economic criteria on the Galaure River, France. *Regulated Rivers-Research & Management*, 13(5), pp.433–448.

Rowntree, K. (1991). An Assessment of the Potential Impact of Alien Invasive Vegetation on the Geomorphology of River Channels in South Africa. *Southern Africa Journal of Aquatic Sciences*, 17(1-2), pp. 28-43.

Saayman, I.C., Scott, D.F., Prinsloo, F.W., Moses, G., Weaver, J. M. C. (2003). Isotopes in the Identification of the Dominant Streamflow Generation: Evaluation of the application of natural isotopes in the identification of the dominant streamflow generation mechanisms in TMG catchments Report to the Water Research Commission. Report No. 1234/1/03. ISBN No. 1-86845-989-6

Sang, J., Allen, P. & Dunbar, J., (2015). Determination of critical shear stress of non-cohesive soils using submerged jet test and turbulent kinetic energy. *Earth Surface Processes and Landforms*, 40(9), pp.1182–1190. Available at: <http://doi.wiley.com/10.1002/esp.3710>.

Savenije, H. H. G. (2010). HESS opinions “topography driven conceptual modelling (FLEX-Topo).” *Hydrology and Earth System Sciences*, 14(12), 2681–2692. <https://doi.org/10.5194/hess-14-2681-2010>



Schulze, R. E. (2011). A 2011 Perspective on Climate Change and the South African Water Sector. An Evaluation of the Sensitivity of Socio-Economic Activities to Climate Change in Climatically Divergent South African Catchments. WRC Report TT 518/12

Schulze, R. E. & Pike, A. (2003). Development and Evaluation of an Installed Hydrological Modelling System. WRC Report No. 1155/1/04. ISBN No. 1-77005-127-9. Available at: www.wrc.org.za/Knowledge%20Hub%20Documents/.../1155-1-04.pdf

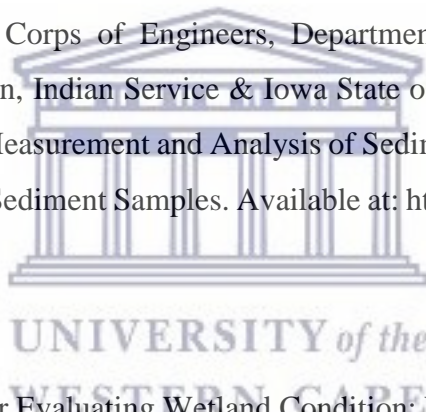
Schulze, R. E., Warburton, M. L., Jewitt, G. P. W. (2010). Confirmation of ACRU model results for applications in land use and climate change studies. *Hydrology and Earth System Sciences*, 14(12), 2399–2414. Available at: <http://doi.org/10.5194/hess-14-2399-2010>

Stroosnijder, L. (1992). Principles of Soil Water and Conservation. Department of Irrigation and Soil & Water Conservation. Lecture notes of Course K200-500/510.

Tal, M. & Paola, C., (2010). Effects of vegetation on channel morphodynamics: results and insights from laboratory experiments. *Earth Surface Processes and Landforms*, 35(9), pp.1014–1028. Available at: <http://doi.wiley.com/10.1002/esp.1908>.

Tanner, J. L., & Hughes, D. A. (2015). Understanding and Modelling Surface Water-Groundwater Interactions Water Research Commission. Available at: <http://www.wrc.org.za/Knowledge Hub Documents/Research Reports/2056 -2-14.pdf>

Tennessee Valley Authority, Corps of Engineers, Department of Agriculture, Geological Survey, Bureau of Reclamation, Indian Service & Iowa State of Hydraulic Research. (1941). A Study of Methods Used in Measurement and Analysis of Sediment Loads in Streams. Report No. 4: Methods of Analyzing Sediment Samples. Available at: <https://doi.org/10.1007/s13398-014-0173-7.2>



U.S. EPA. (2008). Methods for Evaluating Wetland Condition: Wetland Hydrology. Office of Water, U.S. Environmental Protection Agency, Washington, DC. EPA-822-R-08-024.

Vaze, J., Jordan, P., Beecham, R., Frost, A., Summerell, G. (2012). Guidelines for rainfall-runoff modelling: Towards best practice model application. Available from: [http://ewater.org.au/uploads/files/eWater-Modelling-Guidelines-RRM-\(v1-Mar-2012\).pdf](http://ewater.org.au/uploads/files/eWater-Modelling-Guidelines-RRM-(v1-Mar-2012).pdf)

Wilcox, B. P. (2010). Ecohydrology Bearing - Invited Commentary Transformation ecosystem change and ecohydrology: ushering in a new era for watershed management. *Ecohydrology*, 130(February), 126–130. Available at: <https://doi.org/10.1002/eco>

Williams, L., Harrison, S., & O'Hagan, A. M. (2012). The Use of Wetlands for Flood Attenuation. *Report for An Taisce by Aquatic Services Unit, University College Cork*.

Wolski, P., Savenije, H. H. G., Murray-Hudson, M., and Gumbricht, T. (2006). Modelling of the flooding in the Okavango Delta, Botswana, using a hybrid reservoir-GIS model. *Journal of Hydrology*, 331, 58–72, doi:10.1016/j.jhydrol.2006.04.040.

World Meteorological Organization (WMO). (2008). Guide to Hydrological Practices. Hydrology – From Measurement to Hydrological Information. 1:(6), WMO-No. 168. ISBN 978-92-63-10168-6

World Meteorological Organization (WMO). (2010). Manual on Stream Gauging: Volume 1, Fieldwork. WMO-No. 1044. ISBN 978-92-63-11044-2

Wu, W. (2002). Derivation of tree canopy cover by multiscale remote sensing approach. Workshop on Geospatial Data Infrastructure: from data acquisition and updating to smarter services. pp.142–149. Available at: <ftp://ftp.glcf.umiacs.umd.edu/modis/VCF>.

World Wide Fund for Nature, South Africa (WWF-SA) and Council for Scientific & Industrial Research (CSIR) . (2013). An Introduction to South Africa's Water Source Areas. Available at: http://dtnac4dfluyw8.cloudfront.net/downloads/wwf_sa_watersource_area10_lo.pdf

Wynn, T. & Mostaghimi, S., (2006). The effects of vegetation and soil type on streambank erosion, southwestern Virginia, USA. *Journal of the American Water Resources Association*, 42(1), pp.69–82. Available at: <Go to ISI>://000236554000009.

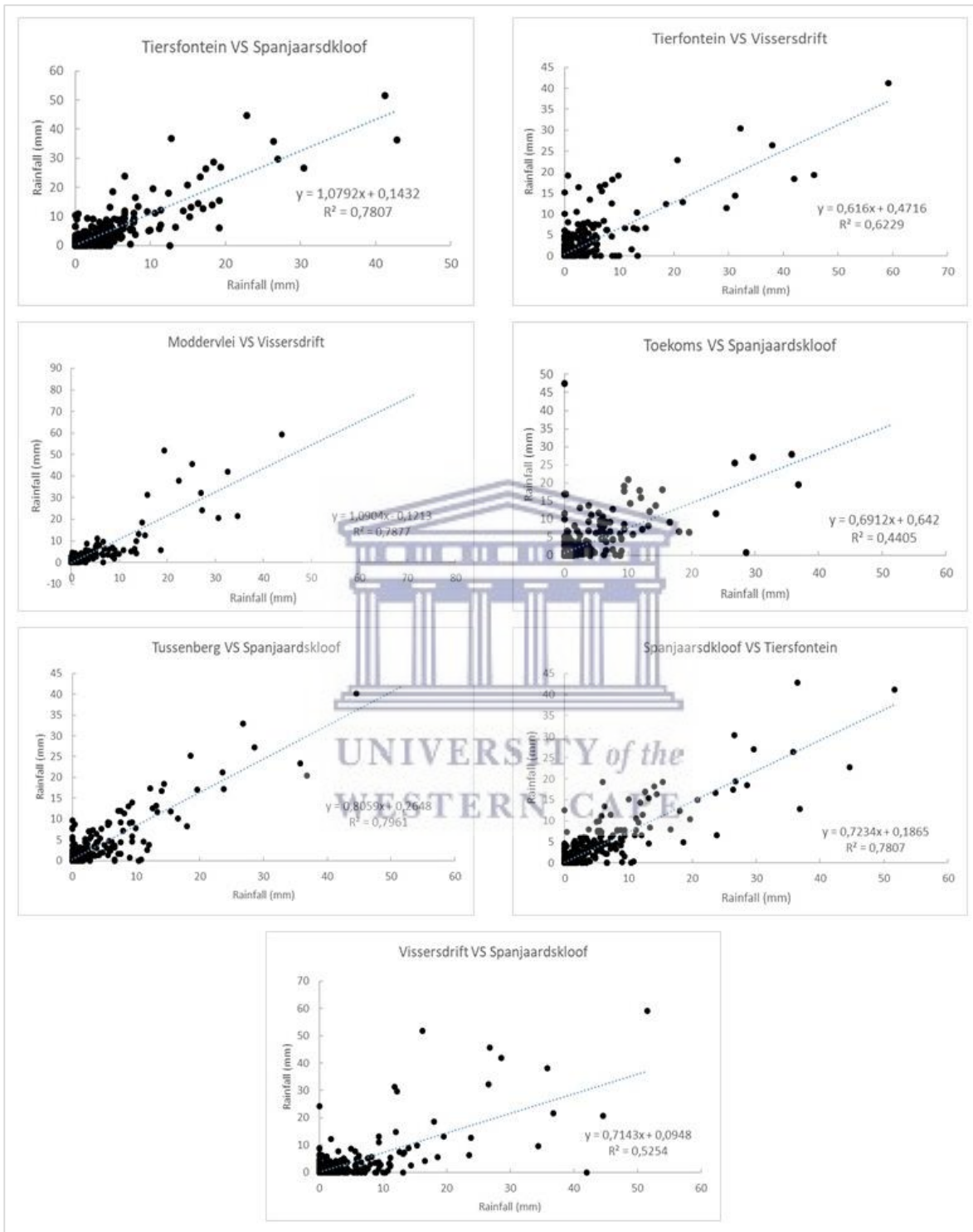
Xu, Y., Colvin, C., van Tonder, G. J., Hughes, S., le Maitre, D., Zhang, J. Braune, E. (2002). Towards the Resource Directed Measures : Groundwater Component Version 1.1. Water Research Commission: Report No.: 1090-2/1/03.

Zaimes, G.N., Schultz, R.C. & Isenhardt, T.M., (2006). Riparian land uses and precipitation influences on stream bank erosion in central Iowa. *Journal of the American Water Resources Association*, 42(1), pp.83–97.

Zribi, M., Chahbi, A., Shabou, M., Lili-Chabaane, Z., Duchemin, B., Baghdadi, N. Chehbouni, A. (2011). Soil surface moisture estimation over a semi-arid region using ENVISAT ASAR radar data for soil evaporation evaluation. *Hydrology and Earth System Sciences*, 15(1), 345–358. Available at: <https://doi.org/10.5194/hess-15-345-2011>



8. ANNEXURES



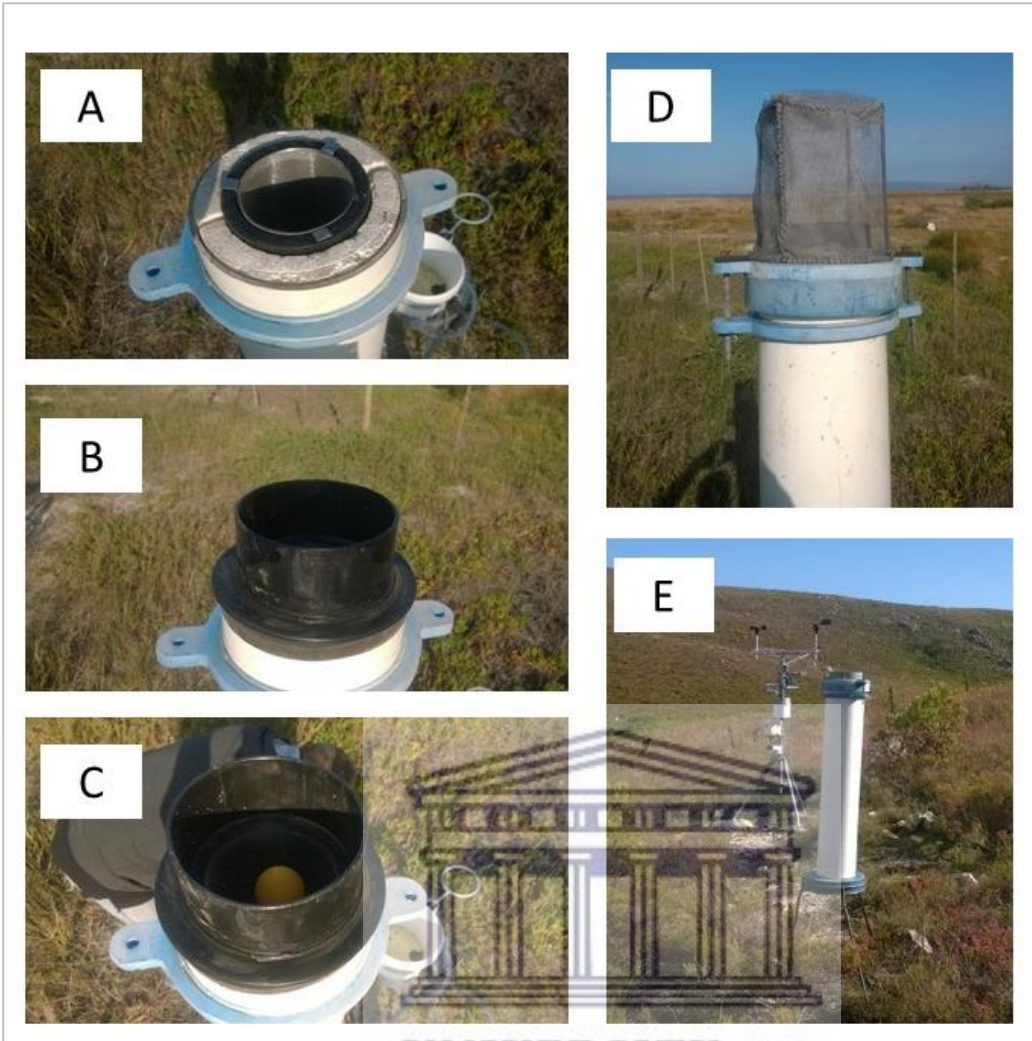
Annexure 1: Rainfall data of each of the sites used for infilling of the rainfall data.



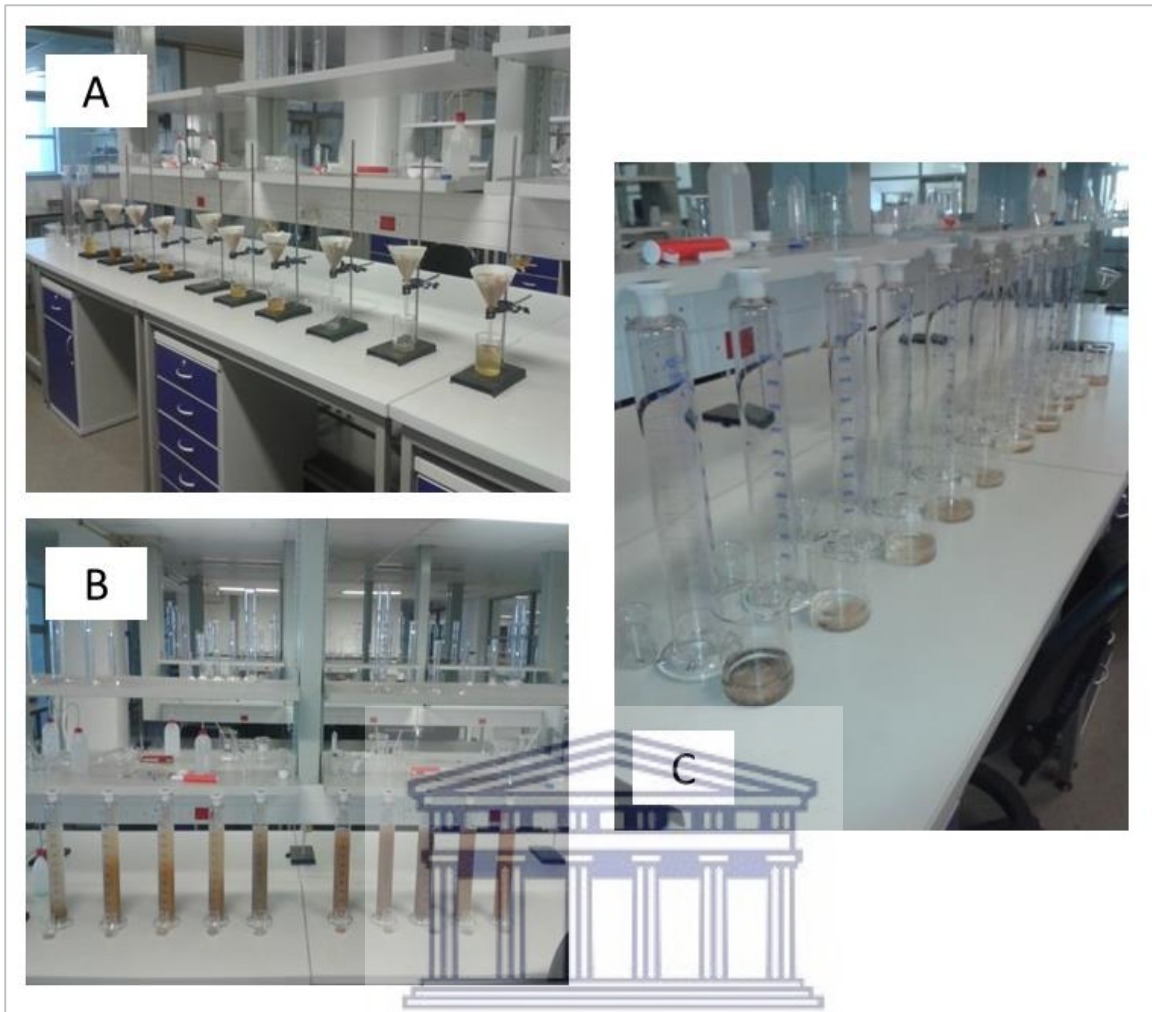
Annexure 2: Fabric mesh (A), PVC cap and 14 mm bolt with lock-nut (B), and slits being cut into the 75 mm PVC pipes used as stilling wells (C).



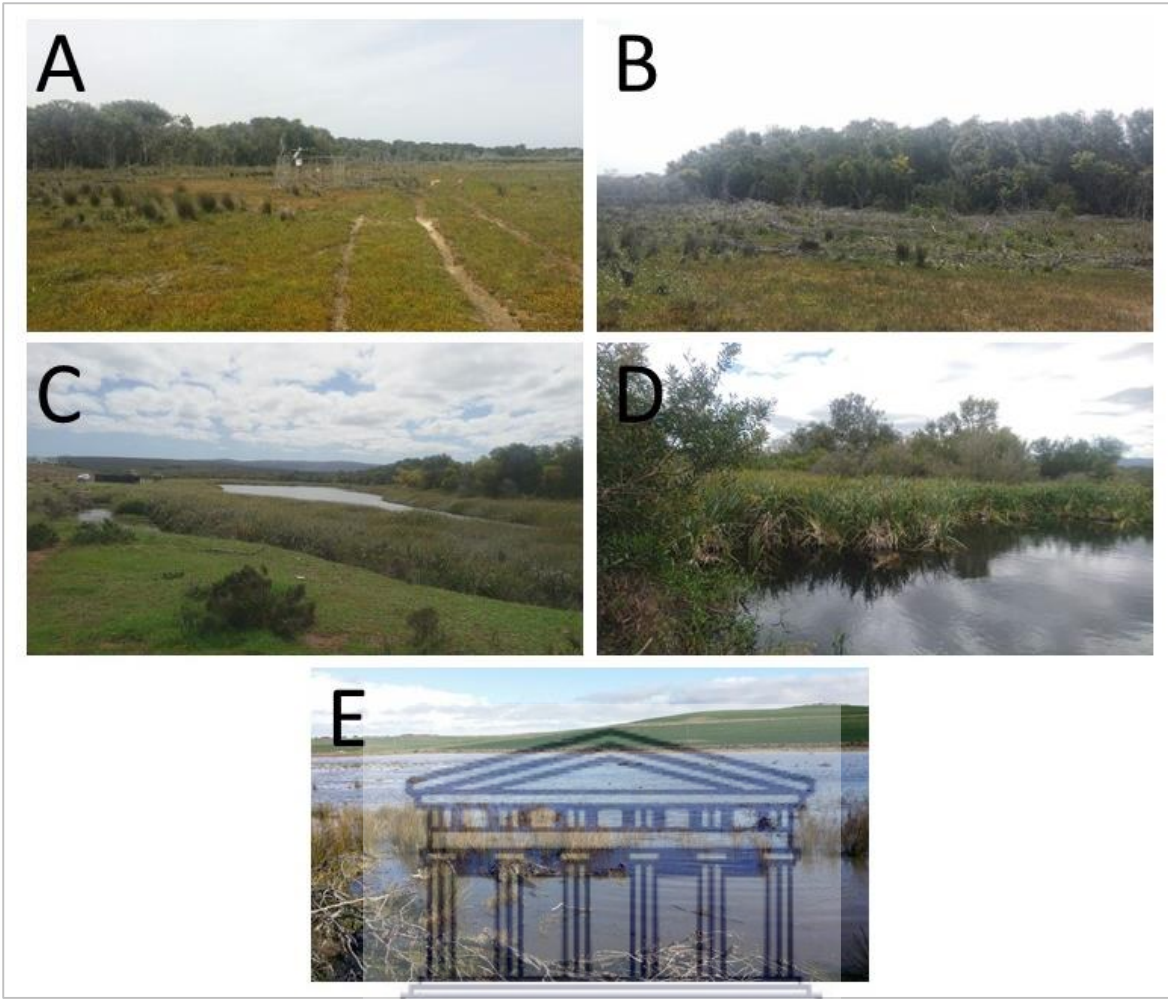
Annexure 3: High flows experienced on the 26th July 2016 during the peak flows at Pietersielieskloof (A), the Melkery Bridge (B) and Jan Swartskraal flow monitoring site (C) which limited the ability of conducting flow measurements.



Annexure 4: Internal structure (A), cone and rubber seal (B), table tennis ball inside the cone (C), anti-bird and insect net (D), and the Isotope sampler installed alongside the Tiersfontein weather station (E).



Annexure 5: Soil samples being filtered after the organic matter was removed (A), soil samples placed in settling tubes before the 8-hour extraction (B) and the sand portion of the analysis following the removal of silt and clay (C).



Annexure 6: Grasses, reeds and *Acacia* species on the banks of the Nuwejaars River (A), upstream of the Moddervlei weather station (B), Wilde Palmiet upstream of transect 5 (C), downstream of transect 4 (D), and flooding of the wetland on 25th July 2016 (E).